CHARLES UNIVERSITY IN PRAGUE

Faculty of Science

Study programme: Biology

Study field: Parasitology

Bc. Tomáš Macháček

Role of glial cells in the immune response of mice infected by neurotropic fluke *Trichobilharzia regenti*

Role gliových buněk v imunitní odpovědi myší infikovaných neurotropní motolicí *Trichobilharzia regenti*

MASTER'S THESIS

Supervisor: RNDr. Lucie Panská, Ph.D.

Prague 2015

PROHLÁŠENÍ

Prohlašuji, že jsem závěrečnou práci zpracoval samostatně a že jsem uvedl všechny použité informační zdroje a literaturu. Tato práce ani její podstatná část nebyla předložena k získání jiného nebo stejného akademického titulu.

V Praze dne 4. května 2015

.....

Tomáš Macháček

ACKNOWLEDGEMENTS

My warmest gratitude goes to my supervisor Lucie Panská for her guidance during my experimental work and completing this thesis; to Libuše Turjanicová, Jana Bulantová and Petr Horák for listening to my ideas and problems, encouraging me when it was necessary and for introducing me to some of the methods; to Jan Černý for sharing his incredible enthusiasm with me, providing me with knock-in mice and giving me an advice anytime I needed; to Tatiana Košťálová for her aid with statistics; to Tom and my friends for cheering me up. Finally yet importantly, I am deeply indebted to my loving family which has been supporting me during my studies.

Experimental work performed within this thesis was funded by Czech Science Foundation (project GA13-29577S).

ABSTRACT

A central nervous system (CNS) can be invaded by plenty of parasites, including parasitic helminths. Host's immune response during such infections includes not only participation of peripheral lymphocytes, but also astrocytes and microglia, resident glial cells present in the CNS. Activation of astrocytes and microglia has been recently demonstrated also in mice infected by neurotropic avian trematode *Trichobilharzia regenti* (Digenea: Schistosomatidae) for which mammals represent accidental hosts. The parasite does not mature in them and elicits development of inflammatory reaction in the CNS which may take part in parasite's destruction.

Employing *in vitro* experiments, this thesis aimed at evaluation of the possible role of astrocytes and microglia in murine immune response to *T. regenti*. For this purpose, primary astrocyte and microglia culture preparations were established and the cells were then stimulated by antigens of *T. regenti* (homogenate of transformed cercariae, recombinant cathepsins B1.1 and B2). After that, production of nitric oxide and proinflammatory cytokines (IL-1 beta, IL-6, TNF-alpha) was measured. The results revealed that *in vitro* stimulated astrocytes and microglia increase production of nitric oxide, IL-6 and TNF-alpha. Such response to parasite's antigens could influence the course of the infection *in vivo*. Apart from *in vitro* stimulation experiments, those *in vivo* were performed using MHC II-EGFP knock-in mice. In these experiments, MHC II+ cells were observed in the spinal cords of infected mice in proximity of the migrating parasites. It suggests the possible role of these cells in mediating T-lymphocytes based immune response.

To conclude, the data presented in this thesis represent the first report of *in vitro* response of murine glial cells to antigens of *T. regenti*; MHC II+ cells in the CNS of infected mice were noticed for the first time as well. Collectively, these data contribute to understanding of immune processes occurring during the infection of mice by neurotropic trematode *T. regenti*.

Keywords: central nervous system, astrocytes, microglia, *Trichobilharzia regenti*, schistosomulum, cathepsin B, cytokines, nitric oxide.

ABSTRAKT

Centrální nervová soustava (CNS) může být napadena celou řadou cizopasníků, včetně parazitických helmintů. Imunitní odpověď hostitele zahrnuje při těchto infekcích nejenom účast periferních leukocytů, ale mohou se na ní podílet i astrocyty a mikroglie, rezidentní gliové buňky CNS. Aktivace astrocytů a mikroglií byla v poslední době potvrzena i při infekci myších hostitelů neurotropní ptačí motolicí *Trichobilharzia regenti* (Digenea: Schistosomatidae), pro niž savci představují náhodné hostitele. Parazit v nich nedospívá a vyvolává v CNS rozvoj zánětlivé odpovědi, která se může podílet na jeho destrukci.

Hlavním cílem této práce bylo zhodnotit na základě *in vitro* experimentů možnou úlohu astrocytů a mikroglií v imunitní odpovědi myší proti motolici *T. regenti*. Za tímto účelem byly zavedeny postupy pro přípravu primárních kultur myších astrocytů a mikroglií a tyto buňky byly následně stimulovány antigeny *T. regenti* (homogenátem transformovaných cerkárií a rekombinantními katepsiny B1.1 a B2). Následně byla v těchto kulturách vyhodnocována produkce oxidu dusnatého a vybraných prozánětlivých cytokinů (IL-1 beta, IL-6, TNF-alfa). Získané výsledky ukázaly, že *in vitro* stimulované astrocyty a mikroglie zvyšují produkci oxidu dusnatého, IL-6 a TNF-alfa. Taková odpověď může mít vliv na průběh infekce *in vivo*. Kromě stimulačních *in vitro* experimentů byly provedeny také *in vivo* pokusy využívající MHC II-EGFP knock-in myši. Při nich byly v okolí migrujícího parazita pozorovány MHC II pozitivní buňky, které se mohou podílet na regulaci odpovědi závislé na T-lymfocytech.

Závěrem lze konstatovat, že data prezentovaná v této práci přestavují první popis *in vitro* odpovědi myších gliových buněk na stimulaci antigeny *T. regenti*; poprvé byl také prokázán výskyt MHC II pozitivních buněk v CNS infikovaných myší. Celkově tak tato data přispívají k pochopení imunitních dějů, k nimž dochází během infekce myších hostitelů neurotropní motolicí *T. regenti*.

Klíčová slova: centrální nervová soustava, astrocyty, mikroglie, *Trichobilharzia regenti*, schistosomulum, katepsin B, cytokiny, oxid dusnatý.

TABLE OF CONTENTS

LIST OF ABBREVIATIONS

CCL	chemokine (C-C motif) ligand
CXCL	chemokine (C-X-C motif) ligand
CD	cluster of differentiation
CNS	central nervous system
DAPI	4',6-diamidino-2-phenylindole
DIV	day(s) *in vitro*
dH_2O	distilled water
DPI	day(s) *post* infection
EDTA	ethylenediaminetetraacetic acid
EGFP	enhanced green fluorescent protein
ELISA	enzyme-linked immunosorbent assay
E/S	excretory/secretory (products)
GFAP	glial fibrillary acidic protein
GM-CSF	granulocyte-macrophage colony-stimulating factor
hom.	homogenate of transformed cercariae
hps	hour(s) *post* stimulation
HRP	horseradish peroxidase
ICC	immunocytochemistry
IL	interleukin
IFN	interferon
(e, i, n)NOS	(endothelial, inducible, neuronal) nitric oxide synthase
M-CSF	macrophage colony-stimulating factor
MG	medium for glial cell cultivation
MHC	major histocompatibility complex
MIP	macrophage inflammatory protein
MMP	matrix metalloprotease
PBS	phosphate-buffered saline
PBS-Tw	phosphate-buffered saline with Tween 20
NGS	normal goat serum
NO	nitric oxide
PCR	polymerase chain reaction
PLL	poly-L-lysine
RA	reactive astrogliosis

RNS	reactive nitrogen species
rpm	revolutions per minute
RPMI	Roswell Park Memorial Institute medium
RT	room temperature
SDS-PAGE	sodium dodecyl sulfate polyacrylamide gel electrophoresis
SE	standard error (of mean)
SEM	scanning electron microscope
SNARF	seminaphthorhodafluor
TBS	Tris buffered saline
TGF	transforming growth factor
TLR	Toll-like receptor
TMB	3,3',5,5'-tetramethylbenzidine
TNF	tumor necrosis factor
TREM	triggering receptor expressed on myeloid cells
TrCB	*Trichobilharzia regenti* cathepsin B

1. INTRODUCTION

Invasion of the central nervous system (CNS) by parasites during their development in mammalian hosts, including humans, is a well-known phenomenon recognised in many parasitic protists and helminths (for review see Table 1.1). For some of them, a spinal cord and/or a brain represent a common and natural site of invasion (e.g. *Toxoplasma gondii*, *Trypanosoma brucei* or *Angiostrongylus cantonensis*).

On the other hand, several parasites enter the CNS rarely, mostly accidentally, during their migration or dissemination in the host's body (e.g. *Schistosoma* spp., *Paragonimus* spp., *Toxocara* spp.); in that case, the CNS represents the ectopic localisation. Clinical manifestation of CNS parasitoses depends on the affected part of the brain/spinal cord, but generally comprises of headache, epilepsy, mental decline, impaired consciousness, confusion, coma or focal neurological deficits (Finsterer and Auer 2013).

Table 1.1. Parasites affecting the CNS of mammals with emphasis on human infections. Adapted from Brown and Voge (1982), Finsterer and Auer (2013) and Garcia *et al*. (2013).

Parasite		Disease	CNS invasion
PROTISTS	*Acanthamoeba* spp.	granulomatous amoebic encephalitis	common
	Balamuthia mandrillaris	granulomatous amoebic encephalitis	common
	Encephalitozoon cuniculi	microsporidial encephalitis	common
	Entamoeba histolytica	amoebic brain abscess	rare
	Leishmania spp.	leishmaniasis	rare
	Naegleria fowleri	primary amoebic meningoencephalitis	common
	Plasmodium falciparum	cerebral malaria	common
	Toxoplasma gondii	toxoplasmosis	common
	Trypanosoma brucei	sleeping sickness	common
	Trypanosoma cruzi	cerebral Chagas disease	common
HELMINTHS	*Angiostrongylus cantonensis*	angiostrongyliasis	common
	Baylisascaris procyonis	baylisascariasis	rare
	Echinococcus spp.	cerebral echinococcosis	rare
	Gnathostoma spp.	neurognathostomiasis	common
	Paragonimus westermani	neuroparagonimiasis	rare
	Schistosoma spp.	neuroschistosomiasis	common
	Spirometra spp.	neurosparganosis	common
	Taenia multiceps	coenurosis	common
	Taenia solium	neurocysticercosis	common
	Toxocara spp.	neurotoxocariasis	common
	Trichinella spp.	neurotrichinelliasis	rare

Although the CNS used to be considered an immune privileged site without anti-infection surveillance, it possesses arms that can be used to fight against invaders. This includes recruitment of peripheral leukocytes as well as activating CNS-resident immune cells, namely microglia and astrocytes. These immune mechanisms in the CNS are well mapped especially in case of neurodegenerative diseases. However, the research of the host immune response in helminthic neuroinfections is nearly neglected despite a high medical importance of some of them, e.g. neurocysticercosis which is suspected of triggering epilepsy (Carpio 2002, Ndimubanzi *et al*. 2010, Kelvin *et al*. 2011, Moyano *et al*. 2014).

Unfortunately, studies evaluating the role of particular cell types, emphasizing glial cells, in helminthic neuroinfections remain scarce. Characterisation of and understanding the regulation of their activation followed by secretion of immunoactive molecules may help us to grasp the course of the infection and the origin of detrimental effects impairing both parasites and hosts. This kind of data would also enrich the general knowledge of the host-parasite interactions and mechanisms of the CNS immune response.

In order to participate at accomplishing what has been mentioned above, the interactions of neurotropic bird schistosome *Trichobilharzia regenti* with its hosts have been studied in the Laboratory of Helminthology (Charles University in Prague, Department of Parasitology) for nearly twenty years. The recent paper by Lichtenbergová *et al*. (2011) revealed activation of glial cells in response to the presence of the parasites in a murine CNS. Nevertheless, no functional assays exploring the anti-parasitic activities of these cells have been done yet. Thus, the presented thesis focuses on the evaluation of the role of astrocytes and microglia in the immune response of mice experimentally infected by *T. regenti*.

2. AIMS OF THE THESIS

The main aim of this thesis was to evaluate the role of astrocytes and microglia in the immune response of mice experimentally infected by neurotropic fluke *Trichobilharzia regenti*. The specific aims were to:

- establish preparation of *in vitro* primary cell cultures of astrocytes and microglia in the Laboratory of Helminthology,
- evaluate nitric oxide production by astrocytes and microglia after their *in vitro* stimulation by antigens of *T. regenti*,
- assess production of proinflammatory cytokines by astrocytes and microglia after their *in vitro* stimulation by antigens of *T. regenti*,
- examine *in vivo* the presence of major histocompatibility complex (MHC) class II positive cells around *T. regenti* schistosomula migrating through a murine spinal cord and prepare samples of the spinal cord for ultramicroscopic examination.

3. LITERATURE REVIEW

3.1. *Trichobilharzia regenti*

Trichobilharzia regenti Horák, Kolářová and Dvořák 1998 is an avian schistosome (Trematoda: Schistosomatidae) with a two-host life cycle originally described from the Czech Republic (Horák *et al*. 1998). Adult worms dwell in a nasal tissue of anatid birds which serve as definitive hosts (Jouet *et al*. 2010). After mating, females lay eggs from which ciliated miracidia hatch directly in the nasal tissue after contact with water. As they get into water, when the bird is drinking/feeding, they search for and penetrate pulmonate snails *Radix lagotis* (intermediate hosts). After the penetration, miracidium changes into a primary sporocyst that gives rise to a secondary sporocyst. It produces large amounts of cercariae, infective larvae emerging from the snail, which actively search for the avian final host (Horák *et al*. 1998). Apart from birds, *T. regenti* cercariae are able to penetrate the skin of accidental mammalian hosts (e.g. mice or humans). This may result in skin allergic reaction, cercarial dermatitis (Kouřilová *et al*. 2004a, Horák *et al*. 2008, 2015, Horák and Kolářová 2011).

3.1.1. *T. regenti* migration in vertebrate hosts

When cercariae find either avian or mammalian host, they penetrate its skin. For this purpose, they are equipped with cysteine peptidases present in their excretory/secretory (E/S) products, which are capable of keratin and collagens degrading (Mikes *et al*. 2005, Kasný *et al*. 2007). The experiments with laboratory prepared recombinant form of the cysteine peptidase cathepsin B2 of *T. regenti* (TrCB2) confirmed its ability to cleave skin proteins (collagen, keratin and elastin) (Dolecková *et al*. 2009). By using specific antibodies, the authors localised TrCB2 in post-acetabular glands of *T. regenti* cercariae implying its possible role in the penetration of host skin.

After penetration the skin, cercariae transform to schistosomula and start a migration through the host's body. It was observed that *T. regenti* schistosomula display, contrary to larval stages of other schistosomes, neurotropic behaviour. They avoid penetration into blood capillaries and rather prefer entering peripheral nerves in host's limbs (Hrádková and Horák 2002). In the cited study, schistosomula were found in peripheral nerves of ducks and mice as soon as 1.5 and 1 day *post* infection (DPI), respectively. In both types of hosts, schistosomula show a high affinity to the CNS and use it as a migratory route. As demonstrated by Lichtenbergová *et al*. (2011), spinal roots represent a gate to the CNS for schistosomula.

The next course of the infection differs in final and accidental hosts. In ducks, schistosomula are observed in synsacral segments of a spinal cord 3 DPI and 7–8 days latter (10–11 DPI) they reach the brain. In their final localisation (the nasal tissue), they occur 13–14 DPI and laying eggs starts 15 DPI (Hrádková and Horák 2002, Chanová and Horák 2007).

In contrast, the progression of infection in mice is different. The first schistosomula are found in a lumbar spinal cord as early as 2 DPI and *medulla oblongata* is invaded the day after in some individuals. However, most of schistosomula stay localised in the thoracic and cervical spinal cord and only exceptionally migrate to the brain (Horák *et al*. 1999, Hrádková and Horák 2002). Neither the presence of worms has been detected in a nasal cavity nor has their maturation been noticed in the nervous tissue. As revealed by Blažová and Horák (2005), schistosomula development in mice is suppressed. According to the authors, this may be caused by the immune response of murine hosts to migrating schistosomula and/or by the presence/absence of some essential (nutritional, stimulatory) host factors.

The supposed crucial role of host immune response on the regulation of the parasite migration in accidental hosts is supported by several observations within experimental infections of immunocompetent and immunodeficient mouse strains:

(i) Hrádková and Horák (2002) reported that immunodeficient mice (SCID) had relatively higher schistosomula burden than immunocompetent ones (BALB/c, hr/hr). These schistosomula also migrated faster and reached the brain hemispheres more often; they were found even in *bulbus olfactorius*. The similar trend was described by Kouřilová *et al*. (2004b). Furthermore, it was shown that damaged schistosomula can be detected in the CNS from 7 DPI in immunocompetent mice whereas in immunodeficient ones, the parasite destruction appears two weeks later (Lichtenbergová *et al*. 2011).

(ii) In challenge (repeated) infections of immunocompetent mice (hr/hr), most of schistosomula are entrapped and damaged in the skin where a strong inflammatory response develops thus preventing schistosomula from entering the CNS (Kouřilová *et al*. 2004a, 2004b).

During the migration through a body of a vertebrate host, *T. regenti* may cause more or less severe pathologies. These might be elicited directly by parasite actions (mechanical damage of the tissues) or indirectly as a side effect of the host immune response.

3.1.2. Pathogenicity of *T. regenti* in vertebrate hosts

In vertebrate hosts infected by *T. regenti*, pathological states might be caused by all stages of the parasite, i.e. (i) by penetrating cercariae transforming to schistosomula in the skin, (ii) by schistosomula migrating through the CNS, and (iii) by adults laying eggs in nasal mucosa (only in avian hosts, thus being omitted here). Although being accidental hosts, most of the studies dealing with the pathological effects of *T. regenti* were conducted on mice because of possible implications to human's health.

In the initial phase of the infection, early transformed schistosomula are localised in the skin. Information about the immune response in the skin of birds has not been completed yet. In mice, immediate oedema and thickening of the site appear as early as 30 minutes after the penetration of cercariae; erythema is evident as well. Within 48 hours, inflammatory foci containing neutrophils, eosinophils, macrophages, CD4+ lymphocytes and degranulating mast cells develop around the parasites (Kouřilová *et al*. 2004a, 2004b). In case of challenge infections, the cellular infiltration is substantially elevated and the extensive inflammation may lead to formation of large abscesses or even epidermal and/or dermal necrosis (Kouřilová *et al*. 2004a).

In humans, the clinical symptoms of cercarial penetration comprise of macules/papules formation at the sites where the parasite entered the skin accompanied by intensive itching. The manifestation is more severe in previously sensitised people. This disease caused not only by *T. regenti* but also by cercariae of other bird schistosome species is called cercarial dermatitis. It is regarded as a neglected allergic disease (Kolářová *et al*. 2013).

The next phase of *T. regenti* infection is represented by schistosomula migration through the CNS. This is accompanied by serious neurological malfunctions in birds that suffer from leg paralysis and balance disorders (Horák *et al*. 1999). At this stage, a high number of undetermined cells/granules from the surrounding tissue were found in schistosomula intestines so the authors suggested that schistosomula feed on nervous tissue. In a murine model, this was proved by Lichtenbergová *et al*. (2011) who detected oligodendrocytes and neurons in the lumen of parasite's intestine. Possible utilizing of the nervous tissue as a source of nutrition is supported by the presence of a cysteine peptidase cathepsin B1 of *T. regenti* (TrCB1) in intestines of migrating schistosomula because this enzyme is capable of myelin basic protein degradation (Dvorák *et al*. 2005).

Nonetheless, Lichtenbergová *et al*. (2011) stated that the nervous tissue ingestion had likely only a minor pathogenic effect on the host CNS. This is consistent with previous observations of mice infected by *T. regenti*. Leg paralysis was, except for Horák *et al*. (1999), noted only in immunocompromised hosts (Kouřilová *et al*. 2004b, Lichtenbergová *et al*. 2011), whereas in experiments with immunocompetent mouse strains, the infected animals did not reveal any neurological disorders (Hrádková and Horák 2002, Kouřilová *et al*. 2004b, Lichtenbergová *et al*. 2011).

Based on what has been mentioned above, it may be concluded that the neurological symptoms originate probably in mechanical damage of nervous tissue leading to dystrophic or even necrotic changes of neurons and axonal injury. The cause of it is large migrating schistosomula (approximately 340×80 μm) which are not destroyed by proper immune response (Kolářová *et al*. 2001, Kouřilová *et al*. 2004b, Lichtenbergová *et al*. 2011).

3.1.3. Immune response to *T. regenti* in the CNS of vertebrate hosts

Formerly, the CNS was supposed to be "the immunologically privileged site" where no immune reactions take place (Niederkorn 2006). Nevertheless, now it is clear that there is active immune surveillance too (Carson *et al*. 2006, Ransohoff and Engelhardt 2012). In case of *T. regenti* infection, inflammatory reaction is triggered within the nervous tissue in response to schistosomula migration (Kolářová *et al*. 2001).

In ducks, eosinophilic meningitis with parasites surrounded by eosinophils and heterophils was noted. Additionally, leukocytes infiltrated perivascular spaces and tissues adjacent to the central canal (Kolářová *et al*. 2001). Despite inflammatory cells recruitment, most of the parasites are able to continue migration and reach the final localisation in nasal mucosa.

On the other hand, a strong cellular response consisting of mononuclear cells, granulocytes, plasma cells, and histiocytes was observed in immunocompetent mice especially around the damaged schistosomula (Kolářová *et al*. 2001, Kouřilová *et al*. 2004b). Lichtenbergová *et al*. (2011) specified the mononuclear cells present in the lesions as macrophages and cluster of differentiation (CD) 3+ lymphocytes which possibly cooperate in schistosomula destruction. As a consequence, CD3-deficient mice developed no or only mild inflammation which was accompanied by neurological symptoms described above (Kouřilová *et al*. 2004b, Lichtenbergová *et al*. 2011).

Additionally, two more CNS-resident cell types capable of mediating immune response, microglia and astrocytes, were detected in the CNS of mice infected by *T. regenti* (Lichtenbergová *et al*. 2011). Activated microglia were observed in the migratory tracks of schistosomula and in the inflammatory lesions containing parasite residues. Therefore, they were suggested to take part in schistosomula destruction either alone or in cooperation with macrophages and CD3+ lymphocytes. In addition, hypertrophy and activation of astrocytes located in the migratory tracks and in the proximity of the schistosomula were seen. This implies their role in immune response and reparation of the tissue, likely in forming of a glial scar (Lichtenbergová *et al*. 2011).

However, no functional assays evaluating the role of these cells, abounding in plenty of possible anti-infection effector mechanisms, in host-parasite interactions have been performed.

3.2. Microglia

Microglia, a type of glial cells present in the CNS, are usually regarded as innate immune cells of the nervous tissue responsible for elimination of threats (Olson and Miller 2004, Glezer *et al*. 2007, Kofler and Wiley 2011). Admittedly, their pathological role in brain aging and development of neurodegenerative diseases caused by increased production of proinflammatory agents was suggested as well (Smith *et al*. 2012, Norden and Godbout 2013, Heneka *et al*. 2014). On the other

hand, in a healthy brain, they carry out irreplaceable physiological functions during neural development and adult neurogenesis or in synaptic interactions (Graeber 2010, Paolicelli *et al*. 2011, Wake *et al*. 2013). However, with respect to the topic of this thesis, the role of microglia in immunity will be in focus.

Traditionally, functions of microglia were deduced from observations of their *in vivo* morphology and behaviour. As a result, two main functional stages of microglia differing in effector capability were described: resting/ramified microglia and activated/reactive microglia (Streit and Kreutzberg 1987, Davis *et al*. 1994). In spite of the first having been thought to be very quiescent, a crucial role of resting microglia in brain parenchyma surveillance was demonstrated by Nimmerjahn *et al*. (2005). Their time-lapse imaging experiments revealed that while the bodies of resting microglia mostly remain fixed at one site, the processes display high motility scanning their vicinity actively. This is in consistency with the idea of microglia sensing for pathological events in the CNS (Kreutzberg 1996).

In response to the CNS disturbances, e.g. infection, trauma, ischaemia, neurodegenerative disease or even altered neuronal activity, microglia become activated. Depending on the signals triggering the activation, it is called "classical" or "alternative" applying the same "paradigm" as for macrophage activation (Mills *et al*. 2000). Classically activated microglia (also termed M1 microglia) appear after lipopolysaccharide (LPS) or interferon (IFN)-gamma stimulation and express pro-inflammatory phenotype. This is characterised by interleukin (IL)-1, IL-6 and tumor necrosis factor (TNF)-alpha secretion and production of reactive oxygen species and nitric oxide (NO). On the other hand, alternatively activated (M2) microglia originate from IL-4 and IL-13 treatment and display anti-inflammatory properties; they participate in tissue repair and extracellular matrix reconstruction too. This phenotype might be expressed also by microglia "deactivated" by IL-10 or transforming growth factor (TGF)-beta or by ingestion of apoptotic cells (Crain *et al*. 2013, Martinez and Gordon 2014, Tang and Le 2015). With regard to the focus of this thesis, classically activated microglia functions will be discussed mostly.

3.2.1. Functions of classically activated microglia

Microglia activation *in vivo* is accompanied by their rapid transformation from ramified to amoeboid cells (Stence *et al*. 2001). At the beginning of the conversion, existing ramified branches retract back being resorbed into the cell body. New protrusions then emerge and reactive microglia start to migrate through the nervous tissue towards the site of the insult, even farther than hundreds of micrometres (Carbonell *et al*. 2005). To cope with the pathological insult, either intrinsic, or extrinsic, reactive microglia are capable of exhibiting several activities: proliferation,

phagocytosis, antigen presentation, secretion of immunoregulatory and/or antimicrobial molecules (Miller *et al*. 2013).

Proliferation of microglia is stimulated by proinflammatory cytokines such as IL-1 beta, IL-6 and TNF-alpha (Streit *et al*. 2000, Mander *et al*. 2006). Other cytokines including macrophage and granulocyte-macrophage colony-stimulating factors (M-, GM-CSF, respectively) were shown to promote microglial division as well (Lee *et al*. 1993, 1994, Smith *et al*. 2013). Moreover, beta-amyloid peptides present in senile plaques accumulations in the nervous tissue of patients suffering from Alzheimer's disease are able to induce increase in microglial number (Jekabsone *et al*. 2006). Microglial proliferation results in amplification of the response against the insult.

In order to dispose of detrimental agents, microglia are capable of phagocytosis. Several receptors may be involved in initiation of this process. Toll-like receptors (TLR) recognize bacterial lipopolysaccharide (LPS) but also fibrillary beta-amyloid which implies their role in neurodegenerative disorders (Ribes *et al*. 2009, Liu *et al*. 2012, Redlich *et al*. 2013, Rajbhandari *et al*. 2014). Triggering receptors expressed on myeloid cells (TREM)-2 are responsible for recognition of cellular debris, including apoptotic neurons (Hsieh *et al*. 2009). Fc, complement and scavenger receptors may be also employed to detect the damaged cells (Peress *et al*. 1993, Bell *et al*. 1994, Reichert and Rotshenker 2003).

Following phagocytosis, residues of ingested particles are presented on MHC II molecules on the cell surface. Therefore, the question if microglia are able to serve as antigen presenting cells capable of T-lymphocytes activation was raised. In a resting state, ramified microglia do not function as antigen presenting cells and even elicit apoptosis of T-lymphocytes (Ford *et al*. 1995, 1996). However, activated reactive microglia increase expression of MHC II and costimulatory molecules which makes them effective antigen presenting cells able to participate in T-lymphocyte activation (Matsumoto *et al*. 1992, De Simone *et al*. 1995, Iglesias *et al*. 1997, Aloisi *et al*. 1998, Mack *et al*. 2003, Wlodarczyk *et al*. 2014).

To mediate the response against insults and to deal with them, microglia possess a repertoire of secretory products, mainly cytokines, chemokines, free radicals (superoxide, nitric oxide), matrix metalloproteases (MMP) and many others (Rock *et al*. 2004). It is out of scope of this review to describe extensively microglial secretion elicited by different stimuli, it will be rather disused solely in context of parasitic infections.

3.2.2. The role of microglia in the CNS parasitic infections

Among parasite-caused neuroinfections, the importance of microglia and immunoactive agents secreted by them has been studied mainly in protozoan infections in both human patients and animal models. Toxoplasmosis (caused by *Toxoplasma gondii*) has been the leading model, being

followed by cerebral malaria (*Plasmodium* spp.) and infections caused by trypanosomes, i.e. African trypanosomiasis and cerebral Chagas disease (*Trypanosoma brucei* and *T. cruzi*, respectively). Data for helminthic neuroinfections are rarer and fragmentary. Available studies deal especially with angiostrongyloidosis (*Angiostrongylus* spp.) and neurocysticercosis (*Taenia solium*).

3.2.2.1. Toxoplasmosis

Initial studies in murine cell cultures revealed that microglia activated by LPS, TNF-alpha and IFN-gamma inhibit toxoplasma proliferation *via* destruction of tachyzoites by nitric oxide (Chao *et al*. 1993a, 1993b, Jun *et al*. 1993). Contrary to what was observed in mice, microglia-produced NO is probably not a key effector molecule in human infections, in which T-lymphocytes probably play the more important role (Chao *et al*. 1994).

In response to toxoplasma infection, microglia produce proinflammatory cytokines such as IL-1 beta, IL-6, TNF-alpha and IFN-gamma (Fischer *et al*. 1997b, Schlüter *et al*. 1997, Benedetto *et al*. 2001, Suzuki *et al*. 2005, Wang and Suzuki 2007, Zhang *et al*. 2014). Recruitment of other effector inflammatory cells is provided by chemokine (C-C motif) ligand (CCL)-5 and chemokine (C-X-C motif) ligand (CXCL)-9 secretion by activated microglia (Strack *et al*. 2002).

During toxoplasma-triggered cerebral inflammation (encephalitis), activated microglia can cause neuronal apoptosis (Zhang *et al*. 2014). Likely in order to prevent such deleterious effects, microglia secrete IL-10 and TGF-beta which attenuate the inflammatory immune response and lead to asymptomatic persistence of the infection (Deckert-Schlüter *et al*. 1997, Fischer *et al*. 1997b, Rozenfeld *et al*. 2003, 2005, Blanchard *et al*. 2015).

3.2.2.2. Cerebral malaria

Although the accumulation of microglia around small brain blood vessels in patients with cerebral malaria was noticed by Janota and Doshi (1979), the proof for microglia activation leading to migration towards capillaries and TNF-alpha release causing pathology in murine model came many years later (Medana *et al*. 1997a, 1997b, Jennings *et al*. 1998, Schluesener *et al*. 1998). In humans, the expression of proinflammatory IL-1 beta and TNF-alpha in brain was proved *post mortem* in patients with cerebral malaria but without attribution of the production to any cell type (Brown *et al*. 1999).

Nitric oxide production by microglia during cerebral malaria has not been evaluated. The only known is that, contrary to macrophages, NO and TNF-alpha secretion in LPS-activated microglia is not inhibited by malaria pigment beta-haematin (Taramelli *et al*. 1995). This suggests that microglia could potentially help to regulate the infection, however, not with enough efficacy.

Similar to toxoplasmosis, microglia were shown to express anti-inflammatory molecules such TGF-beta or metallothionein (a cysteine-rich protein able to capture free radicals) during cerebral malaria, likely to regulate the course of inflammation and avoid excessive tissue damage (Deininger *et al*. 2000, Wiese *et al*. 2006).

3.2.2.3. Infections caused by trypanosomes

Activation of microglia concomitant with the onset of sleep abnormalities was shown by Chianella *et al*. (1999) in a rat model of sleeping sickness caused by *T. brucei*. Interestingly, activation of microglia in horse brain was detected also in case of equine trypanosome *T. evansi* (Lemos *et al*. 2008).

In vitro experiments demonstrated that living trypanosomes stimulate microglia to only slight increase in NO production. However, if IFN-gamma, which is naturally released during the infection (Bancroft *et al*. 1983), is added, the NO production rises four times (Girard *et al*. 2003). Elevated levels of NO in brains infected by *T. brucei* were confirmed by *in vivo* observation in the rat model (Amrouni *et al*. 2010).

Masocha *et al*. (2006) hypothesised that microglia could be a source of proinflammatory cytokines (IL-1 alpha, IL-1 beta, IL-6 and IFN-gamma) and MMPs, since they observed their depletion after administration of minocycline to *T. brucei*-infected mice. Minocycline is an inhibitor of microglial activation preventing its proinflammatory M1 polarization (Kobayashi *et al*. 2013). *In vivo* experiments also revealed rat microglia as a source of chemokines (macrophage inflammatory proteins [MIP] 1 and 2, CCL-5) responsible for peripheral leukocyte recruitment into the brain (Sharafeldin *et al*. 2000).

Histopathological examination of mice infected by *T. cruzi* (experimental model for Chagas disease) confirmed the presence of activated reactive microglia in the CNS (Morocoima *et al*. 2012). Unfortunately, no studies dealing with functional analysis of these cells are available.

3.2.2.4. Angiostrongyloidosis

The role of microglia in angiostrongyloidosis has been elucidated by series of recent papers. Wei *et al*. (2013) demonstrated differences in activation of rat and murine microglia stimulated by *Angiostrongylus cantonensis* larval antigens. While murine microglia increased production of IL-1 beta, IL-5, IL-6, IL-13, TNF-alpha, inducible NO synthase (iNOS) and eotaxin, microglia isolated from rats displayed higher levels of only IL-5, IL-13 and eotaxin (Wei *et al*. 2013).

The authors speculate that elevated levels of proinflammatory cytokines and predicted NO production might be a reason for incomplete development of worms in mice contrary to the

situation in rats in which they mature naturally (Wei *et al*. 2013). On the other hand, parasite's response to the host's inflammatory reaction was described by Z. Li *et al*. (2014). In larvae migrating through the CNS they detected high levels of microRNAs which were able to downregulate the mRNA expression of IL-1 beta, IL-6 and TNF-alpha in murine microglia (Z. Li *et al*. 2014).

Since eosinophilic meningitis is a usual manifestation of angiostrongyloidosis, microglial chemokine secretion, which would be responsible for eosinophils recruitment in the CNS, was studied too. Two major chemokines, eosinophilic chemotactic factor Ym1 and eotaxin, were reported to be localised in and released from activated microglia of *Angiostrongylus*-infected mice suggesting their role in peripheral leukocytes attraction (Zhao *et al*. 2013, S. Li *et al*. 2014).

3.2.2.5. Neurocysticercosis

Neurocysticercosis is the infection of high medical importance since it is a widespread disease suspected of triggering epilepsy (Carpio 2002, Ndimubanzi *et al*. 2010, Kelvin *et al*. 2011, Moyano *et al*. 2014).

The presence of activated microglia in vicinity of cysticerci was described by Alvarez *et al*. (2002). According to the authors, microglia expressed MHC II, costimulatory molecule CD86 and proinflammatory cytokines IFN-gamma and IL-18 (Alvarez *et al*. 2002). However, their results seem to be questionable as they based the attribution of cytokine production to microglia only on cell morphology without applying double staining or at least serial sections analysis.

The same objection should be raised in case of IL-18 detection in microglia in the study by Restrepo *et al*. (2001) dealing with cytokine profiling in brains of patients with neurocysticercosis. They detected IFN-gamma, IL-18, IL-4, IL-10, IL-13 and TGF-beta (i.e. both Th1 and Th2 profile) by immunohistochemistry but matching it with a particular cell type is lacking. If admitted that microglia take part in proinflammatory secretion, the parasite may be able to modulate such reaction by disruption of Ca^{2+}-dependent signalization as shown by Sun *et al*. (2014). In a murine model of neurocysticercosis using tapeworm *Mesocestoides corti*, such disruption caused by helminth soluble factors led to decrease of IL-6 and TNF-alpha (Sun *et al*. 2014).

Alvarez and Teale (2008) also suggested that CD11b+ cells, possibly microglia, are an important source of MMPs whose expression is strongly upregulated during neurocysticercosis. However, a credible proof of MMPs activity localisation has not been published.

3.2.2.6. Neurotoxocariasis

The first report of microglia proliferation in parasite-containing granulomas during neurological manifestation of toxocariasis was carried by Dent *et al*. (1956), but not much more data about

microglia participation in the immune response have accumulated. Recently, Janecek *et al*. (2014) observed activated microglia in brain of infected mice speculating about their possible role in demyelination. Cytokines produced during neurotoxocariasis were analysed by Hamilton *et al*. (2008) who detected increased expression of IL-5, IL-10, IFN-gamma and iNOS as well. However, the cellular source of them remains unknown.

3.2.2.7. Paragonimiasis

Despite a rare occurrence of *Paragonimus westermani* in the CNS, several experiments exploring the influence of its E/S products on microglial activity were performed. Lee *et al*. (2006) observed *in vivo* microglia migration towards the site where E/S products were injected, the lesion also displayed iNOS positivity. The proof of NO production by microglia upon *in vitro* stimulation by *P. westermani* E/S products was brought later (Jin *et al*. 2006, 2009).

3.3. Astrocytes

Astrocytes represent the most abundant type of glial cells present in the CNS. They participate in various processes under both physiological and pathological conditions. In a healthy CNS, three general scopes of astrocyte activities can be recognized.

First, astrocytes guide migrating neurons during CNS development, provide them with mechanical support and regulate synaptogenesis (Rakic 1971, Powell and Geller 1999, Christopherson *et al*. 2005). Second, they induce blood-brain barrier formation by endothelial cells and isolate brain capillaries from the nervous tissue by encasing them with cellular end-feet processes (Braak 1975, Janzer and Raff 1987, Haseloff *et al*. 2005, Abbott *et al*. 2006). Third, the balance of ions, transport of nutrients and metabolism of neurotransmitters is maintained by astrocytes in order to keep homeostasis (Henn *et al*. 1972, Kacem *et al*. 1998, Voutsinos-Porche *et al*. 2003, Brown and Ransom 2007, Perea *et al*. 2009). Recently, murine astrocytes were also observed to abound in a neurogenic capacity suggesting their possible role in neuronal replacement (Magnusson *et al*. 2014).

Undoubtedly, these physiological functions of astrocytes are crucial and appreciable. However, considering the topic of this thesis, the role of astrocytes in non-physiological states of the CNS will be pointed out.

3.3.1. Astrocyte response to CNS insults

Similar to microglia, astrocytes are capable of responding to various CNS insults, both intrinsic and extrinsic. The complex process of astrocyte activation in response to miscellaneous stimuli is called

reactive astrogliosis (RA) which has traditionally been regarded as a hallmark of CNS pathology. Nonetheless, RA consequences can be both detrimental and beneficial (Sofroniew and Vinters 2010, Pekny *et al*. 2014).

Traditionally, canonical markers of RA consisted of increased expression of glial fibrillary acidic protein (GFAP), an intermediate filament component, and astrocyte hypertrophy (Hozumi *et al*. 1990, Vijayan *et al*. 1990, Eddelston and Mucke 1993). On the contrary, Wilhelmsson *et al*. (2006) showed that even though reactive astrocytes increased the thickness of their main cellular processes after injury, the volume occupied by them remained the same as for nonreactive ones (i.e. technically, no hypertrophy was observed).

RA must be understood not as "all-or-non response", but as a "finely gradated continuum of progressive changes" as stated by Sofroniew (2009). Therefore, the classification of RA into three grades depending on the severity of the triggering pathological event was introduced (Sofroniew 2009, Sofroniew and Vinters 2010):

1. Mild to moderate RA develops after non-penetrating and non-contusive trauma or innate immune activation (viral or bacterial infections) and is reversible. Astrocytes usually do not proliferate and preserve their individual domains so the cellular processes do not intermingle (Bushong *et al*. 2002).
2. Severe diffuse RA is usually found around focal lesions elicited by an infection or neurodegeneration. It is characterised by disruption of individual astrocyte domains accompanied by overlapping of cellular processes. Astrocyte proliferation occurs which may results in reconstruction of tissue architecture (Bush *et al*. 1999).
3. Severe diffuse RA with formation of a compact glial scar is associated with sites of extensive tissue damage, necrosis and/or inflammatory infiltration. The glial scar is composed of extracellularly secreted chondroitin sulphate proteoglycans (McKeon *et al*. 1999, Tang *et al*. 2003).

Implications of RA are ambiguous. Several studies identified mechanisms that could be employed by reactive astrocytes in order to protect the nervous tissue. For example, they mitigate oxidative stress by production of anti-oxidative glutathione (Dringen *et al*. 2000, Chen *et al*. 2001), facilitate blood-brain barrier repair and reduce post-traumatic oedema (Bush *et al*. 1999) and are capable of glutamate uptake preventing its excitotoxicity (Vermeiren *et al*. 2005). Moreover, the glial scar has a crucial role in isolation of the insulted site from the healthy tissue which limits the leakage of inflammatory cells and deleterious agents (Roitbak and Syková 1999). Additionally, astrocytes are able to prevent tissue damage mediated by infiltrating autoreactive T-helper lymphocytes. They initiate their apoptosis *via* Fas-FasL interaction (Bechmann *et al*. 2002) or induce upregulation of inhibitory coreceptors on surface of T-lyphocytes (Gimsa *et al*. 2004).

On the other hand, detrimental effects associated with RA are known as well. The most prominent is the inhibition of neurite outgrowth by the glial scar after the CNS insult. It was observed both *in vitro* and *in vivo* (Rudge and Silver 1990, McKeon *et al*. 1991, Smith-Thomas *et al*. 1994) and chondroitin sulphate proteoglycans secreted by reactive astrocytes were identified to be responsible for the neuronal regeneration impairment (Fidler *et al*. 1999, Asher *et al*. 2000, Jones *et al*. 2003, Monnier *et al*. 2003, Tang *et al*. 2003).

Additionally, in response to the infection, reactive astrocytes release a wide repertoire of molecules including antimicrobial substances (e.g. NO), cytokines and chemokines. Their functions are to eliminate the threat, activate neighbouring cells (especially microglia), amplify the immune response, modify the blood-brain barrier permeability and attract peripheral immune cells from the blood circulation (Farina *et al*. 2007). Comprehensive review of papers dealing with the secretion of these molecules under different conditions would go beyond the range of this thesis. Therefore, it will be discussed in context of the CNS parasitic infections.

3.3.2. The role of astrocytes in the CNS parasitic infections

Just like in case of microglia, the role of astrocytes in parasitic neuroinfections has been examined mostly in diseases caused by parasitic protists among which toxoplasmosis, infections caused by trypanosomes and cerebral malaria are in focus most often. Considering helminthic neuroinfections, a little information about participation of astrocytes in the immune response is available only for neurocysticercosis. Otherwise, it is usually restricted to statement about astrocyte activation omitting any functional consequences.

3.3.2.1. Toxoplasmosis

It has been shown by many studies that astrocytes represent a suitable cell type for *Toxoplasma gondii* multiplication which allows to use them for *T. gondii* cultivation and *in vitro* experiments (Jones *et al*. 1986, Peterson *et al*. 1993, Halonen *et al*. 1996, Fischer *et al*. 1997a, Lüder *et al*. 1999). Identification of factors (primarily cytokines and NO) responsible for regulation of toxoplasma growth and development in astrocytes was challenging for many years.

Jones *et al*. (1986) reported that the medium intermittently supplemented with IFN-gamma enables a long-term cultivation of toxoplasma since IFN-gamma controls its intracellular multiplication. Upon cytokine detection in toxoplasma-infected CNS, Hunter *et al*. (1993) stated that both IFN-gamma and TNF-alpha are involved in T-cell-independent mechanisms of mouse resistance to the infection by toxoplasma. Other studies also revealed the importance of

proinflammatory cytokines IFN-gamma, TNF-alpha and IL-1 for toxoplasma control (Peterson *et al*. 1995, Halonen *et al*. 1998).

Although nitric oxide was suggested by Peterson *et al*. (1995) to mediate anti-toxoplasma effects, Halonen *et al*. (1998, 2000) rejected the hypothesis and showed that neither iron depletion is responsible for toxoplasma growth inhibiton. The solution came in 2003, when Oberdörfer *et al*. (2003) revealed that IFN-gamma initiated tryptophan depletion is crucial for toxoplasma control. The same effect of tryptophan depletion was described in case of toxoplasma-infected fibroblasts (Pfefferkorn 1984, Pfefferkorn *et al*. 1986).

Based on several observations of astrocyte activation, including their perivascular cuffing, (Hunter *et al*. 1992a, 1993, Burke *et al*. 1994), it was expected that astrocyte could produce agents (especially cytokines and chemokines) participating in the immune response to toxoplasma infection. Hunter *et al*. (1992a, 1992b) detected elevated levels of IL-1 alpha, IL-1 beta, IL-4, IL-6, IFN-gamma, TNF-alpha, GM-CFS and MIP-1 concurrently with astrocyte activation and increase of their cellular volume. However, the exact cell type responsible for the cytokine production could not have been defined since they used polymerase chain reaction (PCR) applied on whole tissue samples for the analysis (Hunter *et al*. 1992a, 1992b).

Experiments combining particular cell type labelling with the molecule of interest targeting or those performed *in vitro* with well-defined cell cultures helped us to uncover which immunomodulatory molecules are secreted by astrocytes during toxoplasmosis. Fischer *et al*. (1997b) observed that astrocytes infected by *T. gondi* increase IL-1 alpha, IL-6 and GM-CSF production implying their role in initiation of local inflammation. This can be enhanced by peripheral leukocytes recruitment regulated by interferon gamma-induced protein 10, CCL-2, MMP-2 and MMP-9 produced by astrocytes (Strack *et al*. 2002, Brenier-Pinchart *et al*. 2004, Durand *et al*. 2004, Lu and Lai 2013a, 2013b).

Astrocytes can also participate in attenuation of host inflammatory reaction in order to forestall nervous tissue damage. They secrete prostaglandin E2 that promotes suppression of NO production by activated microglia which protects other cells from oxidative stress (Rozenfeld *et al*. 2003). A significant role in nervous tissue protection has recently been ascribed also to TGF-beta signalling in astrocytes. It prevents CCL-5 expression by them which normally leads to recruitment of peripheral leukocytes causing severe neuronal damage (Cekanaviciute *et al*. 2014).

3.3.2.2. Infections caused by trypanosomes

Invasion of the CNS by trypanosomes in course of sleeping sickness results in widespread astrocyte activation and proliferation (Hunter *et al*. 1991, Keita *et al*. 1997). Activated astrocytes stimulated

by trypanosomes were shown to produce NO *in vitro*, the expression of iNOS was detected in astrocytes *in vivo* as well (Girard *et al*. 2000, Amrouni *et al*. 2010).

Hunter *et al*. (1991) and Quan *et al*. (1999) characterised the cytokine production during the infection, but did not determine the cellular source of the upregulated cytokines (IL-1, IL-4, IL-6, IFN-gamma, TNF-alpha, MIP-1). Only INF-gamma was shown to be produced particularly by astrocytes in response to trypanosomal antigen (Bakhiet *et al*. 2002a). On the contrary, astrocytes were demonstrated as a source of many chemokines, namely IL-8, MIP-1, MIP-2, MCP-1, CCL-5, CXCL-10, and interferon gamma-induced protein 10 (Sharafeldin *et al*. 2000, Bakhiet *et al*. 2002b, Amin *et al*. 2009). These chemokines likely promote recruitment of peripheral leukocytes into the CNS where they participate in the ongoing inflammatory response.

In case of infection by *T. cruzi*, it has been observed many times that trypanosomes are able to proliferate and dwell in astrocytes, but further characterisation of the cellular response against the parasite is lacking (Da Mata *et al*. 2000, Guarner *et al*. 2001, Morocoima *et al*. 2012, Vargas-Zambrano *et al*. 2013). A surprising interaction of *T. cruzi* with astrocytes has been recently described by Silva *et al*. (2015). They revealed that uptake of trypanosomes and their proliferation are enhanced by IFN-gamma which stimulates NO and TNF-alpha production by astrocytes. Unexpectedly, these two agents were shown to promote persistence of the infection (Silva *et al*. 2015).

3.3.2.3. Cerebral malaria

In contrast to microglia, only a little information is available about the role of astrocytes during cerebral malaria. In a murine model of the infection, axonal demyelination and damage associated with astrogliosis were noted (Ma *et al*. 1997). Astrocytes may contribute to such pathogenesis by secretion of TNF-alpha which can be harmful to myelin (Medana *et al*. 1997b). On the other hand, to moderate the tissue oxidative stress, astrocytes, likewise microglia, produce metallothionein, which exerts antioxidant function (Wiese *et al*. 2006).

3.3.2.4. Helminthic neuroinfections

The role of astrocytes in helminthic neuroinfections has been understudied despite the fact that astrocyte activation has been reported in many cases including baylisascariasis (Furuoka *et al*. 2003), neuroparagonimiasis (Lee *et al*. 2006), neuroschistosomiasis (Pittella 1985), neurosparganosis (Huh *et al*. 1993) or neurotoxocariasis (Liao *et al*. 2008).

The astrocyte contribution to course of the infection is in focus only in case of neurocysticercosis. Reactive astrogliosis was observed in porcine and murine models of

neurocysticercosis with IL-6 reactivity detected in the glial scar (Alvarez *et al*. 2002, Londoño *et al*. 2002, Alvarez and Teale 2006, Sikasunge *et al*. 2009). Due to rapid angiogenesis occurring in the parasite lesion, astrocytes do not manage to participate in blood-brain formation which results in infiltration of the nervous tissue by leukocytes (Sikasunge *et al*. 2009). Astrocytes can boost leukocyte recruitment by secretion of chemokines (MCP-1, IL-8, CXCL-10) which is triggered by TNF-alpha (Uddin *et al*. 2005). Furthermore, Mishra *et al*. (2006, 2008) described increase in TLR-2, TLR-3, TLR-6, TLR-7, and TLR-13 expression by astrocytes in infected brains but their role remains to be elucidated.

3.4. Nitric oxide

NO is a reactive gas which performs several essential functions in living organisms. Apart from its role in blood vessel dilatation, neurotransmission or penile erection, it carries out crucial functions in immune response to especially intracellular yet also extracellular pathogens that is to be emphasized here.

In vertebrates, NO is produced by NO-synthase (NOS) which converts L-arginine to L-citrulline and NO. Three isoforms encoded by separate genes are recognised: neuronal NOS (nNOS), endothelial NOS (eNOS) and inducible (iNOS). The first and the second are named according to their predominant tissue distribution where they are expressed constitutively being dependant on Ca^{2+} signalling. By contrast, iNOS expression is induced *ad hoc* in different cells by immunological stimuli in Ca^{2+}-independent manner (Stuehr 1999).

Production of NO by immune cells was initially studied in murine macrophages. They were shown to synthesise high levels of nitrites and nitrates in response to stimulation by IFN-gamma and LPS from *Escherichia coli* (Stuehr and Marletta 1985, 1987). At the same time, L-arginine was identified to be necessary for the reaction producing NO which undergoes oxidative degradation to nitrites and nitrates in aqueous solutions (Hibbs *et al*. 1987a, 1987b, Iyengar *et al*. 1987).

As early as in late 1980s, the macrophage cytotoxicity mediated by NO was also shown to kill tumour cells and schistosomula of *Schistosoma mansoni* (Esparza *et al*. 1987, James and Glaven 1989). However, prior to review of the role of NO in elimination of parasitic helminths, a brief summary of potential molecular mechanisms employed in the parasite destruction will be presented.

3.4.1. Nitric oxide reactivity

NO reactivity is determined by the unpaired electron present in the molecule; thus, technically, NO is sometimes regarded as the radical. It is even more reactive when combined with the superoxide

anion (O_2^-) to form peroxynitrite ($ONOO^-$) that is thought to be responsible for many reactions described below which were formerly ascribed to NO itself (Pacher *et al*. 2007). In cells, there are several molecular targets which NO or peroxynitrite (reactive nitrogen species, RNS) can react with.

Proteins represent the first group of molecules, which are at risk of RNS-caused damage; this has been studied especially in case of metabolic enzymes. RNS are able to react with transition metal centres (iron-sulphur or zinc-sulphur clusters) which constitute catalytic sites of the enzymes; this results in enzyme inactivation (Castro *et al*. 1994). The other deleterious effects of RNS to proteins are oxidation and/or nitration of amino acids. This happens mainly to thiol (–SH) groups of cysteine and hydroxyl (–OH) groups of tyrosine; the modification alters protein structure and function (Quijano *et al*. 1997, Wong *et al*. 2001). Furthermore, RNS interact with unsaturated fatty acids in membrane lipids which ends up in changes of membrane fluidity and permeability (O'Donnell *et al*. 1999). Finally yet importantly, nucleic acids are prone to modification by RNS, including base nitration or deamination; such DNA damage may trigger mutagenesis and strand breaks (Burney *et al*. 1999).

The above mentioned molecular mechanisms of RNS cytotoxicity have both direct and indirect effects on pathogen cell physiology and survival. Direct effects include mainly metabolic blockade and DNA mutagenesis that stops pathogen proliferation and cause its death. By contrast, in case of indirect effects, RNS influence host cells behaviour (e.g. initiation of cell apoptosis or autophagy, iron deprivation etc.) which subsequently abolishes the pathogen (Bogdan 2015). Considering the topic of this thesis, the role of nitric oxide in elimination of parasitic helminths will be in focus.

3.4.2. The role of nitric oxide in elimination of parasitic helminths

Although the role of NO is primarily studied in case of protozoan infections, several studies dealing with those caused by helminths are available too. They usually aim at indirect analysis of NO by means of (i) detection of iNOS, the main source of NO during the infection, or (ii) measurement of concentration of NO oxidation products (nitrates and nitrites). These data are put into the context of parasite burden and viability or features of the immune response (cytokine production, leukocyte proliferation etc.).

Although particular molecular mechanisms of how NO affects worms are mostly lacking, coherent idea about its role in control of the parasites exists in case of most studied infections such as schistosomiasis, echinococcosis, trichinellosis and filariasis.

3.4.2.1. Schistosomiasis

One of the earliest demonstrations of antiparasitic effects of NO at all was series of papers published in late 1980s. In 1985, McLaren and James (1985) described the detrimental effects of macrophage-mediated cytotoxicity on schistosomula of *S. mansoni*. The authors incubated schistosomula with peritoneal macrophages from *S. mansoni* infected mice and examined ultrastructure of schistosomula at different time points. One hour of incubation was enough to cause structural changes of subtegumental mitochondria and muscle cells being followed by progressive internal disintegration of schistosomula with increasing incubation time. Surprisingly, the tegument and tegumental outer membrane remained intact (McLaren and James 1985).

Similar results were obtained by Esparza *et al*. (1987); they incubated schistosomula with macrophages stimulated by IFN-gamma and TNF-alpha which induced schistosomula killing as well. The mechanism responsible for the *in vitro* schistosomulicidal effect was elucidated by James and Glaven (1989). They found that schistosomula killing is an arginine-dependent process which results in RNS-caused lethal metabolic inhibition that diminishes schistosomula viability.

In vivo experiments revealed that apart from macrophages, endothelial cells are capable of NO production and schistosomula killing (Oswald *et al*. 1994). Even more, if iNOS activity was inhibited, parasite burden increased (Wynn *et al*. 1994). This strengthened the hypothesis about of the crucial role of NO in parasite control.

However, next experiments pointed out that (i) iNOS inhibiton does not necessarily decrease parasite burden significantly and (ii) only young schistosomula dwelling in lungs are prone to NO toxicity. Thus, it was hypothesised that mitochondrial enzymes involved in aerobic respiration are targets of NO-caused damage (Ahmed *et al*. 1997, Coulson *et al*. 1998).

To make the information complete, the influence of NO on other schistosome life stages has to be mentioned. Except of schistosomula, experiments dealing with NO synthesis have been performed with sporocysts and adults. Considering the first, haemocytes from resistant strains of *Biomphalaria glabrata*, the intermediate host of *S. mansoni*, were reported to exhibit anti-sporocyst behaviour utilizing NO production (Hahn *et al*. 2001). The reaction is provoked by sporocyst E/S products (Zahoor *et al*. 2009). In case of adult worms, data are limited and restricted just to testing soluble adult antigens in eliciting NO production (de Oliveira *et al*. 1998). NO also contributes to granuloma formation around schistosome eggs deposited in the liver (Hirata *et al*. 2001).

3.4.2.2. Echinococcosis

In intermediate hosts (e.g. humans or rodents), echinococcosis represents a chronic infection accompanied by severe pathology. Thus, the host immune response, including NO production, which could stop parasite growth, has been explored.

The early observation of arginine-dependent cytotoxicity of macrophages against parasite's protoscoleces, suggesting NO involvement, was made by Kanazawa *et al*. (1993). The antiparasitic NO production was shown to be IFN-gamma dependent (Amri *et al*. 2007) and NO with peroxynitrite were identified as effector molecules causing parasite damage (Zeghir-Bouteldja *et al*. 2009). However, some components of parasite cysts were able to attenuate NO production by macrophages both *in vitro* and *in vivo*, which suggests the parasite capacity to modulate the injurious immune response (Steers *et al*. 2001, Andrade *et al*. 2004).

Nonetheless, NO action is not potentially deleterious to only the parasite but it impairs host's immune arms as well. Dai *et al*. (1999, 2003) demonstrated *in vitro* that exposure of splenocytes to NO produced during chronic infection by macrophages reduces their proliferation which evokes the state of immunosuppression.

3.4.2.3. Trichinellosis

If speaking about trichinellosis, two phases of infection, the intestinal and the muscular, have to be distinguished. Considering the first one, elevated level of NO in intestinal epithelia was not noted in humans despite the inflammatory reaction evolved (Li *et al*. 1998). In mice, NO was produced during the intestinal phase by epithelial cells. However, it did not accelerate the parasite expulsion (Lawrence *et al*. 2000). NO concentration is likely not high enough to promote antiparasitic effects which may be caused by expression of iNOS inhibitors by the parasite (Bian *et al*. 2001, 2005); however, particular molecules have not been described yet.

During the second phase of the infection, young larvae migrate from the intestine to skeletal muscles. This is accompanied by increased nitrite concentration in serum which suggests increased NO synthesis. For example, peritoneal macrophages isolated from infected mice were shown to upregulate NO production (Wandurska-Nowak and Wiśniewska 2002). Such host reaction may be harmful to growing, migrating larvae which are, contrary to older larvae, susceptible to killing by NO (Gebreselassie *et al*. 2012).

Although older larvae located in muscles are surrounded by cells expressing iNOS (Boczoń *et al*. 2004), NO does not seem to have protective function for host since its exogenous administration increased the intensity of the infection *via* unidentified manner (Wandurska-Nowak *et al*. 2003). Because the treatment with iNOS inhibitors curtails the infection (Kołodziej-Sobocińska *et al*. 2006),

it can be hypothesised that systemic increase in NO observed during the infection (Wandurska-Nowak and Wiśniewska 2002) supress the immune response in a manner analogous to that in case of echinococcosis (see above).

3.4.2.4. Filariasis

Infections caused by filarial worms represent a quite well studied field in terms of the role NO in parasite control. A few studies were done with *Onchocerca* spp. (causative agent of river blindness), and more data are available for *Brugia* spp. (lymphatic filariasis). As the results seem to be complementary, they will be reviewed as a whole.

The necessity of NO for infection control was reported by Rajan *et al*. (1996). The authors observed that inhibition of iNOS leads to development of infection in otherwise resistant hosts and, *vice versa*, NO releasing drugs make hosts, naturally sensitive to the infection, free of parasites. In the contrary, Gray and Lawrence (2002) suggested that another, IFN-gamma/NO-independent mechanism may participate in parasite clearance because they reported decrease in parasite burden even after iNOS inhibition and IFN-gamma neutralisation.

Nevertheless, the role of NO in parasite elimination cannot be excluded. For example, it was demonstrated that NO-mediated toxicity leads to impairment of microfilarial motility and viability, even death was observed (Taylor *et al*. 1996). Similarly to schistosomes, alterations in hypodermal mitochondria ultrastructure (organelle vacuolisation, decline of cristae) were noted after NO treatment suggesting metabolic disruption (Thomas *et al*. 1997).

In addition, high levels of nitrates and nitrites were found in the sera of patients who underwent anti-filarial therapy (Winkler *et al*. 1998) and NO was shown to be necessary for effective treatment of infection with routinely used diethylcarbamazine (McGarry *et al*. 2005). These data advocate for NO participation in parasite elimination, even though NO-triggered immunosuppression was noted too (O'Connor *et al*. 2000, O'Connor and Devaney 2002).

Several studies have also identified molecules which might be responsible for stimulation of NO production. These are mainly proteins of parasite origin, such as cystatins (cysteine proteases inhibitors), or tropomyosin and calponin (proteins of muscle tissue) (Hartmann *et al*. 2002, Verma *et al*. 2015). However, antigens of *Wolbachia* sp., endosymbiotic bacteria of filariae, may also be potent stimuli eliciting inflammatory reaction, including NO release (Taylor *et al*. 2000).

4. MATERIAL AND METHODS

4.1. Buffers, media, solutions

Phosphate-buffered saline (PBS)

PBS was used as a basic buffer in many experiments as washing or dissolving agent. To prepare 0.1 M PBS, two solutions (0.2 M Na_2HPO_4 and 0.2 M NaH_2PO_4) were mixed in a defined ratio depending on the final pH required, see Table 4.1. After that, the same volume of distilled water and NaCl to final concentration 120 mM were added. The buffer was mixed well and the pH was checked using a laboratory pH meter (inoLab, WTW).

Table 4.1. Solution ratios used for preparation of PBS of different pH. Adjusted to the volume of 500 ml (resulting in 1 litre of 0.1 M PBS), pH measured at room temperature (RT).

Required pH	Volume of 0.2 M Na_2HPO_4	Volume of 0.2 M NaH_2PO_4
7.2	360 ml	140 ml
7.4	405 ml	95 ml
8.0	465 ml	35 ml

Tris-buffered saline (TBS)

TBS was used for sample washing during *in situ* schistosomula staining (see 9.1.2.). Its composition was 50 mM Trizma® base (Sigma-Aldrich) and 150 mM NaCl (Sigma-Aldrich) in dH_2O. pH was set to 7.2 with 1 M HCl.

Lysis buffer

This was used for preparation of lysates of astrocytes and microglia intended for western blot analysis. The composition was:

- 125 mM Trizma® base (Sigma-Aldrich), pH set to 6.8 with 1 M HCl,
- 2% (v/v) sodium dodecyl sulphate (Sigma-Aldrich),
- 1% (v/v) 2-mercaptoethanol (Sigma-Aldrich),
- 5% (v/v) glycerol (Penta).

Medium for glial cell cultivation (MG)

MG was used for *in vitro* cultivation of astrocytes and microglia and cercariae after mechanical transformation. It consisted of:

- Roswell Park Memorial Institute medium (RPMI) 1640 without L-glutamine with phenol red (Lonza); for experiments where the concentration of nitric oxide was

assessed, RPMI 1640 without phenol red was used so that its colour does not interfere with the analysis,

- 10% (v/v) foetal calf serum (Labtech), inactivated before use at 56 °C for 30 minutes,
- 1% (v/v) L-glutamine (Lonza), final concentration 2 mM,
- 1% (v/v) penicillin-streptomycin (Lonza), final concentration 100 U/ml, 100 mg/ml.

Aliquots of all components were mixed and filtered using Nalgene™ Rapid-Flow™ Sterile Disposable Filter Units with PES Membrane (Thermo Scientific). Medium was stored at 4 °C and always handled under sterile conditions.

Anaesthetic cocktail

The mixture for deep mouse anaesthesia was prepared under sterile conditions in 1 ml insulin syringe in this composition:

- sterile normal saline (Mayrhofer Pharmazeutika),
- 10% (v/v) Rometar (Bioveta), final concentration of xylazine: 2 mg/ml,
- 20% (v/v) Narketan (Vétoquinol), final concentration of ketamine: 20 mg/ml.

The cocktail was mixed well and 250–300 µl (depending on the size of the animal) were injected into the peritoneum of the mouse.

4.2. Model organisms

4.2.1. *Trichobilharzia regenti*

The life cycle of *T. regenti* is maintained in the Laboratory of Helminthology (Charles University in Prague, Department of Parasitology) using *Radix lagotis* and *Anas platyrhynchos* f. *domestica* as intermediate and definitive hosts, respectively. Cercariae were the life stage used in experiments and were collected as follows.

Snails infected with *T. regenti* in patent period were put into the beaker with dechlorinated tap water and exposed to artificial light (Olympus KL 1500 LCD, 3000 K) for 40–60 minutes; this provoked shedding of cercariae. The water with cercariae was poured to a flask wrapped in aluminium foil nearly up to the neck. The flask was filled up and its neck was illuminated from a side. Positively phototactic cercariae were continuously rising up to the water surface. There they were collected by Pasteur pipette and moved into the 50 ml conical centrifuge tube placed on ice; the flask was refilled after each collection.

Cercariae were left on ice until they fell onto the bottom of the tube. Then, approximately ¾ of volume of water were poured off, the rest was agitated and cercariae were counted. The

calculation was performed as summation of cercariae in twenty 50 µl samples and extrapolation of this result to the total volume of water with cercariae in the tube.

4.2.2. Accidental hosts

Inbred mice of C57BL/6 strain (AnLab) served as accidental hosts. They were bred in the Centre for experimental biomodels (Charles University in Prague, 1st Faculty of Medicine) and their pups were used for glial cell cultures establishment (see 4.3.1.). To obtain *ex vivo* schistosomula for stimulation experiments, adults of inbred C57BL/6 and outbred ICR mice (8–12-week-old males) were infected as described below (see 4.3.2.). For *in vivo* experiments dealing with MHC II expression, C57BL/6 MHC II-EGFP knock-in mice (8-week-old females) generously gifted by Dr. Jan Černý (Charles University in Prague, Department of Cell biology) were used.

All experiments were accomplished in accordance with animal welfare laws of Czech Republic and were approved by the Animal welfare committee of Charles University in Prague, Faculty of Science (project ID: MSMT-31114/2013-9). Author of this thesis is authorised to design and perform the experiments with animals (certificate number CZ 02542).

4.3. *In vitro* experiments: stimulation assays

Stimulation experiments were carried out to elucidate the response of glial cells (astrocytes and microglia) to antigens of *T. regenti*. After glial cell cultures were established (see 4.3.1.), the cells were stimulated by different antigens for 48 hours (see 4.3.2. and 4.3.3.). It was followed by measurement of nitric oxide (see 4.3.4.) and proinflammatory cytokines (see 4.3.5.) concentrations. To evaluate the iNOS expression, western blot was employed to detect the enzyme in lysates of both astrocytes and microglia (see 4.3.6.). Cell culture purity was examined by immunocytochemistry (ICC) (see 4.3.7.). Morphology of the cells was observed by the scanning electron microscope (SEM, see 4.3.8.). The scheme of stimulation experiments is presented in Figure 4.1.

Figure 4.1. The scheme of stimulation experiments.

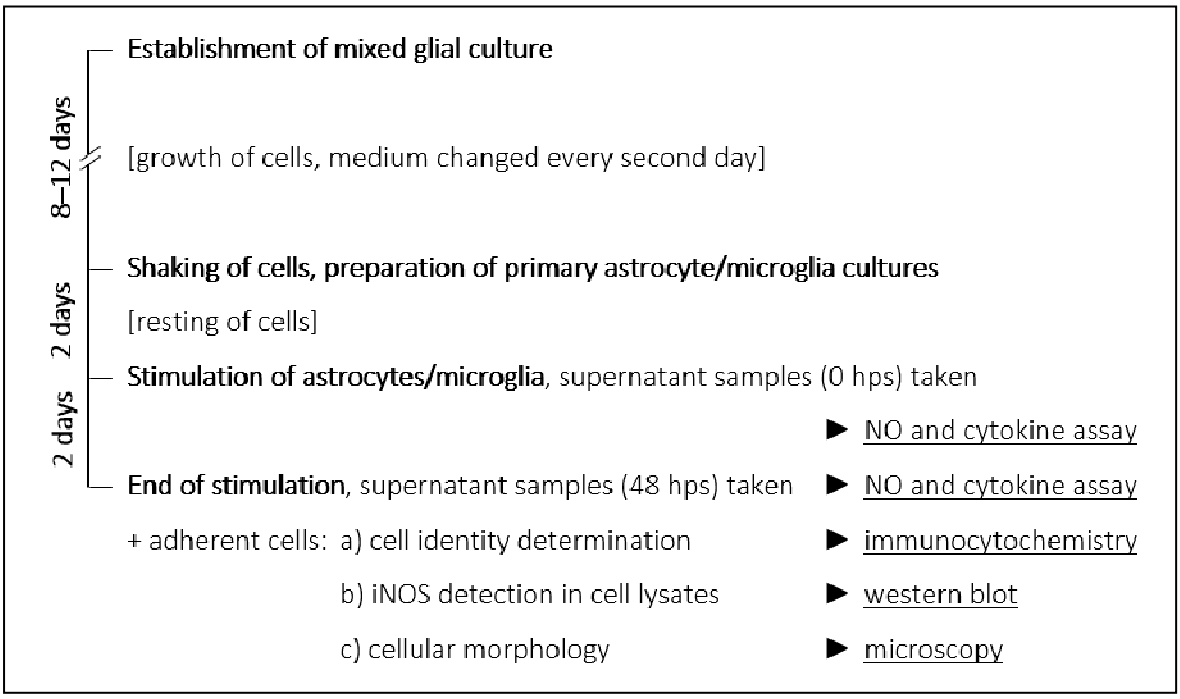

4.3.1. Obtaining glial cells

4.3.1.1. Mixed glial cultures

Mice pups of C57BL/6 strain not older than 48 hours were used for establishment of mixed glial cell cultures according to modified protocol by Giulian and Baker (1986) and McCarthy and de Vellis (1980). After decapitation of a pup, the head was disinfected in 70% ethanol for 3–5 seconds and placed in a sterile Petri dish with MG.

A brain was dissected out of a cranium. Meninges and visible vessels were removed carefully. After that, the brain was moved to the other Petri dish with MG where it was cut into pieces. Remnants of meninges were disposed of if present. The tissue was homogenized mechanically by pipetting up and down in a 10 ml pipette. The cell suspension of two brains was placed into a 75 cm^2 tissue culture flask (Sigma-Aldrich) coated by 5 µg/ml poly-L-lysine (PLL, Sigma-Aldrich) (coating at least for 2 hours at 37 °C, washed twice with sterile PBS before use). Tissue cultures were put into the incubator (37 °C, 5% CO_2 if not stated otherwise), medium was changed on the next day and then every second day.

During the cultivation, cells were checked for bacterial or fungal contamination and the culture appearance was monitored; for both the inverted microscope equipped with a phase contrast was used (Olympus IX50). Approximately 1–2 days after cells reached confluence, the flasks were placed in an orbital shaker (Lab-Line MaxQ™ 4000) and shaken 6–8 hours at 200 revolutions per minute (rpm) at 37 °C. Afterwards, primary microglia and/or astrocytes cultures were obtained as follows.

4.3.1.2. Primary microglia cultures.

To obtain microglia, supernatants from flasks (after shaking) were gathered in sterile 50 ml centrifugation tubes and centrifuged (Schoeller, Universal 320R) at 300 *g* and 4 °C for 1 min per millilitre of suspension volume in one tube. Cell pellet was then resuspended in MG and cells were counted as follows. Ten microliters of cell suspension were mixed with 10 µl of trypan blue, put onto a special slide and inserted into Countess™ Automated Cell Counter (Invitrogen) with this setting: cell size 8–13 µm, sensitivity 5, roundness 80. Apart from counting the cells, the counter also performed trypan blue exclusion assay to assess cell viability. Analysis of cells was done in a duplicate and the average was taken as a result.

Cells were seeded in cell culture treated 12- or 6-well plates (Nunc) at densities of 2.0×10^5 or 1.2×10^6 cells/well, respectively. If cells were intended for immunocytochemistry or SEM examination, there were PLL-coated (see above) coverslips (15×15 mm) in the wells where cells were seeded. Plates were placed into the incubator for 10 minutes to let microglia adhere. Cells were then washed 3 times with MG (37 °C) and put back into the incubator for 48 hours to settle down before stimulation.

4.3.1.3. Primary astrocyte cultures

After shaking and processing the supernatant, culture flasks with astrocyte monolayer were washed twice with sterile PBS and 2 ml of trypsin-EDTA (Sigma-Aldrich) were added. Flasks were put into the incubator for 8–12 minutes until astrocytes detached. Trypsinisation was stopped by adding 2 ml of MG and the cell suspension was centrifuged at 300 *g* and 4 °C for 1 min per millilitre of suspension volume. Following centrifugation, the pellet was resuspended in MG and the cells were counted as described above (only the cell size was set to 8–20 µm).

After that, astrocytes were seeded in 12- or 6-well plates (Nunc) at densities of 2.0×10^5 or 1.2×10^6 cells/well, respectively. For SEM observation, astrocytes were seeded at density 0.5×10^5 cells/well. If cells were intended for immunocytochemistry or SEM examination, there were PLL-coated (see above) coverslips (15×15 mm) in the wells where cells were seeded. Prior to stimulation, astrocytes were let to calm down for 48 hours in the incubator.

4.3.2. Antigen preparation

Several antigens of *T. regenti* origin were used as stimuli for astrocytes and microglia: *ex vivo* isolated schistosomula, homogenate of transformed cercariae and *T. regenti* recombinant cathepsins 1.1 and 2. They were prepared according to following protocols.

Ex vivo isolated schistosomula. Healthy mouse was put into the high, narrow beaker with 1–2 cm of water (RT) in order to defecate and urinate. After an hour, the dirty water was discarded and water with 3.000 cercariae was added. Exposure of the mouse to cercariae lasted 60 minutes and was performed in the dark. Five days *post* infection (DPI), the mouse was sacrificed by cervical dislocation and the spinal cord was dissected out. Extracted nervous tissue was cut into pieces and torn by forceps in a Petri dish. After 30–60-minute exposure to artificial light, it was examined under a stereomicroscope for presence of schistosomula. Parasites were collected and washed three times in MG before being used as a stimulant.

Homogenate of transformed cercariae, according to Chanová *et al*. (2009), the protocol modified. Cercariae were collected as described above (4.2.1.) and passed through a 23G-syringe needle (0.6 mm in diameter) at least 20 times. After that, they were moved into a sterile Petri dish where MG was added. Whirling the dish, cercariae concentrated in the middle and MG was changed; cercariae were washed two more times by this way. Subsequently, they were put into the incubator and cultivated in MG for three days. These *in vitro* transformed cercariae ("schistosomula-like stages") were rinsed in MG three times. MG in the last wash was supplemented by cOmplete Mini protease inhibitors (one tablet per 10 ml MG; Roche). After that, the transformed cercariae were homogenised by sonicator (3×30 seconds, amplitude 60 W, cooled on ice; Vibra Cell). To remove debris, the suspension was centrifuged (Eppendorf, 5804R) 2×10 minutes at 16.000 *g*. The protein concentration in supernatant was determined by Quant-iT™ Protein Assay Kit (Invitrogen) following the manufacturer's instructions. Samples were measured in a triplicate, the average being taken as a result. Supernatants were stored in –80 °C until used.

Recombinant cathepsins. Lyophilised samples of purified *T. regenti* recombinant cathepsins B1.1 and B2 expressed in *Pichia pastoris* (kindly provided by Mgr. Hana Dvořáková, Charles University in Prague, Department of Parasitology) were rehydrated to sterile PBS and filtered by Amicon Ultra Centrifugal Filters (Merck Millipore) for 10 minutes at 14.000 *g* (4 °C). After that, the filtration unit was refilled with sterile PBS and centrifuged again; the same was then repeated one more time while the filtrate was discarded after each centrifugation. Finally, the concentrated protein dissolved in the residue of sterile PBS was collected by reverting the filtration unit and spinning for 10 minutes at 1.000 *g* (4 °C). The concentration of protein was measured in the same way as in case of homogenate (see above) and the samples were stored in –80 °C until used.

4.3.3. Cell stimulation

Astrocytes and microglia stimulation was conducted under sterile conditions in a laminar flow hood (ESCO). At the beginning, MG itself (as a negative control) or supplemented by different stimulants (see Table 4.2.) was added to the cells.

Table 4.2. Antigens used for glial cell stimulation.

Stimulant	Final concentration in MG
Lipopolysaccharide (Sigma-Aldrich), positive control	0.5 μg/ml
Ex vivo isolated schistosomula	1 schistosomulum/well
Homogenate of transformed cercariae (hom.)	50 μg/ml
T. regenti recombinant cathepsin 1.1	1 μg/ml
T. regenti recombinant cathepsin 2	1 μg/ml

The plate was gently shaken and supernatant aliquots were taken for NO and/or cytokine concentration analysis (0 hour *post* stimulation, hps). Plates with cells were then moved to the incubator and left there for 48 hours. After this time (48 hps), supernatant aliquots were taken for NO and/or cytokine concentration analysis. Cell morphology was examined under the inverted microscope with a phase contrast. Some samples were alternatively prepared for observation under the scanning electron microscope. Cells from 6-well plates were utilised for western blot detection of iNOS, those from 12-well plates (if intended) underwent immunocytochemical processing.

4.3.4. Measurement of nitric oxide production

Nitric oxide production was assessed by indirect measurement of nitrite (a stable breakdown product of NO) concentration by the Griess assay. It is based on a reaction of nitrite from examined sample with sulphanilamide which results in forming of diazonium salt. After adding the azo dye agent (N-α-naphthyl-ethylenediamine), a pink colour develops.

In order to measure the nitrite concentration, 100 μl of cell supernatant were mixed with the same volume of solution A (58 mM sulphanilamide [Sigma-Aldrich] in 2.5% H_3PO_4/dH_2O) and incubated for 10 minutes. Subsequently, 100 μl of solution B (12 mM N-α-naphthyl-ethylenediamine [Sigma-Aldrich] in 2.5% H_3PO_4/dH_2O) were added and incubated for 10 minutes in the dark. The absorbance was then measured by a microplate reader (Tecan Infinite M200) at 550 nm.

Ten milimolar $NaNO_2$/dH_2O was used as a working solution from which a calibration curve comprising of 100, 50, 25, 12.5, 6.25, and 3.125 μM standards (two-fold serial dilution) was obtained. Standards were prepared in a duplicate for each analysis; they were mixed with solutions A and B in the same manner as samples and concurrently with them. Griess assay was performed in a 96-well plate (Nunc) suitable for measuring of absorbance.

4.3.5. Measurement of cytokine production

Concentration of selected proinflammatory cytokines (IL-1 beta, IL-6, and TNF-alpha) was measured in glial cell supernatants using indirect "sandwich" enzyme-linked immunosorbent assay (ELISA).

Concentration of the cytokines was analysed in supernatants from cells cultivated in 12-well plates using ELISA MAX™ standard sets (BioLegend). One day before running ELISA, 96-well plate (Nunc) suitable for this assay was coated by the capture antibody diluted 1:200 in a coating buffer (100 mM $NaHCO_3$ and 33.5 mM Na_2CO_3 in dH_2O, pH 9.5). The plate was sealed and incubated overnight in 4 °C in a humidified chamber.

Next day, the plate was washed 4 times with 0.05% Tween 20 (Bio-Rad) in PBS (PBS-Tw) and blocked by 1% bovine serum albumin (BSA, Sigma-Aldrich) in PBS for 1 hour being shaken. After washing the plate 4 times with 0.05% PBS-Tw, sample (undiluted supernatant) was added and incubated for 2 hours in a sealed plate being shaken. Afterwards, the plate was washed 4 times with 0.05% PBS-Tw and the detection antibody diluted 1:200 in 1% BSA/PBS was added for 1 hour being shaken. Avidin-horseradish peroxidase (HRP) diluted 1:1000 in 1% BSA/PBS was then added for 30 minutes and subsequently, the plate was washed 5 times (each for 1 minute) with 0.05% PBS-Tw. The reaction was visualised by adding 3,3',5,5'-tetramethylbenzidine (TMB) Liquid Substrate System for ELISA (Sigma-Aldrich). This incubation was performed in the dark and was stopped by pipetting of equal volume of 1 M H_2SO_4 when TMB substrate turned blue (usually in 5–10 minutes). The absorbance of samples was immediately measured at 450 nm by a microplate reader (Tecan Infinite M200).

To assess the concentration of cytokines in samples, a calibration curve from recombinant cytokines dissolved in 1% BSA/PBS was constructed. Standards for each cytokine were prepared in two-fold serial dilution in these ranges: 2,000–31.25 pg/ml for IL-1 beta and 500–7.8 pg/ml for IL-6 and TNF-alpha. Standards were run within a triplicate in each analysis and handled in the same manner as samples and concurrently with them.

Controls of unspecific direct binding of avidin/HRP to either capture antibody or blocking agent were done. In blank samples, stock solution of MG only was added, detection antibody and avidin-HRP being omitted. Blank was run in a duplicate and the average of its absorbance was subtracted from absorbance of all other samples and standards before calculating the final concentration.

4.3.6. iNOS detection by western blot

To detect the presence of iNOS in the cells, both astrocytes and microglia seeded in 6-well plates were washed twice with PBS and lysed by 100 µl of lysis buffer per well. Following the cell lysis, the samples were boiled for 5 minutes and sonicated (Vibra Cell).

The protein separation was performed by sodium dodecyl sulfate polyacrylamide gel electrophoresis (SDS-PAGE) in 7% gel (1 mm) under reducing conditions. Thirty micrograms of total protein (measured by Quant-iT™ Protein Assay Kit, Invitrogen) were loaded into each well. The constant voltage was set to 100 V (PowerPack Universal™, Bio-Rad) and the separation was carried out in Tris/Glycin/SDS Buffer (Bio-Rad) in Mini-Protean® 3 Cell (Bio-Rad). Precision Plus Protein Dual Xtra Standards (Bio-Rad) were used within each separation to calculate the molar weight of bands.

After separation, proteins in the gel were either stained by Coomassie Brilliant Blue R-250 (Serva Electrophoresis) or transferred onto Immun-Blot® polyvinylidene difluoride (PVDF) membrane (Bio-Rad) by Trans-Blot Turbo Transfer system (Bio-Rad). The transfer was performed in semi-dry conditions using blotting buffer consisting of 10% (v/v) 10× Tris/Glycine/SDS Buffer (BioRad) and 10% (v/v) methanol in dH_2O. The transfer time was 20 minutes at the constant current set to 1.3 A. To check the transfer quality, the PVDF membrane was reversibly stained by 0.5% Ponceau S (Sigma-Aldrich) in 1% acetic acid/dH_2O. Next, the membrane was processed as whole or cut in 5 mm vertical stripes representing sample lines. In order to prevent non-specific background signal, the membrane was blocked 2 hours in 5% (w/v) non-fat dry milk (Bio-Rad) being shaken all the time. Following three washes with PBS, mouse monoclonal anti-nitric oxide synthase antibody (Sigma-Aldrich) diluted 1:1000 in PBS was added. The incubation was carried out overnight at 4 °C.

Next day, the membrane was washed three times with PBS and incubated with monoclonal anti-mouse IgG (Fc specific)–peroxidase antibody produced in goat (Sigma-Aldrich) diluted 1:2000 in PBS for 2 hours (RT) being shaken. Prior to detection, the membrane was 3× 5 minutes washed with PBS. Opti-4CN™ Substrate Kit (Bio-Rad) was utilised for detection of bound antibodies according to manufacturer's instructions. Developed membranes were scanned by GS-800 Calibrated Densitometer (Bio-Rad).

4.3.7. Immunocytochemistry

To verify the identity of cells used in stimulation experiments, ICC was performed. Microglia and astrocytes were targeted by primary antibodies against Iba1 and GFAP, respectively, and visualised by secondary antibodies with conjugated fluorophores. All the antibodies used and their working dilutions are listed in Table 4.3. The cell culture purity was calculated as a ratio of Iba1/GFAP positive cells to all cells.

Table 4.3. Antibodies used in immunocytochemistry assays and their working concentrations.

Target	Primary antibody	Dilution	Secondary antibody	Dilution
Microglia	Polyclonal rabbit anti-mouse Iba1 (Wako)	1:1000 in 10% NGS/PBS	Goat anti-rabbit Alexa Fluor® 488 (Invitrogen)	1:2000 in PBS
Astrocytes	Polyclonal rabbit anti-GFAP (Dako)	1:2000 in 10% NGS/PBS	Goat anti-rabbit Alexa Fluor® 568 (Invitrogen)	1:2000 in PBS

First, remaining MG was removed and the cells were rinsed quickly with PBS and fixed in freshly prepared 4% paraformaldehyde (Fluka)/PBS (pH 7.4) for 20 minutes. Then they were washed 3 times in PBS and incubated in 0.1% Triton X-100 (Sigma-Aldrich)/PBS for 5 minutes to permeabilize cell membranes. Following permeabilization, the cells were washed 3× 5 minutes in PBS and incubated in 10% normal goat serum (NGS) for 30 minutes to block unspecific binding of antibodies. Afterwards, the cells were incubated with the primary antibody against Iba1 or GFAP overnight at 4 °C in a humidified chamber. To check a non-specific binding of secondary antibodies, negative rabbit serum (Dako) was used instead of the primary antibody as a negative control.

Next day, the cells were rinsed 3× 5 minutes with PBS and incubated with a secondary antibody for 60 minutes in the dark (RT). Finally, the cells were rinsed with PBS and mounted in VectaShield® Mounting Medium with DAPI (Vector Labs). The slides were examined under a fluorescence microscope (Olympus BX51) using proper excitation/emission filters. Photos were taken by Olympus U-TV1 X camera and processed by QuickPHOTO MICRO 2.3 and GIMP 2.8.

4.3.8. Scanning electron microscopy

Morphology of microglia was observed under the scanning electron microscope. The cells grown on cover slips were washed in PBS and immediately immersed into 2.5% glutaraldehyde/PBS for overnight fixation at 4 °C. Next day, the samples were washed 3 times (each for 5 minutes) in PBS and post-fixed in OsO_4 for 1 hour (RT). After that, cells were washed in PBS again and dehydrated in ascending ethanol series: 30%, 50%, 70%, 80%, 96%, 3 times 100% ethanol (5 minutes left in each). Three baths in 100% acetone (5 minutes each) followed and the dehydration was completed by critical point drying method (Bal-Tec CPD 030).

Finally, samples were mounted onto the stubs with double-sided carbon tape, coated with gold in sputter coater (Bal-Tec SCD 050) and observed under the scanning electron microscope JEOL 6380 LV. Sample preparation was performed with technical assistance of Dr. Jana Bulantová (Charles University in Prague, Department of Parasitology).

4.4. *In vivo* experiments

In these experiments, C57BL/6 MHC II-EGFP knock-in mice (see 4.2.2.) were infected by cercariae of *T. regenti* which had been stained prior to the infection (see 4.4.1.). Five days *post* infection, mice were sacrificed and perfused (see 4.4.2.). The spinal cord was used for either preparing squashed-tissue samples or the ultramicroscopical examination (see 4.4.3.). Worms present in the spinal cord were counted and the distribution of MHC II+ cells tagged by EGFP in the proximity of parasite was evaluated.

4.4.1. Staining of cercariae

In order to detect schistosomula migrating through the spinal cord, it was necessary to label them with red fluorescent signal as a counterstaining to a possible green MHC II signal. Several red stains were tested, the only one working was seminaphthorhodafluor (SNARF)-1 carboxylic acid, acetate, succinimidyl ester (Invitrogen, see below). Other stains and methods which were utilised are presented in Supplement 1.

SNARF-1 stock solution was made by dissolving it in dimethyl sulfoxide to reach 5 mM concentration. Two microlitres of this stock solution were mixed with 498 µl of dechlorinated water. Afterwards, 500 µl of water with cercariae concentrated to the density 1000 cercariae per millilitre were added. The microtube was placed into the dark being incubated for 60 minutes (RT). Viability of cercariae and the quality of the staining were then checked under a fluorescence microscope. Labelled cercariae were immediately used for infection of mice; this was done in the same manner as described above (see 4.3.2., *ex vivo* isolated schistosomula). The mouse was sacrificed and the spinal cord examined 3 DPI; an uninfected mouse was taken as a negative control.

4.4.2. Transcardial perfusion of mice and spinal cord processing

The mouse was injected intraperitoneally with 250–300 µl of the anaesthetic cocktail. Thoracic cavity of properly anesthetized mouse was opened and 25G needle connected via tubing to syringe with heparin (10 U/ml, Zentiva)/PBS (pH 7.4) heated to 37 °C was inserted into the posterior end of the left ventricle and the right atrium was cut by scissors. Bloodstream was being perfused until only pure solution flowed from the atrium; usually 30 ml of heparin/PBS was needed. The effectivity of the perfusion was confirmed by the liver decolourisation. The spinal cord was then dissected out carefully and cut to 0.5–0.7 cm long pieces. Squashed-tissue samples were prepared from them and examined under the fluorescence microscope.

If the mouse was intended for the ultramicroscopic examination, it was perfused with freshly prepared 30 ml ice-cold 4% paraformaldehyde/PBS (pH 7.4) after the heparin/PBS perfusion and

post-fixed in it overnight at 4 °C. Next day, the spinal cord was washed in PBS (pH 8.0) and sent for ultramicroscopic examination.

4.4.3. Ultramicroscopic examination

Ultramicroscopy is a technique allowing optical sectioning and subsequent reconstruction of even macroscopic objects like mouse brain or embryos in µm resolution (Dodt *et al*. 2007). It is based on illumination of a translucent specimen by two opposite light sheets of defined wavelength. This causes the excitation of fluorophores in the specimen. Fluorescent signal is emitted and registered by a detector. Optical sections are successively made through the whole specimen placed in a movable glass chamber. All sections are then composed using a graphical software and a 3D reconstruction is created (Jährling *et al*. 2008). A simplified scheme of the ultramicroscope is illustrated in Figure 4.2.

Ultramicroscopic examination of spinal cord samples was performed by Dr. Christian Hahn (Vienna University of Technology, Department of Bioelectronics) in January 2014 according to protocols published by their group (Becker *et al*. 2012, Ertürk *et al*. 2012).

Figure 4.2. The scheme of the ultramicroscope. A transparent sample placed in a chamber is illuminated by thin sheets of light. This causes a fluorescence emission in the excited plane. The emitted light is projected to a camera by an objective. Optical sections are successively made through the whole specimen placed in the chamber which is moved by a stepping motor. Single images are then merged and 3D reconstruction is done by software. Adapted from Jährling *et al*. (2009).

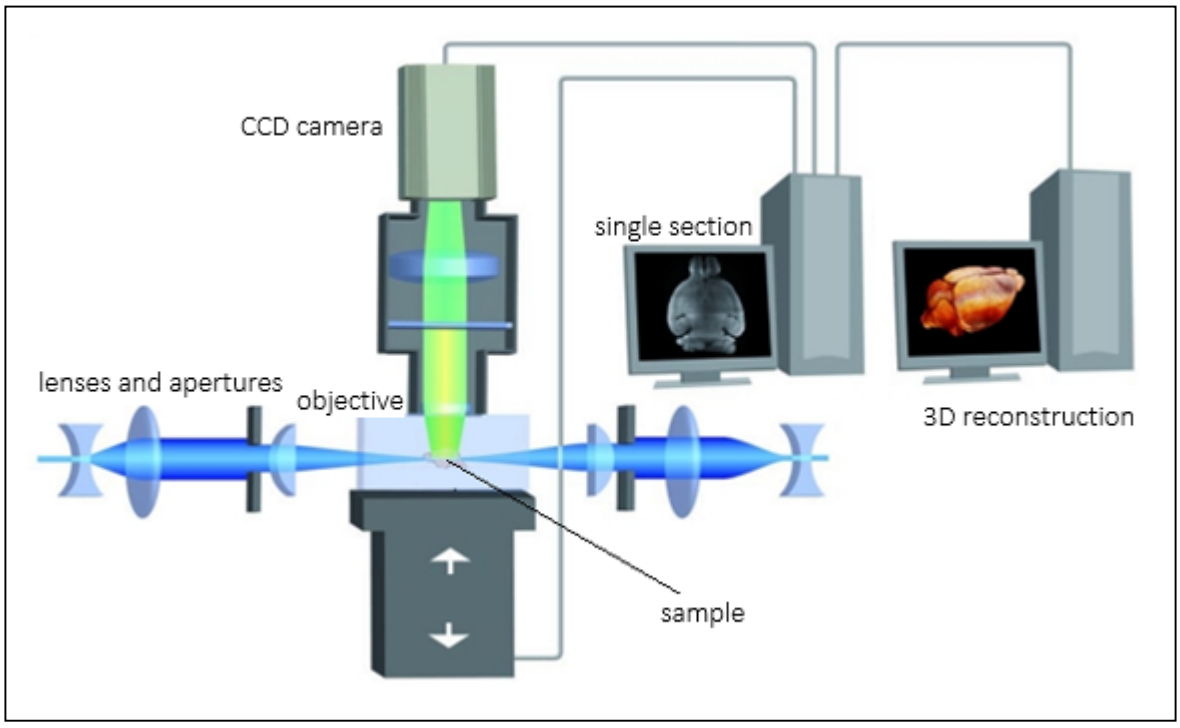

4.5. Statistical analysis

Statistical analysis with R 3.1.3 software was performed to assess the significance of differences in NO and cytokine production by astrocytes and microglia in stimulation experiments. At first, non-transformed data were tested for normality by Shapiro–Wilk test. The difference of NO and cytokine concentrations within the group and between the groups were determined by Wilcoxon signed rank test and Wilcoxon rank sum test, respectively. A value of $p < 0.05$ was used to identify statistically significant differences.

5. RESULTS

5.1. Glial cell cultures establishment

Mixed glial cell cultures were established from mechanically dissociated brains of newborn murine pups. In total, 15 successful cultivations utilizing 198 pups were performed. During first days of the cultivation, a lot of cellular debris was present in the culture among which round cells were located (Fig 5.1A). Sometimes slight bacterial contamination occurred but it deceased in 2–3 days; if not, the flask was discarded. After 2–3 days *in vitro* (DIV), round cells were still present and those with elongated or spindle-like morphology appeared as well (Fig. 5.1B). The debris was still visible but to a lesser extent. In the next 3–4 days (5–7 DIV), the round cells disappeared while the bottom of the flask started to get covered by a monolayer of flattened cells (Fig. 5.1C). Ramified cells occupied free spaces on the bottom or grew on the surface of the flattened ones; the debris was found only sparsely. The lower monolayer reached confluence commonly after 8–9 DIV, when ramified cells were scattered on it (Fig. 5.1D).

Figure 5.1. Appearance of mixed glial cells cultures at different time points. (A) 1 DIV, (B) 3 DIV, (C) 6 DIV, (D) 8 DIV. Detailed description is provided in the text above. Scale bars 25 μm.

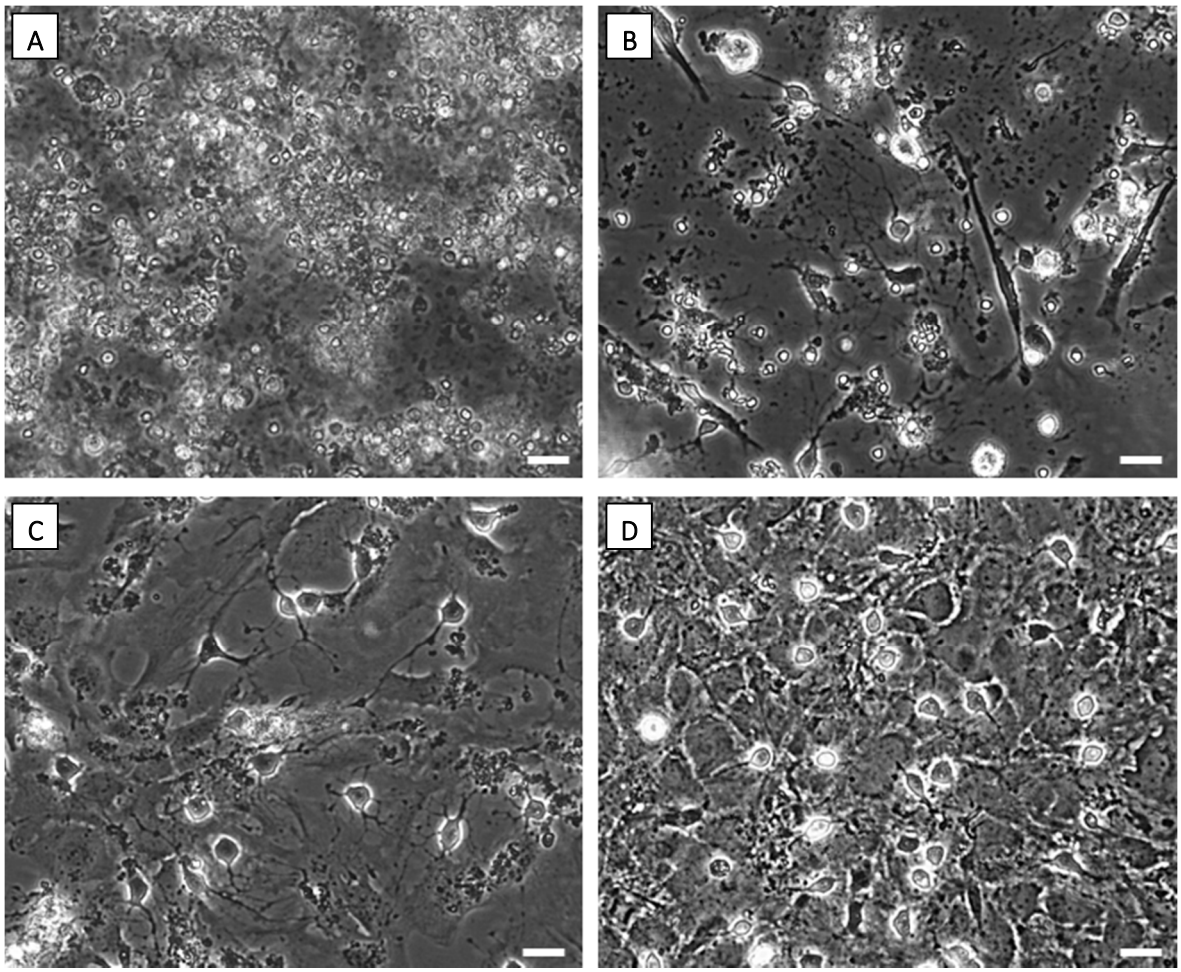

From mixed glial cell cultures, primary astrocyte and microglia cultures were obtained. If counted and adjusted to one murine brain used for cell culture establishment, the yield of live astrocytes was 8.7-fold higher than that of live microglia as shown in Figure 5.2A. Astrocytes also displayed higher viability than microglia when it was evaluated immediately after isolation (Fig. 5.2B). The relatively low amount of obtained microglia was limiting for stimulation experiments. Thus, not all antigens were tested in case of microglia and their *n* is reduced if compared to astrocytes.

Figure 5.2. Primary astrocyte and microglia cell culture preparation. (A) Yields of astrocytes and microglia adjusted to one brain. (B) Viability of astrocytes and microglia after isolation. Data in both graphs are shown as mean ± standard error of mean (SE); *n* (microglia) = 13, *n* (astrocytes) = 9.

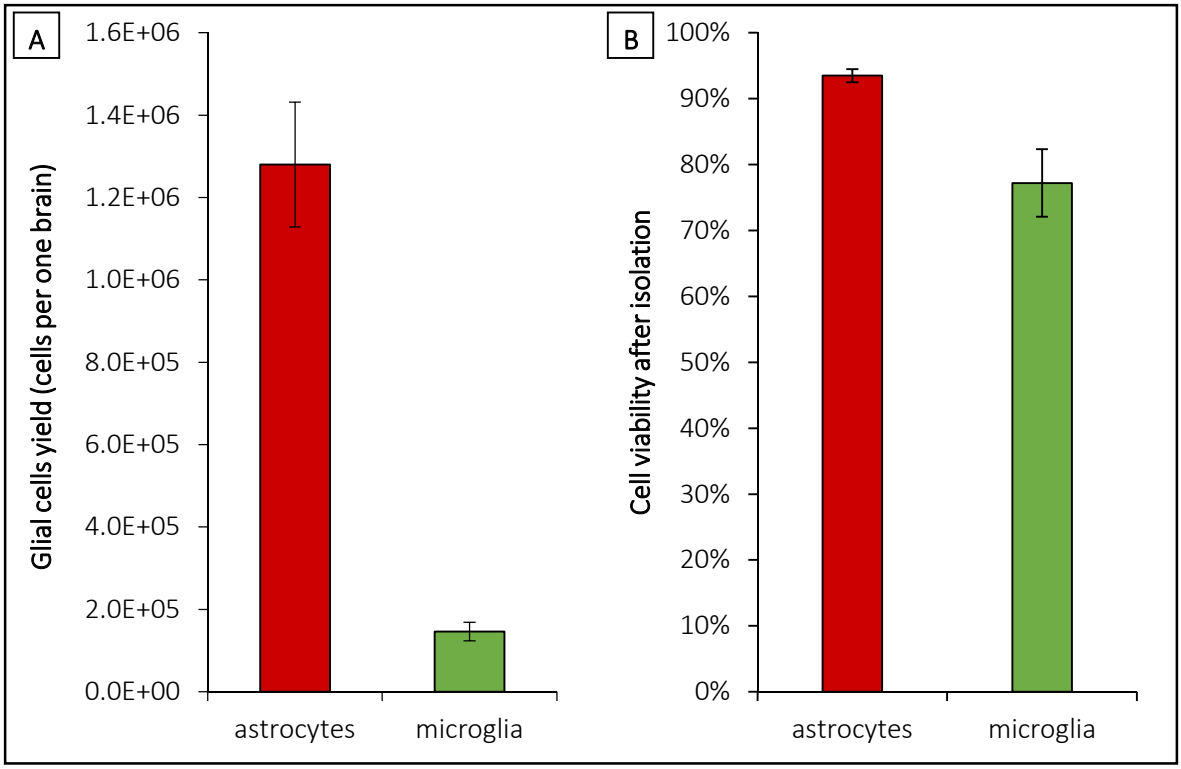

Purity of the cultures was evaluated by immunocytochemistry. In particular, the proportion of GFAP+ and Iba1+ cells was calculated in both astrocyte and microglia cultures in randomly selected wells from minimally three independent cultivations. In each case, at least 25 cells were examined and the proportion of the positive ones was calculated. More than 85% of cells in astrocyte or microglia cultures were positive for GFAP or Iba1, respectively. As revealed by cross-examination (i.e. detection of Iba1+ cells in astrocyte cultures and GFAP+ cells in microglia cultures), the other cell type (i.e. microglia in astrocyte cultures and *vice versa*) constituted more than 50% of all contaminating cells. The results are summarised in Table 5.1.

Table 5.1. Cell culture purity. % represents the mean proportion of cells expressing the marker. *n* stands for the number of wells in which the particular examination was performed.

	GFAP+ cells		Iba1+ cells	
	%	*n*	%	*n*
Astrocyte cultures	85.5	15	8.4	3
Microglia cultures	10.0	5	87.5	15

5.2. Stimulation of glial cells

The response of astrocytes and microglia to antigens of *T. regenti* was examined in terms of changes of cellular morphology (by microscopy), evaluation of expression of marker molecules (by ICC) and production of NO and cytokines (Griess assay and ELISA, respectively).

Contrary to our plans, living schistosomula dissected out from murine spinal cords were not used for stimulation because the infections of mice repeatedly failed. Altogether, eight mice were successively infected and only six schistosomula in total were obtained from the spinal cord 5 DPI. Considering the unpredictability of gaining this stimulus and the large amount of mice that would be necessary to sacrifice, experiments with living schistosomula were stopped. Nevertheless, other stimuli (homogenate of transformed cercariae and recombinant cathepsins) were used as was originally designed.

Total amounts of samples successfully analysed in each group are collectively summarised in Table 5.2. They represent the dataset free of erroneous results (caused for example by contamination of negative control, wrong standard pipetting etc.).

Table 5.2. Summary of analysed samples. *n* represents the total number of samples (separate wells with either astrocytes or microglia) which were analysed before and after stimulation (i.e. 0 and 48 hps, respectively); cell morphology and expression of markers were analysed only after stimulation. *Rep.* stands for number of cultivations, during which samples were collected.

CELL TYPE Analysis	Neg. control		LPS		Homogenate		TrCB1.1		TrCB2	
	n	rep.	*n*	rep.	*n*	repeats	*n*	rep.	*n*	rep.
ASTROCYTES										
Morph. + markers	4	2	4	2	4	2	not done			
NO production	68	7	70	7	56	6	50	2	61	2
IL-1 beta secretion	63	6	79	6	67	6	51	2	63	2
IL-6 secretion	57	6	67	6	63	6	51	2	63	2
TNF-alpha secretion	66	6	60	6	60	5	51	2	63	2
MICROGLIA										
Morph. + markers	4	2	4	2	4	2	not done due to limited amount of microglia			
NO production	17	7	19	7	23	7				
IL-1 beta secretion	18	6	18	7	17	7				
IL-6 secretion	16	7	14	6	16	7				
TNF-alpha secretion	15	6	12	6	15	6				

5.2.1. Changes in cellular morphology

Immediately after seeding into the wells and adding stimuli, both astrocytes and microglia were round in shape (Fig 5.3A and 5.3C, respectively). After 48 hours, appearance of cells changed irrespective of the surface on which they were seeded (plastic well with or without PLL-coated slides).

In case of astrocytes, rod-like or multipolar cells spread on the surface and after 48 hours of stimulation they were nearly confluent (Fig 5.3B). This appearance was the same in all stimulated groups (LPS, homogenate, TrCB1.1, TrCB2) and the negative control group as well.

Microglia underwent morphological changes which differed in particular groups. Unstimulated microglia (the negative control group) usually formed a wide lamellipodium from which a long "tail" was protruded. Elongated, bi-polar cells were also noted, but no amoeboid ones were present (Fig. 5.3D, Fig. 5.4A). In the group of microglia stimulated by homogenate of cercariae, two cell morphologies were common. The first was represented by cells with compact bodies and thick processes with finer secondary ones, the other by flattened, amoeboid cells (Fig. 5.3E, Fig. 5.4B). Microglia stimulated by LPS (the positive control group) formed large flattened amoeboid cells or broad bipolar ones. Vacuole-like structures appeared in them very often and membrane ruffles were sometimes present (Fig. 5.3F, Fig. 5.4C+D).

5.2.2. Expression of marker molecules

Apart from assessing aforementioned cell culture purity, immunocytochemistry was used for rough evaluation of intensity and pattern of GFAP and Iba1 expression in astrocytes and microglia, respectively. This analysis was performed with cells stimulated by LPS and homogenate of cercariae, unstimulated cells were taken as the negative control. The results are presented collectively in Figure 5.5.

In all examined groups of microglia, Iba1 was expressed diffusely in whole cytoplasm; only in some cells, more condensed signal was noted in perinuclear region. In LPS stimulated cells, Iba1 signal seemed to concentrate in ruffle-like structures in the cell periphery (Fig. 5.5C1). No significant differences in signal intensity were noticed by naked eye. Considering GFAP, it was expressed in all examined astrocyte cultures being usually organised in discrete bundle-like structures when the cells were flattened enough. If the cells in any group were elongated (and thus narrower), the signal appeared more intense. Otherwise, no significant differences in signal intensity were observed.

Figure 5.3. Morphology of astrocytes and microglia in phase contrast microscopy. (A) Astrocytes 30 minutes after seeding, cells are round. (B) Astrocytes after 48 hours of stimulation by LPS, cells are rod-like or multipolar. (C) Microglia 30 minutes after seeding, cells are round. (D) Unstimulated microglia after 48 hours of cultivation, cells form wide lamellipodia (wide arrow) or are bipolar (thin arrow). (E) Microglia after 48 hours of stimulation by homogenate of transformed cercariae, cells with compact bodies (thin arrow) or amoeboid ones (wide arrow) are present. (F) Microglia after 48 hours of stimulation by LPS. Cells have vacuole-like structures inside (wide arrow) or form membrane ruffles (thin arrows). Scale bars 25 μm.

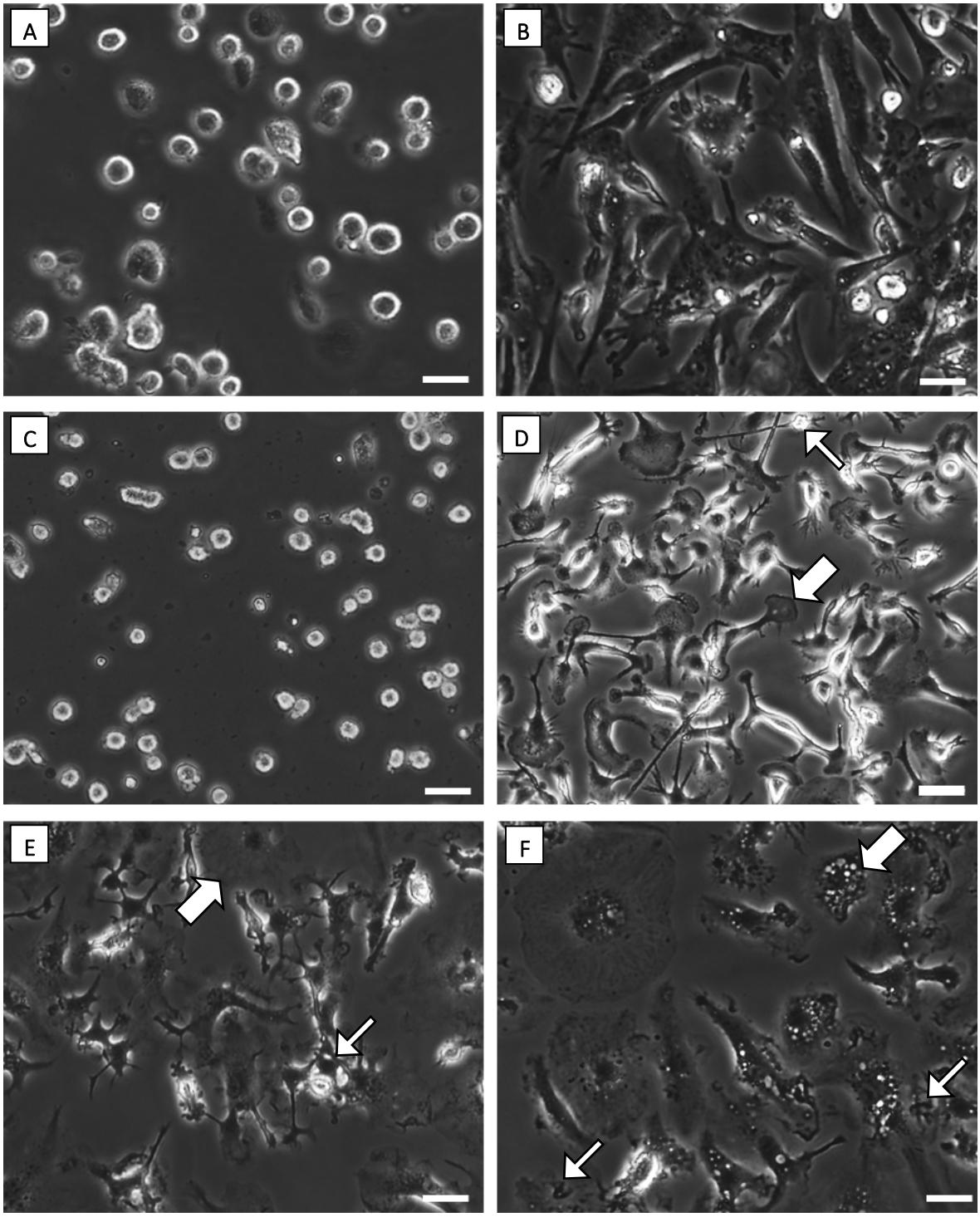

Figure 5.4. Morphology of microglia under SEM. (A) Unstimulated microglia after 48 hours of cultivation, wide lamellipodium is visible (wide arrow). (B) Microglia after 48 hours of stimulation by homogenate of transformed cercariae, secondary processes are present (wide arrow). (C) Microglia after 48 hours of stimulation by LPS, amoeboid form with holes in membrane (wide arrow) that arose probably as an artefact at place where vacuoles were located. Membrane ruffles are visible as well (thin arrows). (D) Microglia after 48 hours of stimulation by LPS, broad bipolar form with membrane ruffles (thin arrow). Scale bars 10 μm.

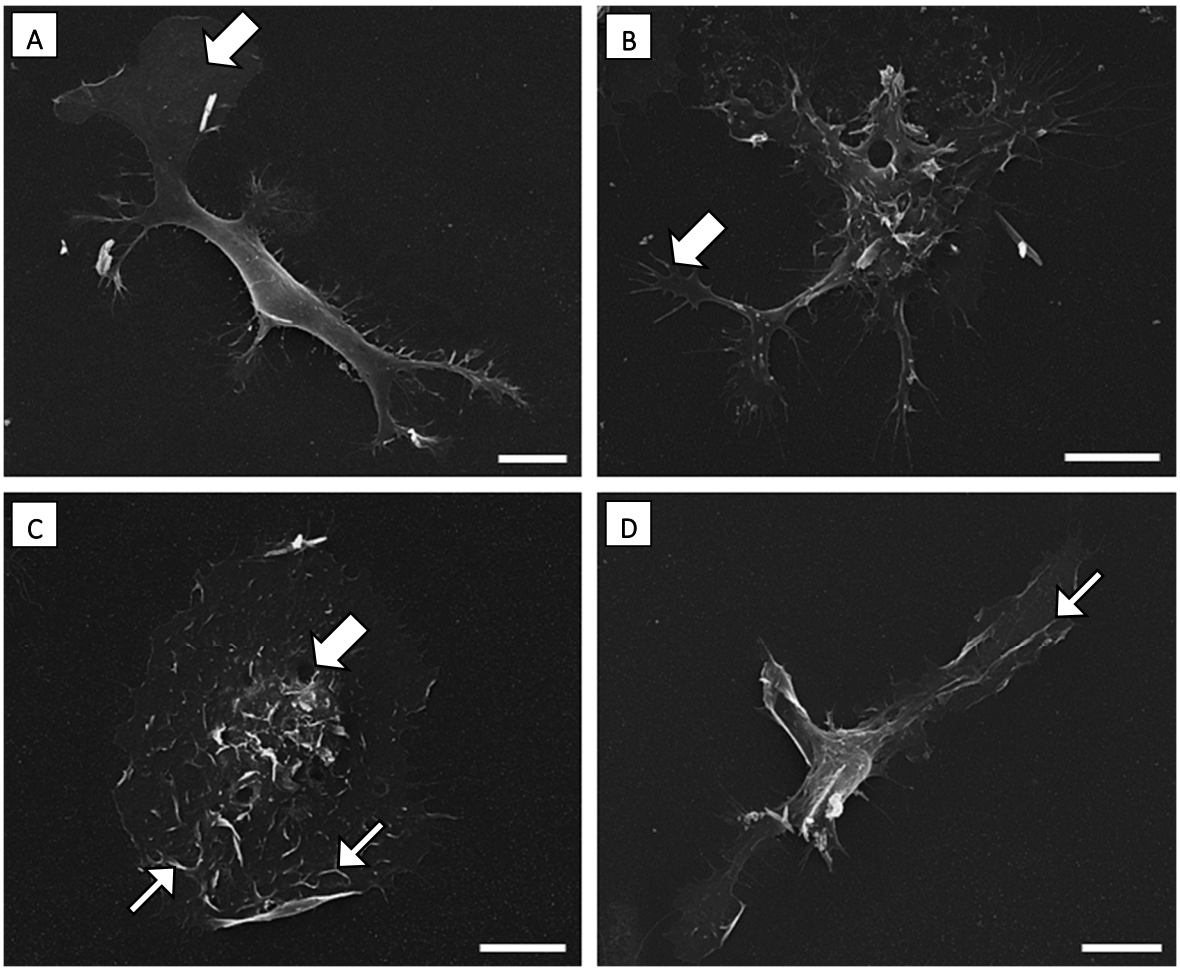

Figure 5.5 (on the next page). Expression of Iba1 and GFAP by microglia and astrocytes, respectively, as detected by immunocytochemistry. (A1/2) The control of unspecific binding of secondary antibody to microglia/astrocytes stimulated by LPS (primary antibody against Iba1/GFAP was omitted). (B1/2) Unstimulated microglia/astrocytes. (C1/2) Microglia/astrocytes after stimulation by LPS. The thin arrows indicate Iba1 signal concentrated in ruffle-like structure. (D1/2) Microglia/astrocytes after stimulation by homogenate of cercariae. In all photos, the green signal stands for Iba1, the red for GFAP and the blue for DAPI. Scale bars 10 μm.

Figure 5.5. Due to spatial limitations, the legend for this figure is on previous page.

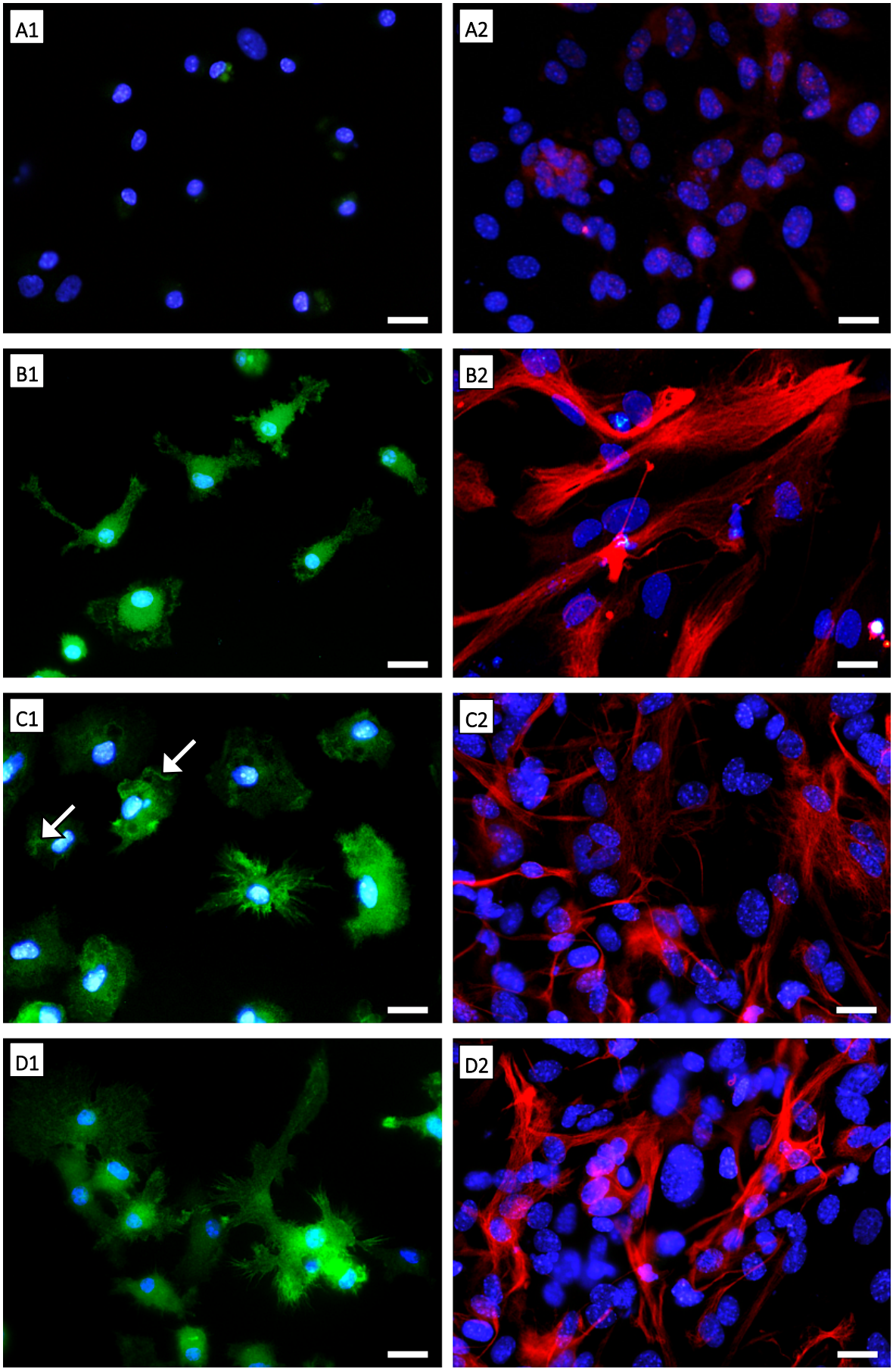

5.2.3. NO production by stimulated astrocytes and microglia and iNOS detection

Concentration of nitrites (breakdown products of NO) was measured in supernatant samples from astrocytes and microglia 0 and 48 hps. The results are summarised in Figure 5.6 and *p*-values obtained by statistical analysis are presented in Table 5.3.

In all groups, nitrite concentration increased significantly during the experiment, if it was compared at 0 and 48 hps within the same group. This is not illustrated by any sign in Figure 5.6 to keep it clear; exact *p*-values for each group are presented in Table 5.3.

Comparison of nitrite concentrations in stimulated groups at 48 hps and negative (unstimulated) control at 48 hps revealed significant differences in all cases which is shown in Figure 5.6. Homogenate of transformed cercariae caused 1.7- and 2.8-fold increase in NO production by microglia and astrocytes, respectively. *T. regenti* recombinant cathepsins B1.1 and B2 stimulated astrocytes to 1.9- and 1.6-fold higher production of NO, respectively. Exact *p*-values are shown in Table 5.3.

Experiments dealing with the detection of iNOS in cell lysates by western blot were performed as well. Cell lysates were successfully separated by electrophoresis as confirmed by Coomassie staining and electrotransferred onto PVDF-membrane as assured by Ponceau staining. However, the primary antibody recognised more than one target so several positive bands were received after the colour reaction was developed. These bands were absent from strips where only buffer or secondary antibodies were used. Neither diluting the primary antibody nor change of the buffer (TBS instead of PBS) nor prolonging blocking time (12 instead of 2 hours) improved the results. Thus, evaluation of iNOS expression was not possible.

Table 5.3. *p*-values obtained in statistical analysis of nitrite concentration differences. The differences were compared both within each group (i.e. concentration at the beginning of and after the stimulation; Wilcoxon signed rank test, the middle column) and between the stimulated and unstimulated groups at 48 hps (Wilcoxon rank sum test, the right column).

	p-value (paired samples, 0 × 48 hps)	*p*-value (sample × neg. control 48 hps)
ASTROCYTES		
Neg. control	$6.141 \cdot 10^{-10}$	1
LPS	$8.591 \cdot 10^{-13}$	$7.318 \cdot 10^{-11}$
Homogenate	$1.015 \cdot 10^{-10}$	$7.374 \cdot 10^{-9}$
TrCB1.1	$9.345 \cdot 10^{-10}$	$2.007 \cdot 10^{-15}$
TrCB2	$1.669 \cdot 10^{-11}$	$9.579 \cdot 10^{-10}$
MICROGLIA		
Neg. control	0.0026	1
LPS	0.0006	0.0409
Homogenate	$2.384 \cdot 10^{-7}$	0.0088

Figure 5.6. NO production by astrocytes and microglia stimulated by antigens of *T. regenti* illustrated as concentration of nitrites in cell supernatants. In case of microglia, TrCB1.1 and TrCB2 were not tested due to limited amount of the cells. Results are presented as mean ± SE. Asterisks refer to significant difference if compared to proper negative control at 48 hps (* $p < 0.05$, *** $p < 0.001$).

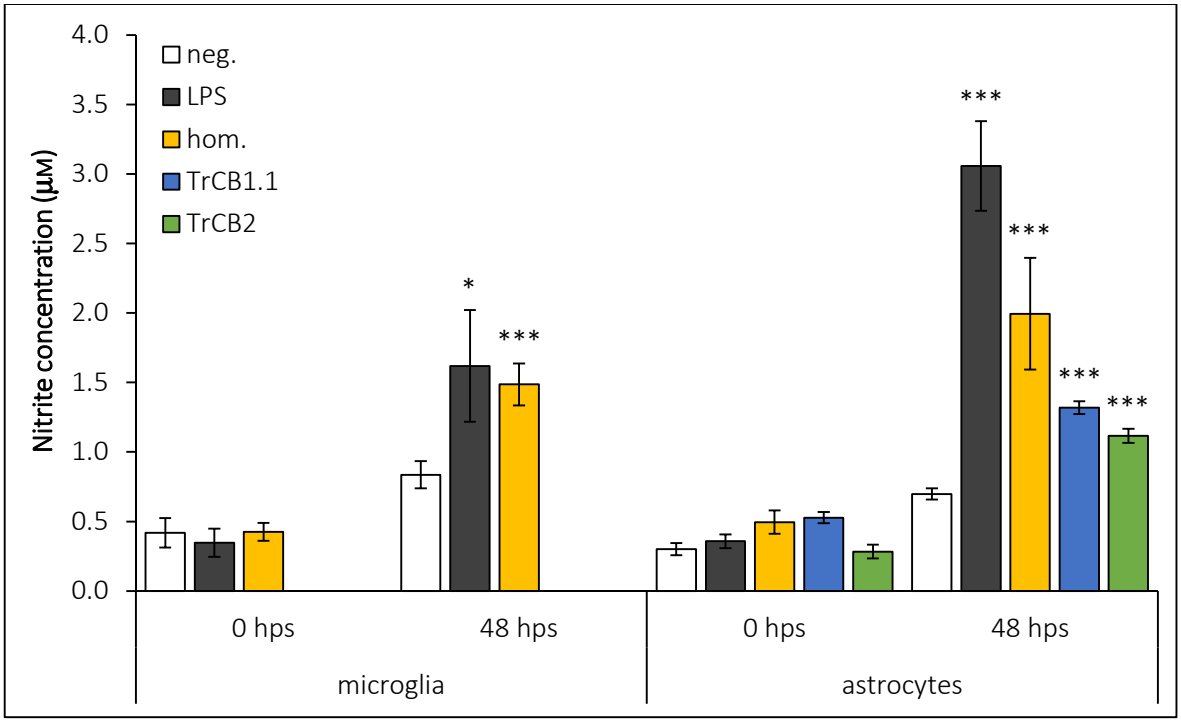

5.2.4. Cytokine production by stimulated astrocytes and microglia

Concentration of proinflammatory cytokines IL-1 beta, IL-6 and TNF-alpha was measured in supernatants from astrocytes and microglia at 0 and 48 hps. The results are shown separately for each cytokine in Figures 5.7, 5.8 and 5.9; exact *p*-values obtained by statistical analysis are presented in comprehensive summary in Table 5.4.

Concentrations of all cytokines increased significantly during the stimulation in all examined groups if samples from 0 and 48 hps were tested. This is not illustrated by any sign in Figures 5.7–5.9 to keep them clear; exact *p*-values for each group are presented in Table 5.4.

If compared to the proper negative control group at 48 hps, concentration of IL-1 beta was significantly increased (1.3-fold) only in case of microglia stimulated by LPS which served as the positive control group (Fig. 5.7). In other groups, either astrocytes or microglia, no significant differences were found. Results for stimulation of astrocytes by TrCB1.1 and TrCB2 are not included because concentrations of IL-1 beta in these samples were calculated to be under the ELISA detection limit at both 0 and 48 hps. Exact *p*-values are shown in Table 5.4.

The production of IL-6 was significantly higher in all groups at 48 hps if compared to the proper negative control (Fig. 5.8). Stimulation with homogenate of transformed cercariae led to 8-fold and 2.6-fold elevation in IL-6 production by microglia and astrocytes, respectively. Astrocytes

stimulated by TrCB1.1 and TrCB2 produced 2.1-fold and 10.9-fold more IL-6 than the negative control group. Exact *p*-values are shown in Table 5.4.

In comparison to the proper negative control group, homogenate of transformed cercariae did not influence the production of TNF-alpha by microglia but diminished its secretion by astrocytes 4.3-fold (Fig. 5.9). On the contrary, concentration of TNF-alpha was significantly higher after stimulation of astrocytes by TrCB1.1 (2-fold increase) and TrCB2 (14.5-fold increase). Exact *p*-values are shown in Table 5.4.

Table 5.4. *p*-values obtained in statistical analysis of cytokine concentration differences. The differences were compared both within each group at 0 and 48 hps ("paired"; Wilcoxon signed rank test) and between the stimulated and unstimulated groups at 48 hps (Wilcoxon rank sum test).

	IL-1 beta		IL-6		TNF-alpha	
	p (paired)	*p* (× neg.)	*p* (paired)	*p* (× neg.)	*p* (paired)	*p* (× neg.)
ASTROCYTES						
Neg. control	$7.697 \cdot 10^{-5}$	1	$5.283 \cdot 10^{-11}$	1	$5.232 \cdot 10^{-12}$	1
LPS	$4.847 \cdot 10^{-11}$	0.1415	$1.145 \cdot 10^{-12}$	$2.200 \cdot 10^{-16}$	$1.671 \cdot 10^{-11}$	$2.200 \cdot 10^{-16}$
Homogenate	$2.220 \cdot 10^{-5}$	0.6887	$5.556 \cdot 10^{-12}$	0.0308	$1.929 \cdot 10^{-8}$	0.0325
TrCB1.1	×	×	$5.301 \cdot 10^{-10}$	$3.990 \cdot 10^{-7}$	$9.036 \cdot 10^{-10}$	$4.419 \cdot 10^{-9}$
TrCB2	×	×	$5.294 \cdot 10^{-12}$	$2.200 \cdot 10^{-16}$	$5.294 \cdot 10^{-12}$	$2.200 \cdot 10^{-16}$
MICROGLIA						
Neg. control	0.0034	1	0.0017	1	$6.104 \cdot 10^{-5}$	1
LPS	$2.289 \cdot 10^{-5}$	0.0257	0.0001	$1.375 \cdot 10^{-8}$	0.0005	$1.150 \cdot 10^{-7}$
Homogenate	0.0013	0.3302	0.0001	0.0426	$6.104 \cdot 10^{-5}$	0.0975

Figure 5.7. Concentration of IL-1 beta in supernatants from astrocytes and microglia. Results are presented as mean ± SE. Asterisk refers to significant difference if compared to proper negative control at 48 hps (* $p < 0.05$).

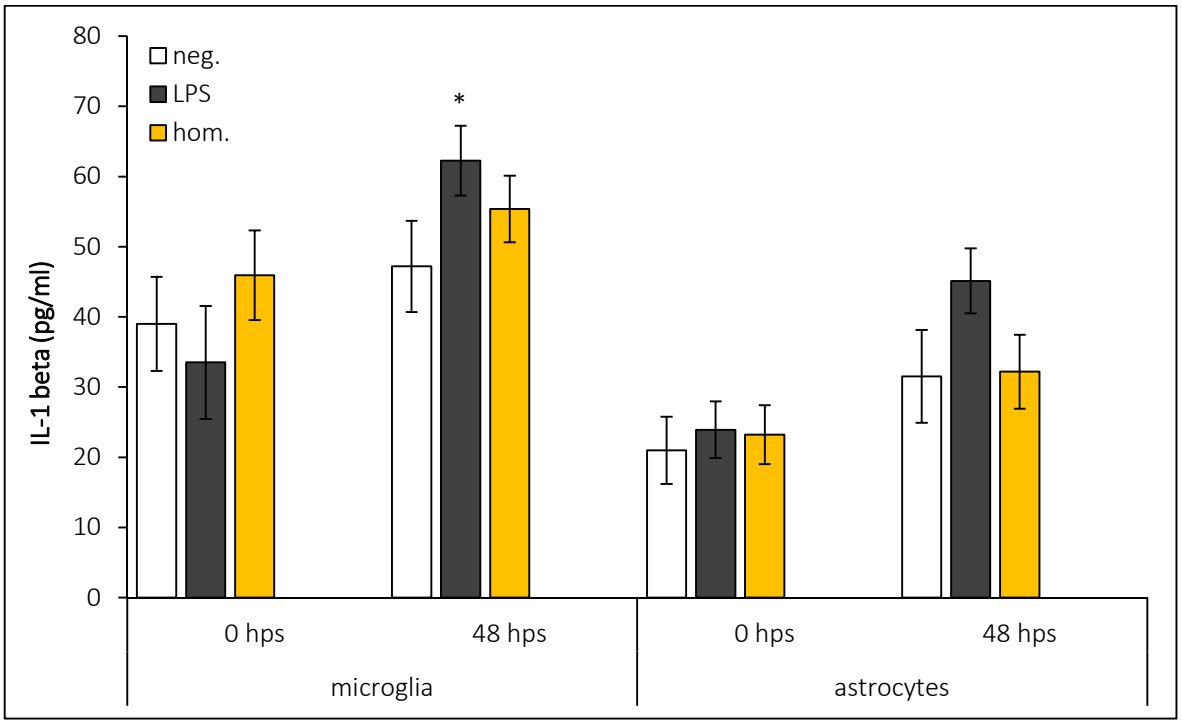

Figure 5.8. Concentration of IL-6 in supernatants from astrocytes and microglia. Results are presented as mean ± SE. Asterisks refer to significant difference if compared to proper negative control at 48 hps (* $p < 0.05$, *** $p < 0.001$).

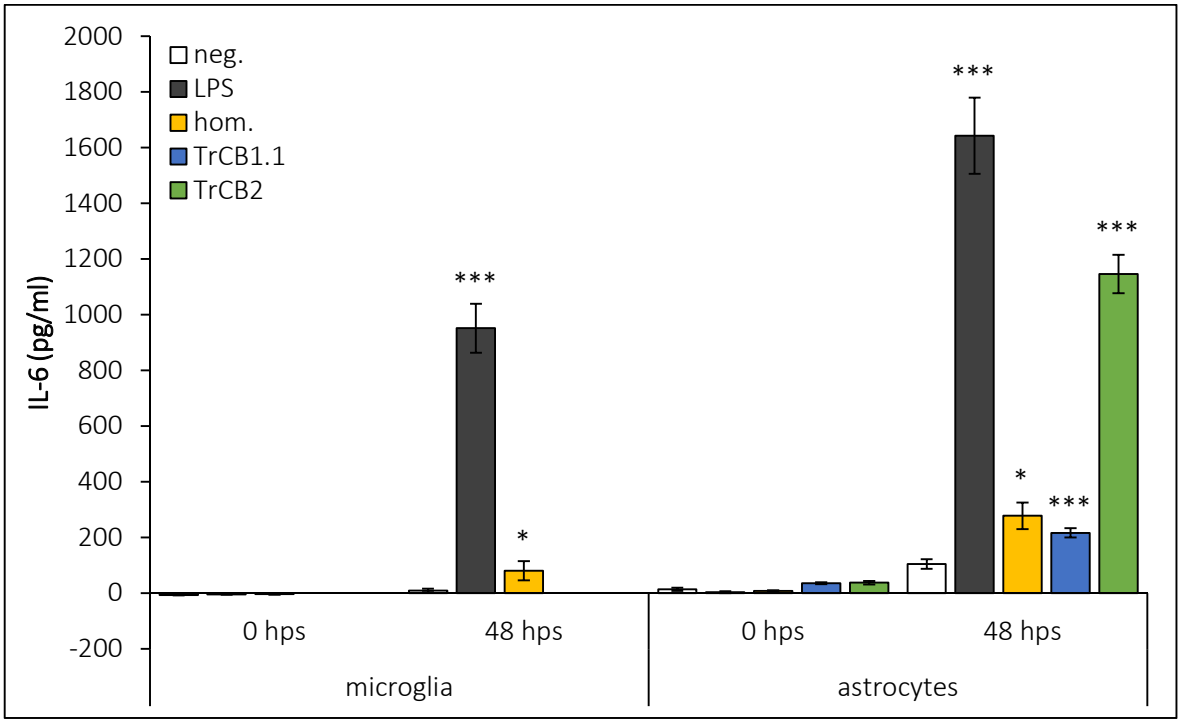

Figure 5.9. Concentration of TNF-alpha in supernatants from astrocytes and microglia. Results are presented as mean ± SE. Asterisks refer to significant difference if compared to proper negative control at 48 hps (* $p < 0.05$, *** $p < 0.001$).

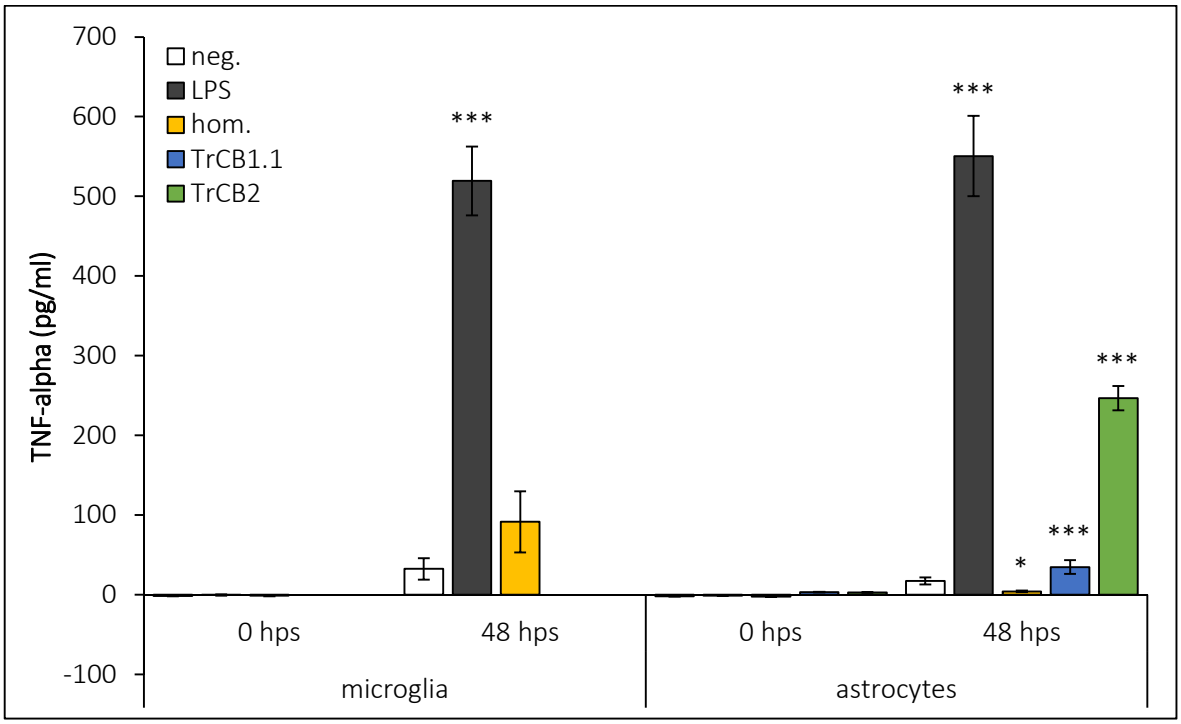

5.3. *In vivo* experiments

To be able to track schistosomula during their migration through the murine CNS, they were stained red with 10 µM SNARF-1 for 60 minutes. Staining procedure did not affect neither viability, nor motility of cercariae. They were freely swimming in water without any sign of non-physiological body contraction, tegument disruption or inner disorganisation; tails were attached (Fig. 5.10A). SNARF-1 labelled both surface of cercariae and unidentified inner structures. Intense signal appeared also in the front part of the body at the site where gland ducts open.

Stained cercariae were used for infection of one C57BL/6 mouse in order to evaluate stability of the red signal and the possible influence of the staining on infectivity of cercariae. The last mentioned was not attenuated by SNARF-1, because three days after infection, 13 schistosomula were successfully extracted from the spinal cord of the infected mouse. The schistosomula were alive and motile, intensity of the red signal was reduced and restricted mostly to the front part of the body (Fig. 5.10B); still it was detectable.

Figure 5.10. Staining of *T. regenti* larvae by SNARF-1. (A) Cercaria is labelled throughout whole body, the most intense signal comes from the front part. (B) In three-day-old schistosomulum, the signal is attenuated, but still detectable especially in the front part of the body. Scale bars 50 μm.

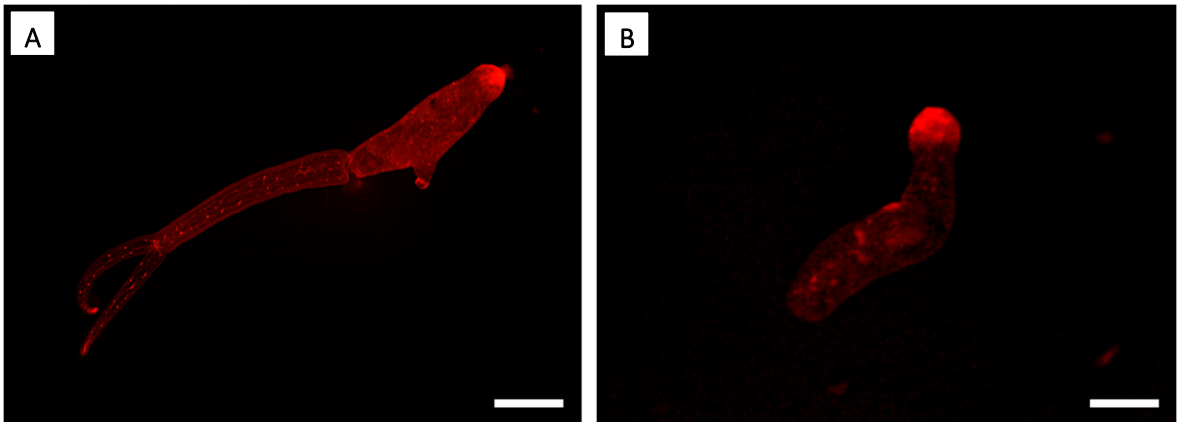

After checking the signal preservation *in vivo*, four C57BL/6 MHC II-EGFP knock-in mice were infected by labelled cercariae and two mice were used as negative controls. During the infection, neither control, nor infected mice exhibited neurological disorders or changes in behaviour. Three days after the infection, they were sacrificed, perfused and squashed-tissue samples were prepared from 0.5 cm long pieces of the spinal cord and examined under the microscope.

In the spinal cords of two infected mice, no migrating schistosomula were found. Spinal cords, thoracic segments in particular, of the third and the fourth infected mouse harboured five and three schistosomula, respectively. They were actively moving in the tissue exhibiting red signal (Fig. 5.11). Green signal emitting MHC II+ structures considered to be cells were detected In the migratory tracks of the schistosomula or in their surroundings (Fig. 5.11). It was not possible to determine whether they were originally in contact with the schistosomula as the tissue was squashed. They did not co-localise with unidentified red structures sporadically occurring in the nervous tissue. No MHC II green signal was detected in spinal cords of uninfected animals.

Figure 5.11. *T. regenti* schistosomula in the spinal cords of C57BL/6 MHC II-EGFP knock-in mice. In the migratory tracks or in the vicinity of schistosomula (red, pointed with an arrow), MHC II+ cells (green) were detected. The pictures represent samples from two infected mice in which schistosomula were found. Scale bars 50 μm.

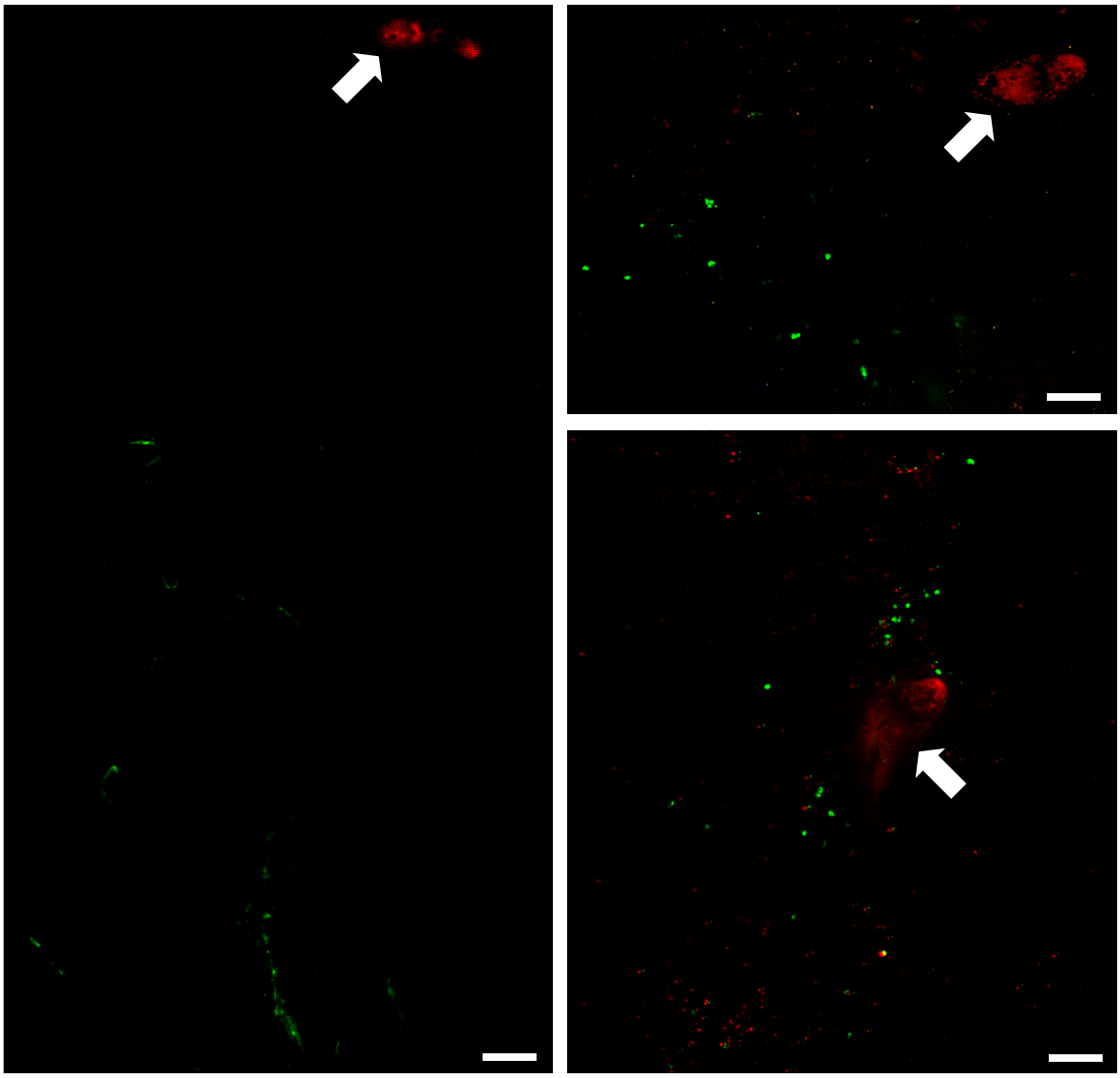

For ultramicroscopic examination, spinal cords from other two C57BL/6 MHC II-EGFP knock-in mice (infected and uninfected) were extracted carefully and sent to Dr. Christian Hahn who performed the imaging. According to his report, ten schistosomula were detected in the spinal cord of the infected mouse; they emitted the signal both in a red and green channel. The spinal cord was broken at several positions probably due to enhancing of micro-ruptures, which appeared during the preparation, by chemical processing of the sample. This thwarted higher resolution imaging, which would evaluate the presence of MHC II+ cells, and then 3D reconstruction.

6. DISCUSSION

Apart from participation of peripheral leukocytes, the host immune response in the CNS includes anti-infection activities of the resident glial cells, in particular astrocytes and microglia. Nevertheless, their role in helminth-caused parasitic infections has been largely understudied although these cells might be helpful in parasite elimination and subsequent tissue repair.

To contribute to the knowledge extension in this field, the neurotropic fluke *T. regenti*, affecting the CNS of both avian and mammalian hosts (Horák *et al*. 1999), was taken as a model. Four years ago, activation of astrocytes and microglia was noticed in the spinal cords of infected mice by immunohistochemistry (Lichtenbergová *et al*. 2011). Thus, astrocyte and microglia cultures were established and several functional assays dealing with their response to antigens of *T. regenti* were carried out *in vitro*. Additionally, *in vivo* experiments focused on the detection of MHC II+ immune cells, were performed as well with murine hosts.

6.1. Cultivation of glial cells

As there had not been almost any experience in isolation and cultivation of astrocytes and microglia in the Laboratory of Helminthology, all necessary procedures had to be established at the beginning of this master's project. Results of our approach are discussed below accompanied by comments on possible improving the protocol in the future.

We performed *in vitro* experiments with primary astrocyte and microglia cultures prepared directly from neonatal murine brains. These cells are routinely used and are supposed to simulate the *in vivo* functional state better than immortalised glial cell lines which may differ in some properties (Fok-Seang *et al*. 1995, Stansley *et al*. 2012). For example, murine-derived BV-2 microglia express less IL-1 beta, IL-6 and TNF-alpha after stimulation with LPS than microglia from primary cultures and nitric oxide synthesis is diminished too (Horvath *et al*. 2008, Henn *et al*. 2009).

Mixed glial cultures for our experiments were prepared by mechanical dissociation of neonatal murine brains, which were then placed into the culture flasks. The tissue dissociation can be followed by disposing of myelin and tissue debris by centrifugation in Percoll gradient or sieving through the cell strainer to enhance cell viability and reduce the content of debris which may cause unspecific activation of the cells (Hsieh *et al*. 2009, Nikodemova and Watters 2012).

Although we removed neither myelin nor debris from the cultures, cell viability and growth did not seem to be attenuated. The cultivation flasks were cover by the confluent cell layer after 8–9 DIV which corresponds with observations in seminal papers dealing with astrocyte and microglia isolation from mixed glial cultures (McCarthy and de Vellis 1980, Giulian and Baker 1986).

The authors identified the confluent cells forming the lower monolayer as astrocytes and the cells sitting on them as oligodendrocytes (ramified) and microglia (round/amoeboid) (McCarthy and de Vellis 1980, Giulian and Baker 1986). In our mixed cultures, we mostly observed only ramified cells sitting on the astrocyte layer; those with round/amoeboid morphology were present only in the first days of cultivation among the debris. We hypothesise, that some of the round/amoeboid cells were microglia which did not grow on the astrocytes but were rather intermingled among them as described by Saura (2007). The other explanation might be that microglia growing in our mixed glial cultures exerted rod-like or tri-polar rather than round/amoeboid morphology, thus resembling oligodendrocytes, as was described in the study performed by Marek *et al*. (2008). Immunocytochemistry or flow cytometry analysis would help to unravel the proportion of particular cell types in our mixed cultures.

There were no troubles with establishing primary astrocyte cultures, which were abundant cells in the mixed glial cultures. The average yield of astrocytes was $1.3 \cdot 10^6$ cells per brain which is comparable to Feldman *et al*. (2014). The proportion of GFAP+ cells in the culture was 84.5% and microglia represented the major contaminant. According to terminology suggested by Saura (2007), such cultures would be still called "mixed-glial", because he restricts the term "astroglial-enriched cultures" to those where astrocytes constitute more than 90% of all cells.

The purity of our astrocyte cultures was lower than that achieved by McCarthy and de Vellis (1980) or Marek *et al*. (2008). It was probably caused by insufficient shaking which did not separated the intermingled microglia. The amount of microglia in astrocyte cultures could be lowered by shaking the mixed cultures immediately after astrocytes are confluent (see below) or by adding inhibitors of microglial proliferation, namely L-leucine methyl ester (Hamby *et al*. 2006). The identity of GFAP–/Iba1– cells present in our astrocyte cultures is unknown, but we speculate that most of them are oligodendrocytes which remained with astrocytes in the cultivation flask after shaking. To dispose of them, another shaking step at higher speed would be necessary (McCarthy and de Vellis 1980).

Microglia cultures displayed 87.5% purity being contaminated by astrocytes most often. More than 90% culture purity stated by Giulian and Baker (1986) and Marek *et al*. (2008) was not reached narrowly probably due to the time left for cell adhesion during which not only microglia but also astrocytes adhered to coverslips or plastic wells. Shortening the time of adhesion should increase the purity (Giulian and Baker 1986). However, it is a trade-off, since the yields could then be reduced, as not all microglia would manage to adhere.

Yields of microglia isolated from mixed cultures were very low: only $1.5 \cdot 10^5$ per one brain on average. Floden and Combs (2007) and Marek *et al*. (2008) reached nearly 2-fold higher amount of microglia by the shaking-off method. The reason is most likely because they changed media every

4–7 days and continued cultivation even after the astrocyte layer became confluent. As a result, microglial growth factors produced by astrocytes (GM-CSF, M-CSF) accumulated in media and enhanced microglial proliferation (Hao *et al*. 1990, Ganter *et al*. 1992, Lee *et al*. 1993, 1994, Smith *et al*. 2013). Such prolonged cultivation or use of astrocyte-conditioned media could be a way to augment microglial yields; however, this may lead to increased microglial contamination in astrocyte cultures as well because intermingled microglia which cannot be replaced by shaking would proliferate too. Additionally, more effective than shaking-off methods, namely mild trypsinization (Saura *et al*. 2003) or magnetic separation (Gordon *et al*. 2011), could be employed to gain more microglia from neonatal brains.

To conclude, we were able to establish the cultivation of astrocytes and microglia in our laboratory but several issues, e.g. augmentation of culture purity and microglia yields by other methods, should be improved in the future.

6.2. Stimulation experiments – glial cell morphology and marker molecules expression

Under non-physiological conditions, astrocytes and microglia were shown to change their morphology and/or expression of GFAP and Iba1, respectively, *in vivo* (Hozumi *et al*. 1990, Vijayan *et al*. 1990, Davis *et al*. 1994, Ito *et al*. 2001). However, *in vitro* morphological transformation following stimulation is usually not studied. Furthermore, expression of marker molecules is routinely evaluated by PCR or Western blot, but not by naked eye using fluorescence microscopy. Thus, we investigated morphological alteration and expression of GFAP and Iba1 in both unstimulated and stimulated astrocytes and microglia.

Examining astrocytes under the microscope equipped with phase contrast, we did not see any differences in cell morphology if we compared astrocytes stimulated by LPS or homogenate of transformed cercariae to unstimulated ones. Analogous results were obtained by Sheng *et al*. (2011) who observed primary rat astrocytes stimulated by LPS + IFN-gamma or IFN-gamma + IL-1 beta + TNF-alpha. They did not notice any changes in astrocyte morphology after *in vitro* stimulation by LPS and/or proinflammatory cytokines (Sheng *et al*. 2011). On the contrary, significant alterations may occur at ultrastructural level that we did not evaluate. For example, dilation of rough endoplasmic reticulum, was observed by transmission electron microscopy in astrocytes after treatment with LPS, TNF-alpha and IL-1 beta (Hu *et al*. 1994).

In contrast, microglial cells exhibited distinct phenotypes depending on stimulation. Unstimulated cells often formed wide lamellipodium from which a long process was protruded. This morphology was reported by Giulian and Baker (1986) for cells cultivated with retinoic acid which prevents M1 polarization in microglia (Dheen *et al*. 2005). These data underpin our assumption of quiescent state of this negative control group.

When microglia were stimulated by LPS, amoeboid and bipolar forms appeared similarly as in the studies of Suzumura *et al*. (1991), Abd-El-Basset and Fedoroff (1995) and Sheng *et al*. (2011) who saw these phenotypes after stimulation by LPS. According to Suzumura *et al*. (1991), amoeboid cells represent activated microglia and those bipolar are actively proliferating cells. Bipolar cells exhibit mixed M1/M2 phenotype while amoeboid ones are classically activated (M1) microglia capable of proinflammatory secretion (Tam and Ma 2014).

Furthermore, two unusual morphological features were noticed in some LPS-stimulated microglia. Membrane ruffles were seen in periphery of some cells by phase contrast microscopy, the same was reported by Sheng *et al*. (2011) for immortalised BV-2 microglial lines stimulated by IL-1 beta, TNF-alpha and IFN-gamma. When examined by immunocytochemistry, we obtained similar Iba1 pattern in some cells suggesting association of membrane ruffles with Iba1 which is actin-associated protein. Abd-El-Basset and Fedoroff (1995) observed these ruffles being positive for phalloidin signal. The association of Iba1 with membrane ruffles was confirmed by Ohsawa *et al*. (2000) who demonstrated that Iba1 co-localises with F-actin in membrane ruffles and is necessary for phagocytosis performed by activated amoeboid microglia.

The other prominent feature of LPS-stimulated microglia was the presence of numerous vacuoles in the cytoplasm as noticed also by Suzumura *et al*. (1991). This was not reported in any case by Sheng *et al*. (2011) but Harms *et al*. (2012) detected vacuoles in LPS-treated microglia from TNF-alpha-deficient mice and Abd-El-Basset and Fedoroff (1995) noticed these structures in unstimulated microglia. None of these studies, however, did not investigated nature of the vacuoles. When we examined the cells by SEM, membrane apertures were present instead of supposedly protuberant vacuoles. The same observation was made by Lee *et al*. (2011) in case of microglia stimulated by the lysate of *Naegleria fowleri*. They interpreted it as the parasite-caused membrane lysis (Lee *et al*. 2011).

Possibly, the vacuoles could be associated with autophagy which is typical for nutrient-deprived or overstimulated cells (Yu *et al*. 2004, Chen and Klionsky 2011). Microglia possess the autophagy pathway which might be activated in LPS-stimulated cells; however, this is associated with suppression of NO and IL-6 secretion (Han *et al*. 2013). This contrasts to our results in which LPS-stimulated microglia increased NO and IL-6 production significantly. Thus, we think that vacuoles, observed in microglia after LPS stimulation, were not related to autophagy and their origin remains unknown. Nevertheless, it is not possible to conclusively exclude their autophagy origin without analysis of the presence of autophagy-specific markers.

Microglia stimulated by homogenate of cercariae exhibited two morphologies: amoeboid cells and those with compact bodies and thick processes. We suggest amoeboid microglia to be identical to the activated M1 microglia with the same morphology observed within aforementioned

microglia stimulated by LPS. The absence of membrane ruffles could be explained by not as highly activated state of cells which was manifested also in lower production of NO and cytokines in comparison to LPS-treated cells. The other type, the cells with compact bodies and thick processes, mostly resemble activated microglia from *in vivo* depicted by Davis *et al*. (1994) and Miller *et al*. (2013); however, transfer to *in vitro* conditions is doubtful. *In vitro*, similar morphology was noticed in rat-derived highly aggressive proliferating immortalized microglial cells after treatment with TNF-alpha + IL-1 beta + IFN-gamma (Sheng *et al*. 2011). Based on that, we hypothesise this form of microglia represents a transient state between resting and proliferating bipolar microglia seen in the LPS-treated group. The delay in development of the "full" proliferating bipolar phenotype could be caused by less stimulatory potential of homogenate of transformed cercariae if compared to LPS.

Considering the expression of GFAP or Iba1, we did not find any differences between unstimulated and stimulated cells when it was evaluated just by fluorescence microscopy. Streit (2013) hypothesised that microglia *in vitro* are permanently activated in comparison to *in vivo* ones due to the way of isolation, which is stressful and during which a lot of cellular debris arises. Neither after resting are they comparable to quiescent microglia observed *in vivo* (Streit 2013). Such "default" activation of the cells may be the reason why we did not observe any differences in expression of GFAP and Iba1, markers of activation (Hozumi *et al*. 1990, Vijayan *et al*. 1990, Ito *et al*. 1998, 2001), in unstimulated and stimulated astrocytes and microglia, respectively.

Summarizing these data, we conclude that evaluation of GFAP or Iba1 expression by immunocytochemistry is not very helpful when assessing the activation state of cells. Nevertheless, conventional phase contrast microscopy could be helpful for gross, "first-glance" evaluation of microglial activation.

6.3. Stimulation experiments – NO and cytokine production

Histological studies revealed inflammatory lesions in the CNS of mice infected by *T. regenti* in proximity of which activated astrocytes and microglia were found too (Kolářová *et al*. 2001, Kouřilová *et al*. 2004b, Lichtenbergová *et al*. 2011). Both astrocytes and microglia were shown to be capable of promoting pathological states by secretion of NO and proinflammatory cytokines (Boje and Arora 1992, Brown *et al*. 1995, Lee *et al*. 2000, Stewart *et al*. 2000, Smith *et al*. 2012, Deng *et al*. 2014). Thus, we analysed the production of NO and proinflammatory cytokines IL-1 beta, IL-6 and TNF-alpha after exposing astrocytes and microglia to antigens of *T. regenti*. Characteristics of used antigens are discussed being followed by comments on NO and cytokine production.

Ex vivo isolated living schistosomula of *T. regenti* and their homogenate would definitely be the most fitting stimuli of glial cells best simulating *in vivo* conditions. They would stand for both

initial and terminal phase of the infection when schistosomula are alive or in the process of destruction, respectively. However, the infections of C57BL/6 mice exhibited decreasing schistosomula yields in course of time so this material was not available for stimulation experiments. C57BL/6 mice were used in previous immunological studies performed with *T. regenti*, but only serum from infected hosts, positive for anti-*T. regenti* antibodies, was taken (Lichtenbergová *et al*. 2008, Chanová *et al*. 2011); the mice were not dissected for schistosomula counting.

We speculated that the problem with infecting C57BL/6 mice might have been in using different mouse strain (predisposed to Th1 response) than in previous studies which detected schistosomula in the spinal cords of infected BALB/c, hr/hr and SCID mice (Kolářová *et al*. 2001, Hrádková and Horák 2002, Kouřilová *et al*. 2004b). Nevertheless, Blank *et al*. (2011) reported no significant differences in strain-specific sensitivity to *Schistosoma mansoni* infection. Furthermore, preliminary data for *T. regenti* suggest that Th1 polarization even accelerates the schistosomula migration in murine hosts (Chanová and Hrdý 2013). As we failed to infect other mouse strains as well (BALB/c, ICR; results not presented in this thesis), we hypothesise that the infectivity and/or virulence of our laboratory strain of *T. regenti* has been attenuated and so it is not capable of proper migration in non-specific murine hosts.

Thus, we replaced aforementioned stimuli with homogenate of transformed cercariae. They exhibit the same immunoreactivity as *ex vivo* schistosomula (Chanová *et al*. 2011) and their homogenate represents a mixture of surface and intrinsic soluble antigens existing in the parasite which are exposed to the immune system during the infection. This kind of stimulus was used also in other studies dealing with glial cell response, e.g. in case of *Mesocestoides corti* and *Angiostrongylus cantonensis* where it was called “helminth soluble factors” (Sun *et al*. 2014) or simply “soluble antigen” (Wei *et al*. 2013), respectively.

Apart from homogenate of transformed cercariae, we tested two recombinant proteins, *T. regenti* cathepsins B1.1 and B2. *In vivo*, TrCB1.1 and TrCB2 are expressed at high levels in schistosomula (Dolecková *et al*. 2010) and both can get in contact with astrocytes. Even though TrCB1.1 was localised in the intestine of schistosomula (Dvorák *et al*. 2005), it can leak from there and be diffused in the nervous tissue when schistosomula regurgitates ingested meal. TrCB2, present in the penetration glands, was suggested to participate primarily in the process of skin invasion. Nonetheless, according to its high expression in schistosomula and ability to cleave myelin basic protein as well, its role in migration during which it can be exposed to the adjacent nervous tissue cannot be excluded (Dolecková *et al*. 2009).

Surprisingly, testing of capability of particular parasite proteins in stimulating astrocytes and microglia to NO or cytokine production is not common. To our knowledge, there is only one paper

describing the effect of helminth recombinant protein on astrocytes and microglia. Li *et al*. (2012) analysed how 16-kDa protein from *Angiostrongylus cantonensis* larvae, which is homologous to the immunodominant hypodermal antigen from *Ancylostoma caninum*, affects NO production in rat astrocytes and microglia (Li *et al*. 2012).

If we summarised our results from stimulation experiments dealing with NO production by the glial cells, significant increase in nitrite concentration, implying NO production by the cells, was noticed in all stimulated groups. This is similar to analogous studies which also confirmed increase in NO production by astrocytes and/or microglia after *in vitro* stimulation by living trypanosomes or their E/S product (Girard *et al*. 2000), E/S products of *Paragonimus westermani* (Jin *et al*. 2006, 2009), soluble antigens of *Angiostrongylus cantonensis* larvae (Wei *et al*. 2013) or its recombinant 16-kDa protein (Li *et al*. 2012). The most prominent elevation of NO production was observed in groups stimulated by homogenate of transformed cercariae which is probably caused by complexity of the stimulus, which is the mixture of antigens. The comparison of our data, in terms of absolute concentrations, is not possible because the study by Wei *et al*. (2013) detected changes in iNOS expression rather than nitrite concentration and others stimulated different amounts of cells for different time periods (Girard *et al*. 2000, Jin *et al*. 2006, 2009, Li *et al*. 2012).

Admittedly, two issues should be pointed out. First, to be sure of exact source of NO in our cultures iNOS detection should be performed by a method with cellular resolution, e.g. double staining immunocytochemistry simultaneously detecting GFAP/Iba1 and iNOS. This is highlighted by Saura (2007), who illustrates that for example even subtle microglial contamination of astrocyte culture may be responsible for NO production which would be erroneously addressed to astrocytes. Second, to assure the effect of cathepsins on NO production, the experiments have to be repeated since they were done only twice due to limited amount of the recombinant proteins.

Nevertheless, we hypothesise that astrocytes and/or microglia might be capable of NO production not only *in vitro*, but also *in vivo* in response to antigens of *T. regenti*. This can participate in parasite elimination in mice in which schistosomula do not survive. Such deleterious effect of NO on helminths potentially leading to control of the infection was demonstrated for instance in case of schistosomula of *Schistosoma mansoni* (James and Glaven 1989, Wynn *et al*. 1994), cysts of *Echinococcus granulosus* (Zeghir-Bouteldja *et al*. 2009), cysticerci of *Taenia crassiceps* (Alonso-Trujillo *et al*. 2007) or microfilariae of *Brugia malayi* (Rajan *et al*. 1996, Taylor *et al*. 1996). Additionally, elevated expression of iNOS (and proinflammatory cytokines) was suggested to be crucial for elimination of *Angiostrongylus cantonensis* larvae in mice which are not suitable hosts for this nematode (Wei *et al*. 2013).

To elucidate the potential role of nitric oxide in control of *T. regenti* infection in mice, more experiments have to be done. First, toxicity of NO, generated by either astrocytes/microglia or NO-

donors, to schistosomula should be tested *in vitro* (Ahmed *et al*. 1997, Thomas *et al*. 1997). Second, mice should be treated with iNOS inhibitors and migrating schistosomula should be then counted (Wynn *et al*. 1994, Rajan *et al*. 1996).

Data obtained in cytokine assays were more diverse. IL-1 beta, which is regarded as the proinflammatory cytokine, is produced by astrocytes and microglia in parasitic infections associated with formation of inflammatory lesions (Fischer *et al*. 1997b, Wei *et al*. 2013). Contrary to our assumptions, we detected elevated levels of IL-1 beta in neither astrocyte nor microglia cultures stimulated by homogenate of transformed cercariae. In the samples from cultures stimulated by recombinant cathepsins, undetectable amounts of IL-1 beta were present. Apart from possible error in sample processing, IL-1 beta depletion caused by proteolytic activities of cathepsins cannot be conclusively excluded even if we did not find the proof for it in literature. Cathepsins of helminth origin are known to cleave host's immunoglobulins (Sajid *et al*. 2003), but to our knowledge, no data about their ability to deplete cytokines have been published. Nevertheless, this should be tested *in vitro* and all cytokines analysed in our experiments should be included.

The situation was completely different for IL-6 whose secretion was upregulated by all stimuli, TrCB2 being the most potent one. Increased production of IL-6, enhanced by TNF-alpha, was noted in astrocytes *in vitro* infected by *Toxoplasma gondi* (Fischer *et al*. 1997b) and microglia stimulated by soluble antigen from *Angiostrongylus cantonensis* (Wei *et al*. 2013). Additionaly, IL-6 reactivity was noticed in glial scars formed around lesions in brains of mice infected by *Mesocestoides corti* (Alvarez and Teale 2006). Thus, IL-6 of glial cell origin is suggested to participate in promotion of local inflammation also *in vivo* which may be the same in case of mice infected by *T. regenti*. On the other hand, neuroprotective effects of exogenous IL-6 during CNS ischemia were demonstrated as well (Loddick *et al*. 1998) implying ambiguous effects of this cytokine. To determine the role of IL-6 and glial cells in its production, *in situ* detection of IL-6 should be performed being followed by experimental infections of IL-6 deficient mice by *T. regenti* or at least administration of neutralizing anti-IL-6 antibodies.

The last proinflammatory cytokine included in our analysis, TNF-alpha, was shown to be produced by microglia infected by *Toxoplasma gondii* (Fischer *et al*. 1997b) and microglia treated with soluble antigen from *Angiostrongylus cantonensis* (Wei *et al*. 2013). In our experiments, its production was not changed after stimulation of microglia by homogenate of transformed cercariae but it decreased significantly if this stimulus was administered to astrocytes. It seems that homogenate of transformed cercariae may cause attenuation of TNF-alpha secretion. This effect was demonstrated in case of microglia exposed to soluble factors from *Mesocestoides corti*; IL-6 and TNF-alpha production was diminished due to disruption of calcium signalling in microglia (Sun *et al*. 2014). On the contrary, recombinant cathepsins, especially TrCB2, triggered induction of TNF-

alpha secretion which might subsequently cause enhanced production of IL-6 as shown by Fisher *et al*. (1997b) in case of microglia infected by *Toxoplasma gondii*. In addition, increased concentration of TNF-alpha may induce chemokine expression in astrocytes as proved by Uddin *et al*. (2005), which could result in recruitment of peripheral leukocytes to the site of infection *in vivo*.

Importantly, prior to making conclusions about the cytokines produced by glial cells, the same notes as in case of NO have to be kept in mind: (i) the exact cell type serving as the source of cytokines has to be determined by the proper method and (ii) more repeating of stimulation experiments with recombinant cathepsins have to be done to confirm the effects. Furthermore, anti-inflammatory cytokines (IL-4, IL-10, TGF-beta) should be analysed as well to get more comprehensive idea about the ongoing immune response.

Being aware of the limitations mentioned above, we conclude that the first *in vitro* functional assays pursuing production of NO and proinflammatory cytokines by astrocytes and microglia stimulated by antigens of *T. regenti* were performed. We found that both astrocytes and microglia exposed to antigens of *T. regenti* are capable of NO synthesis which may take part in schistosomula elimination *in vivo*. Moreover, astrocytes and microglia were demonstrated to secrete IL-6 which *in vivo* might either promote development of inflammatory lesions around schistosomula or, concurrently, mediate protection of nervous tissue. Finally, astrocytes stimulated by *T. regenti* recombinant cathepsins seem to produce high levels of TNF-alpha which may enhance inflammation *in vitro* by enhancing IL-6 production. On the contrary, homogenate of transformed cercariae, the mixture of parasite's antigens, diminished TNF-alpha secretion suggesting possible role of some parasite's molecules in regulation of the host's inflammatory response.

6.4. *In vivo* experiments

To broaden the knowledge about the immune response of murine hosts to the infection by *T. regenti*, we performed *in vivo* experiments dedicated to analysis of MHC II+ cells presence in the CNS as well. MHC II+ cells, typically dendritic cells, B-lymphocytes and macrophages, but also activated microglia, present antigens to T-helper lymphocytes and thus mediate the immune response (Aloisi *et al*. 1998).

To visualise the interaction of MHC II+ cells with the parasite directly in the spinal cord, we used C57BL/6 MHC II-EGFP knock-in mice infected by red-stained cercariae of *T. regenti*. Staining of cercariae was enormously tricky. As they do not feed, ingestion of the dye was not possible; its free diffusion to cercarial body was hampered by a thick surface glycocalyx. In our laboratory, we have used carboxyfluorescein succinimidyl ester for staining cercariae of *T. regenti* (Pech 2013). It was also applied for long-term tracking of *Toxocara canis* larvae in mice (Kolbeková *et al*. 2011) and labelling of *Schistosoma mansoni* cercariae in skin invasion assays (Paveley *et al*. 2009). However,

it gives the green signal which was not suitable for our experiment. Thus, we tested other possibilities of labelling *T. regenti* cercariae or schistosomula (see Supplement 9.1) and only SNARF-1 was found to be suitable for its good penetration into the cercarial body, non-toxicity and signal persistence. This was appreciated also by Ligasová *et al*. (2011) who used other SNARF-1 derivative for estimation of pH in secretory glands of *T. regenti*.

Spinal cords with schistosomula of *T. regenti* were primarily intended for ultramicroscopic examination. It would allow 3D reconstruction of the tissue with the parasites and quantitation of MHC II+ cells would be possible like in the study of Ertürk *et al*. (2012) in which the authors quantified different cellular parameters after spinal cord injury. Unfortunately, the samples for ultramicroscopic examination were destructed, likely during the sample processing; nevertheless, the damage during the transport, e.g. by temperature shock, cannot be excluded.

In helminthic neuroinfections, MHC II+ cells regarded as B-lymphocytes and microglia/macrophages were observed spread diffusely or clustered perivascularly in brain granulomas of patients with neurocysticercosis (Restrepo *et al*. 2001, Alvarez *et al*. 2002). Indicative examination of squashed tissue samples of the spinal cords invaded by *T. regenti* disclosed MHC II+ cells both near schistosomula and in its migratory route. This resembled the distribution of macrophages and microglia observed by Lichtenbergová *et al*. (2011). Macrophages are canonical antigen presenting cells and microglia were also demonstrated to trigger T-lymphocyte proliferation and cytokine secretion which may then influence the course of the infection (Aloisi *et al*. 1998). Brain dendritic cells and, to a lesser extent, astrocytes also express MHC II (Zeinstra *et al*. 2000, Bulloch *et al*. 2008), thus cannot be excluded from the list of potential MHC II+ cells noticed in *T. regenti* infected spinal cords. It is obvious, that additional experiments employing cell-specific markers are needed to determine the identity the MHC II+ cells.

7. CONCLUSIONS

The presented thesis has been focused on evaluation of the role of astrocytes and microglia in the immune response of mice experimentally infected by *Trichobilharzia regenti*, the trematode migrating through the CNS of its vertebrate hosts. During migration, the inflammatory immune response is triggered, parasite's development is inhibited, and schistosomula, are gradually being damaged.

Considering the previously published data on *in situ* activation of astrocytes and microglia around the schistosomula, the capacity of those glial cells to produce nitric oxide and proinflammatory cytokines after *in vitro* stimulation by antigens of *T. regenti* origin was tested. These experiments represent the first *in vitro* functional assays of astrocytes and microglia exposed to *T. regenti* antigens. Furthermore, *in vivo* experiments dedicated to detection of MHC II+ cells in the infected spinal cords were performed as well.

In order to achieve the aims of the thesis, methods of parasitology, immunology, cell biology, and biochemistry were employed and the following results were obtained:

- Preparation of *in vitro* primary astrocyte and microglia cultures from neonatal murine brains, which was a prerequisite for stimulation experiments, was established in the Laboratory of Helminthology.
- Significant increase of NO production was demonstrated in cultures of both astrocytes and microglia after *in vitro* stimulation by homogenate of transformed cercariae of *T. regenti*. Recombinant cathepsins B1.1 and B2 of *T. regenti* were shown to trigger NO synthesis in astrocyte cultures too, but to a lesser extent. These data suggest possible NO production by glial cells during the infection of mice by *T. regenti*, which may participate in schistosomula destruction.
- Concentration of proinflammatory cytokines IL-6 and TNF-alpha was significantly elevated in supernatants from astrocyte and microglia cultures stimulated *in vitro* by *T. regenti* recombinant cathepsins B1.1 and B2, the latter being a very potent stimulus. These observations suggest a possible role of cathepsins in triggering inflammation during the infection. Homogenate of transformed cercariae caused increase in production of IL-6 by both astrocyte and microglia cultures, but decrease of TNF-alpha secretion in astrocyte cultures. It suggests ambiguous character of this mixture of antigens which probably consists of molecules both triggering and diminishing the inflammation *in vivo*.
- MHC II+ cells were detected in the spinal cords of mice infected by *T. regenti* which suggests their possible role in mediating the T-helper lymphocytes based immune

response against migrating schistosomula. The samples of the spinal cords infected by fluorescently labelled schistosomula intended for ultramicroscopic examination were prepared as well.

To summarize, the presented thesis has brought new data that contribute to extension of the knowledge about the host immune response against *T. regenti* with focus on the role of astrocytes and microglia. Based on the obtained results, implications for the *in vivo* infections have been outlined and the future experiments testing these hypotheses have been proposed.

8. REFERENCES

Abbott NJ, Rönnbäck L, Hansson E (**2006**). Astrocyte-endothelial interactions at the blood-brain barrier. *Nat. Rev. Neurosci.* 7, 41–53.

Abd-El-Basset E, Fedoroff S (**1995**). Effect of bacterial wall lipopolysaccharide (LPS) on morphology, motility, and cytoskeletal organization of microglia in cultures. *J. Neurosci. Res.* 41, 222–37.

Ahmed SF, Oswald IP, Caspar P, Hieny S, Keefer L, Sher A, James SL (**1997**). Developmental differences determine larval susceptibility to nitric oxide-mediated killing in a murine model of vaccination against *Schistosoma mansoni*. *Infect. Immun.* 65, 219–26.

Aloisi F, Ria F, Penna G, Adorini L (**1998**). Microglia are more efficient than astrocytes in antigen processing and in Th1 but not Th2 cell activation. *J. Immunol.* 160, 4671–80.

Alonso-Trujillo J, Rivera-Montoya I, Rodríguez-Sosa M, Terrazas LI (**2007**). Nitric oxide contributes to host resistance against experimental *Taenia crassiceps* cysticercosis. *Parasitol. Res.* 100, 1341–50.

Alvarez J, Colegial C, Castaño C, Trujillo J, Teale J, Restrepo B (**2002**). The human nervous tissue in proximity to granulomatous lesions induced by *Taenia solium* metacestodes displays an active response. *J. Neuroimmunol.* 127, 139–44.

Alvarez J, Teale JM (**2008**). Multiple expression of matrix metalloproteinases in murine neurocysticercosis: Implications for leukocyte migration through multiple central nervous system barriers. *Brain Res.* 1214, 145–58.

Alvarez JI, Teale JM (**2006**). Breakdown of the blood brain barrier and blood-cerebrospinal fluid barrier is associated with differential leukocyte migration in distinct compartments of the CNS during the course of murine NCC. *J. Neuroimmunol.* 173, 45–55.

Amin DN, Rottenberg ME, Thomsen AR, Mumba D, Fenger C, Kristensson K, Büscher P, Finsen B, Masocha W (**2009**). Expression and role of CXCL10 during the encephalitic stage of experimental and clinical African trypanosomiasis. *J. Infect. Dis.* 200, 1556–1565.

Amri M, Aissa SA, Belguendouz H, Mezioug D, Touil-Boukoffa C (**2007**). *In vitro* antihydatic action of IFN-gamma is dependent on the nitric oxide pathway. *J. Interferon Cytokine Res.* 27, 781–7.

Amrouni D, Gautier-Sauvigné S, Meiller A, Vincendeau P, Bouteille B, Buguet A, Cespuglio R (**2010**). Cerebral and peripheral changes occurring in nitric oxide (NO) synthesis in a rat model of sleeping sickness: identification of brain iNOS expressing cells. *PLoS One* 5, e9211.

Andrade MA, Siles-Lucas M, Espinoza E, Arellano JLP, Gottstein B, Muro A (**2004**). *Echinococcus multilocularis* laminated-layer components and the E14t 14-3-3 recombinant protein decrease NO production by activated rat macrophages *in vitro*. *Nitric Oxide* 10, 150–155.

Asher R, Morgenstern D, Fidler P, Adcock K, Oohira A, Braistead J, Levine J, Margolis R, Rogers J, Fawcett J (**2000**). Neurocan is upregulated in injured brain and in cytokine-treated astrocytes. *J. Neurosci.* 20, 2427–38.

Bakhiet M, Hamadien M, Tjernlund A, Mousal A, Seiger A (**2002a**). African trypanosomes activate human fetal brain cells to proliferation and IFN-gamma production. *Neuroreport* 13, 53–56.

Bakhiet M, Mousa A, Seiger Å, Andersson J (**2002b**). Constitutive and inflammatory induction of α and β chemokines in human first trimester forebrain astrocytes and neurons. *Mol. Immunol.* 38, 921–929.

Bancroft GJ, Sutton CJ, Morris AG, Askonas BA (**1983**). Production of interferons during experimental African trypanosomiasis. *Clin. Exp. Immunol.* 52, 135–43.

Bechmann I, Steiner B, Gimsa U, Mor G, Wolf S, Beyer M, Nitsch R, Zipp F (**2002**). Astrocyte-induced T cell elimination is CD95 ligand dependent. *J. Neuroimmunol.* 132, 60–5.

Becker K, Jährling N, Saghafi S, Weiler R, Dodt H-U (**2012**). Chemical clearing and dehydration of GFP expressing mouse brains. *PLoS One* 7, e33916.

Bell MD, Lopez-Gonzalez R, Lawson L, Hughes D, Fraser I, Gordon S, Perry VH (**1994**). Upregulation of the macrophage scavenger receptor in response to different forms of injury in the CNS. *J. Neurocytol.* 23, 605–13.

Benedetto N, Folgore A, Romano Carratelli C, Galdiero F (**2001**). Effects of cytokines and prolactin on the replication of *Toxoplasma gondii* in murine microglia. *Eur. Cytokine Netw.* 12, 348–58.

Bian K, Harari Y, Zhong M, Lai M, Castro G, Weisbrodt N, Murad F (**2001**). Down-regulation of inducible nitric-oxide synthase (NOS-2) during parasite-induced gut inflammation: a path to identify a selective NOS-2 inhibitor. *Mol. Pharmacol.* 59, 939–47.

Bian K, Zhong M, Harari Y, Lai M, Weisbrodt N, Murad F (**2005**). Helminth regulation of host IL-4Ralpha/Stat6 signaling: mechanism underlying NOS-2 inhibition by *Trichinella spiralis*. *Proc. Natl. Acad. Sci.* 102, 3936–41.

Blanchard N, Dunay IR, Schlüter D (**2015**). Persistence of *Toxoplasma gondii* in the central nervous system: a fine tuned balance between the parasite, the brain and the immune system. *Parasite Immunol.* 37, 150–8.

Blank WA, Liu SF, Prasad J, Blanton RE (**2011**). Host mouse strain is not selective for a laboratory adapted strain of *Schistosoma mansoni*. *J. Parasitol.* 97, 518–21.

Blažová K, Horák P (**2005**). *Trichobilharzia regenti*: the developmental differences in natural and abnormal hosts. *Parasitol. Int.* 54, 167–72.

Boczoń K, Wandurska-Nowak E, Wierzbicki A, Frydrychowicz M, Mozer-Lisewska I, Zeromski J (**2004**). mRNA expression and immunohistochemical localization of inducible nitric oxide synthase (NOS-2) in the muscular niche of *Trichinella spiralis*. *Folia Histochem. Cytobiol.* 42, 209–13.

Bogdan C (**2015**). Nitric oxide synthase in innate and adaptive immunity: an update. *Trends Immunol.* 36, 161–178.

Boje KM, Arora PK (**1992**). Microglial-produced nitric oxide and reactive nitrogen oxides mediate neuronal cell death. *Brain Res.* 587, 250–6.

Braak E (**1975**). On the fine structure of the external glial layer in the isocortex of man. *Cell Tissue Res.* 157, 367–90.

Brenier-Pinchart M-P, Blanc-Gonnet E, Marche PN, Berger F, Durand F, Ambroise-Thomas P, Pelloux H (**2004**). Infection of human astrocytes and glioblastoma cells with *Toxoplasma gondii*: monocyte chemotactic protein-1 secretion and chemokine expression *in vitro*. *Acta Neuropathol.* 107, 245–249.

Brown AM, Ransom BR (**2007**). Astrocyte glycogen and brain energy metabolism. *Glia* 55, 1263–71.

Brown GC, Bolaños JP, Heales SJR, Clark JB (**1995**). Nitric oxide produced by activated astrocytes rapidly and reversibly inhibits cellular respiration. *Neurosci. Lett.* 193, 201–204.

Brown H, Turner G, Rogerson S, Tembo M, Mwenechanya J, Molyneux M, Taylor T (**1999**). Cytokine expression in the brain in human cerebral malaria. *J. Infect. Dis.* 180, 1742–1746.

Brown J, Voge M (**1982**). Neuropathology of parasitic pnfections, 1st ed. Oxford University Press.

Bulloch K, Miller M, Gal-Toth J, Milner T, Gottfried-Blackmore A, Waters EM, Kaunzner UW, Liu K, Lindquist R, Nussenzweig MC, Steinman RM, McEwen BS (**2008**). CD11c/EYFP transgene illuminates a discrete network of dendritic cells within the embryonic, neonatal, adult, and injured mouse brain. *J. Comp. Neurol.* 508, 687–710.

Burke JM, Roberts CW, Hunter CA, Murray M, Alexander J (**1994**). Temporal differences in the expression of mRNA for IL-10 and IFN-gamma in the brains and spleens of C57BL/10 mice infected with *Toxoplasma gondii*. *Parasite Immunol.* 16, 305–314.

Burney S, Caulfield JL, Niles JC, Wishnok JS, Tannenbaum SR (**1999**). The chemistry of DNA damage from nitric oxide and peroxynitrite. *Mutat. Res.*

Bush T, Puvanachandra N, Horner C, Polito A, Ostenfeld T, Svendsen C, Mucke L, Johnson M, Sofroniew M (**1999**). Leukocyte infiltration, neuronal degeneration, and neurite outgrowth after ablation of scar-forming, reactive astrocytes in adult transgenic mice. *Neuron* 23, 297–308.

Bushong EA, Martone ME, Jones YZ, Ellisman MH (**2002**). Protoplasmic astrocytes in CA1 stratum radiatum occupy separate anatomical domains. *J. Neurosci.* 22, 183–92.

Carbonell WS, Murase S-I, Horwitz AF, Mandell JW (**2005**). Infiltrative microgliosis: activation and long-distance migration of subependymal microglia following periventricular insults. *J. Neuroinflammation* 2, 5.

Carpio A (**2002**). Neurocysticercosis: an update. *Lancet Infect. Dis.* 2, 751–62.

Carson MJ, Doose JM, Melchior B, Schmid CD, Ploix CC (**2006**). CNS immune privilege: hiding in plain sight. *Immunol. Rev.* 213, 48–65.

Castro L, Rodriguez M, Radi R (**1994**). Aconitase is readily inactivated by peroxynitrite, but not by its precursor, nitric oxide. *J. Biol. Chem.* 269, 29409–15.

Cekanaviciute E, Dietrich HK, Axtell RC, Williams AM, Egusquiza R, Wai KM, Koshy AA, Buckwalter MS (**2014**). Astrocytic TGF-β signaling limits inflammation and reduces neuronal damage during central nervous system *Toxoplasma infection*. *J. Immunol.* 193, 139–49.

Chanová M, Bulantová J, Máslo P, Horák P (**2009**). *In vitro* cultivation of early schistosomula of nasal and visceral bird schistosomes (*Trichobilharzia* spp., Schistosomatidae). *Parasitol. Res.* 104, 1445–52.

Chanová M, Horák P (**2007**). Terminal phase of bird schistosomiasis caused by *Trichobilharzia regenti* (Schistosomatidae) in ducks (*Anas platyrhynchos* f. *domestica*). *Folia Parasitol.* 54, 105–7.

Chanová M, Hrdý J (**2013**). The impact of Th1/Th2 balance on migration of *Trichobilharzia* sp. schistosomula in mice. *In: Kuchta R, Soldánová M, Hodová I (Eds), 20th Helminthological Days: Programme & Abstracts*. Masaryk University, Brno, p. 15.

Chanová M, Lichtenbergová L, Bulantová J, Mikeš L, Horák P (**2011**). *Trichobilharzia regenti*: Antigenic structures of intravertebrate stages. *Cent. Eur. J. Biol.* 7, 83–90.

Chao CC, Anderson WR, Hu S, Gekker G, Martella A, Peterson PK (**1993a**). Activated microglia inhibit multiplication of *Toxoplasma gondii* via a nitric oxide mechanism. *Clin. Immunol. Immunopathol.* 67, 178–83.

Chao CC, Gekker G, Hu S, Peterson PK (**1994**). Human microglial cell defense against *Toxoplasma gondii*. The role of cytokines. *J. Immunol.* 152, 1246–52.

Chao CC, Hu S, Gekker G, Novick WJ, Remington JS, Peterson PK (**1993b**). Effects of cytokines on multiplication of *Toxoplasma gondii* in microglial cells. *J. Immunol.* 150, 3404–10.

Chen Y, Klionsky DJ (**2011**). The regulation of autophagy – unanswered questions. *J. Cell Sci.* 124, 161–70.

Chen Y, Vartiainen N, Ying W, Chan P, Koistinaho J, Swanson R (**2001**). Astrocytes protect neurons from nitric oxide toxicity by a glutathione-dependent mechanism. *J. Neurochem.* 77, 1601–10.

Chianella S, Semprevivo M, Peng ZC, Zaccheo D, Bentivoglio M, Grassi-Zucconi G (**1999**). Microglia activation in a model of sleep disorder: an immunohistochemical study in the rat brain during *Trypanosoma brucei* infection. *Brain Res.* 832, 54–62.

Christopherson KS, Ullian EM, Stokes CCA, Mullowney CE, Hell JW, Agah A, Lawler J, Mosher DF, Bornstein P, Barres BA (**2005**). Thrombospondins are astrocyte-secreted proteins that promote CNS synaptogenesis. *Cell* 120, 421–33.

Coulson PS, Smythies LE, Betts C, Mabbott NA, Sternberg JM, Wei XG, Liew FY, Wilson RA (**1998**). Nitric oxide produced in the lungs of mice immunized with the radiation-attenuated schistosome vaccine is not the major agent causing challenge parasite elimination. *Immunology* 93, 55–63.

Crain JM, Nikodemova M, Watters JJ (**2013**). Microglia express distinct M1 and M2 phenotypic markers in the postnatal and adult central nervous system in male and female mice. *J. Neurosci. Res.* 91, 1143–1151.

Da Mata JRC, Chiari SER, Machado E, Da Mata CRS, Camargos JR (**2000**). *Trypanosoma cruzi* infection and the rat central nervous system: Proliferation of parasites in astrocytes and the brain reaction to parasitism. *Brain Res. Bull.* 53, 153–162.

Dai WJ, Gottstein B (**1999**). Nitric oxide-mediated immunosuppression following murine *Echinococcus multilocularis* infection. *Immunology* 97, 107–16.

Dai WJ, Waldvogel A, Jungi T, Stettler M, Gottstein B (**2003**). Inducible nitric oxide synthase deficiency in mice increases resistance to chronic infection with *Echinococcus multilocularis*. *Immunology* 108, 238–44.

Davis EJ, Foster TD, Thomas WE (**1994**). Cellular forms and functions of brain microglia. *Brain Res. Bull.* 34, 73–8.

De Oliveira DM, do Carmo SA, Silva-Teixeira DN, Goes AM (**1998**). Immunization with PIII, a fraction of *Schistosoma mansoni* soluble adult worm antigenic preparation, affects nitric oxide production by murine spleen cells. *Mem. Inst. Oswaldo Cruz* 93 Suppl 1, 175–80.

De Simone R, Giampaolo A, Giometto B, Gallo P, Levi G, Peschle C, Aloisi F (**1995**). The costimulatory molecule B7 is expressed on human microglia in culture and in multiple sclerosis acute lesions. *J. Neuropathol. Exp. Neurol.* 54, 175–87.

Deckert-Schlüter M, Buck C, Weiner D, Kaefer N, Rang A, Hof H, Wiestler OD, Schlüter D (**1997**). Interleukin-10 downregulates the intracerebral immune response in chronic *Toxoplasma* encephalitis. *J. Neuroimmunol.* 76, 167–76.

Deininger MH, Kremsner PG, Meyermann R, Schluesener HJ (**2000**). Differential cellular accumulation of transforming growth factor-beta1, -beta2, and -beta3 in brains of patients who died with cerebral malaria. *J. Infect. Dis.* 181, 2111–5.

Deng Y, Xie D, Fang M, Zhu G, Chen C, Zeng H, Lu J, Charanjit K (**2014**). Astrocyte-derived proinflammatory cytokines induce hypomyelination in the periventricular white matter in the hypoxic neonatal brain. *PLoS One* 9, e87420.

Dent J, Nichols R, Beaver P, Carrera G, Staggers R (**1956**). Visceral *larva migrans*; with a case report. *Am. J. Pathol.* 32, 777–803.

Dheen ST, Jun Y, Yan Z, Tay SSW, Ling EA (**2005**). Retinoic acid inhibits expression of TNF-alpha and iNOS in activated rat microglia. *Glia* 50, 21–31.

Dodt H-U, Leischner U, Schierloh A, Jährling N, Mauch CP, Deininger K, Deussing JM, Eder M, Zieglgänsberger W, Becker K (**2007**). Ultramicroscopy: three-dimensional visualization of neuronal networks in the whole mouse brain. *Nat. Methods* 4, 331–6.

Dolecková K, Albrecht T, Mikes L, Horák P (**2010**). Cathepsins B1 and B2 in the neuropathogenic schistosome *Trichobilharzia regenti*: distinct gene expression profiles and presumptive roles throughout the life cycle. *Parasitol. Res.* 107, 751–5.

Dolecková K, Kasný M, Mikes L, Cartwright J, Jedelský P, Schneider EL, Dvorák J, Mountford AP, Craik CS, Horák P (**2009**). The functional expression and characterisation of a cysteine peptidase from the invasive stage of the neuropathogenic schistosome *Trichobilharzia regenti*. *Int. J. Parasitol.* 39, 201–11.

Dringen R, Gutterer JM, Hirrlinger J (**2000**). Glutathione metabolism in brain metabolic interaction between astrocytes and neurons in the defense against reactive oxygen species. *Eur. J. Biochem.* 267, 4912–6.

Durand F, Brenier-Pinchart MP, Berger F, Marche PN, Grillot R, Pelloux H (**2004**). Phosphatidylcholine-specific phospholipase C but not gamma interferon regulate gene expression and secretion of CC chemokine ligand-2 (CCL-2) by human astrocytes during infection by *Toxoplasma gondii*. *Parasite Immunol.* 26, 419–422.

Dvorák J, Delcroix M, Rossi A, Vopálenský V, Pospísek M, Sedinová M, Mikes L, Sajid M, Sali A, McKerrow JH, Horák P, Caffrey CR (**2005**). Multiple cathepsin B isoforms in schistosomula of *Trichobilharzia regenti*: identification, characterisation and putative role in migration and nutrition. *Int. J. Parasitol.* 35, 895–910.

Eddelston M, Mucke L (**1993**). Molecular profile of reactive astrocytes – implications for their role in neurologic disease. *Neuroscience*.

Ertürk A, Mauch CP, Hellal F, Förstner F, Keck T, Becker K, Jährling N, Steffens H, Richter M, Hübener M, Kramer E, Kirchhoff F, Dodt HU, Bradke F (**2012**). Three-dimensional imaging of the unsectioned adult spinal cord to assess axon regeneration and glial responses after injury. *Nat. Med.* 18, 166–71.

Esparza I, Männel D, Ruppel A, Falk W, Krammer PH (**1987**). Interferon gamma and lymphotoxin or tumor necrosis factor act synergistically to induce macrophage killing of tumor cells and schistosomula of *Schistosoma mansoni*. *J. Exp. Med.* 166, 589–94.

Farina C, Aloisi F, Meinl E (**2007**). Astrocytes are active players in cerebral innate immunity. *Trends Immunol.* 28, 138–45.

Feldmann M, Pathipati P, Sheldon RA, Jiang X, Ferriero DM (**2014**). Isolating astrocytes and neurons sequentially from postnatal murine brains with a magnetic cell separation technique. *J. Biol. Methods* 1, 11.

Fidler P, Schuette K, Asher R, Dobbertin A, Thornton S, Calle-Patino Y, Muir E, Levine J, Geller H, Rogers J, Faissner A, Fawcett J (**1999**). Comparing astrocytic cell lines that are inhibitory or permissive for axon growth: the major axon-inhibitory proteoglycan is NG2. *J. Neurosci.* 19, 8778–88.

Finsterer J, Auer H (**2013**). Parasitoses of the human central nervous system. *J. Helminthol.* 87, 257–70.

Fischer HG, Nitzgen B, Reichmann G, Gross U, Hadding U (**1997a**). Host cells of *Toxoplasma gondii* encystation in infected primary culture from mouse brain. *Parasitol. Res.* 83, 637–41.

Fischer HG, Nitzgen B, Reichmann G, Hadding U (**1997b**). Cytokine responses induced by *Toxoplasma gondii* in astrocytes and microglial cells. *Eur. J. Immunol.* 27, 1539–1548.

Floden AM, Combs CK (**2007**). Microglia repetitively isolated from *in vitro* mixed glial cultures retain their initial phenotype. *J. Neurosci. Methods* 164, 218–24.

Fok-Seang J, Smith-Thomas LC, Meiners S, Muir E, Du J-S, Housden E, Johnson AR, Faissner A, Geller HM, Keynes RJ, Rogers JH, Fawcett JW (**1995**). An analysis of astrocytic cell lines with different abilities to promote axon growth. *Brain Res.* 689, 207–223.

Ford A, Foulcher E, Lemckert F (**1996**). Microglia induce CD4 T lymphocyte final effector function and death. *J.* 184, 1737–45.

Ford AL, Goodsall AL, Hickey WF, Sedgwick JD (**1995**). Normal adult ramified microglia separated from other central nervous system macrophages by flow cytometric sorting. Phenotypic differences defined and direct *ex vivo* antigen presentation to myelin basic protein-reactive CD4+ T cells compared. *J. Immunol.* 154, 4309–21.

Furuoka H, Sato H, Kubo M, Owaki S, Kobayashi Y, Matsui T, Kamiya H (**2003**). Neuropathological observation of rabbits (*Oryctolagus cuniculus*) affected with raccoon roundworm (*Baylisascaris procyonis*) *larva migrans* in Japan. *J. Vet. Med. Sci.* 65, 695–9.

Ganter S, Northoff H, Männel D, Gebicke-Härter PJ (**1992**). Growth control of cultured microglia. *J. Neurosci. Res.* 33, 218–30.

Garcia HH, Tanowitz HB, Del Brutto OH (Eds) (**2013**). Neuroparasitology and tropical neurology, 1st ed*., Handbook of Clinical Neurology*. Elsevier.

Gebreselassie NG, Moorhead AR, Fabre V, Gagliardo LF, Lee NA, Lee JJ, Appleton JA (**2012**). Eosinophils preserve parasitic nematode larvae by regulating local immunity. *J. Immunol.* 188, 417–25.

Gimsa U, ØRen A, Pandiyan P, Teichmann D, Bechmann I, Nitsch R, Brunner-Weinzierl MC (**2004**). Astrocytes protect the CNS: antigen-specific T helper cell responses are inhibited by astrocyte-induced upregulation of CTLA-4 (CD152). *J. Mol. Med. (Berl).* 82, 364–72.

Girard M, Ayed Z, Preux PM, Bouteille B, Preud'Homme JL, Dumas M, Jauberteau MO (**2000**). *In vitro* induction of nitric oxide synthase in astrocytes and microglia by *Trypanosoma brucei brucei*. *Parasite Immunol.* 22, 7–12.

Girard M, Bisser S, Courtioux B, Vermot-Desroches C, Bouteille B, Wijdenes J, Preud'homme J-L, Jauberteau M-O (**2003**). *In vitro* induction of microglial and endothelial cell apoptosis by

cerebrospinal fluids from patients with human African trypanosomiasis. *Int. J. Parasitol.* 33, 713–20.

Giulian D, Baker TJ (**1986**). Characterization of ameboid microglia isolated from developing mammalian brain. *J. Neurosci.* 6, 2163–78.

Glezer I, Simard AR, Rivest S (**2007**). Neuroprotective role of the innate immune system by microglia. *Neuroscience* 147, 867–83.

Gordon R, Hogan CE, Neal ML, Anantharam V, Kanthasamy AG, Kanthasamy A (**2011**). A simple magnetic separation method for high-yield isolation of pure primary microglia. *J. Neurosci. Methods* 194, 287–96.

Graeber MB (**2010**). Changing face of microglia. *Science* 330, 783–788.

Gray CA, Lawrence RA (**2002**). Interferon-gamma and nitric oxide production are not required for the immune-mediated clearance of *Brugia malayi* microfilariae in mice. *Parasite Immunol.* 24, 329–36.

Guarner J, Bartlett J, Zaki SR, Colley DG, Grijalva MJ, Powell MR (**2001**). Mouse model for Chagas disease: Immunohistochemical distribution of different stages of *Trypanosoma cruzi* in tissues throughout infection. *Am. J. Trop. Med. Hyg.* 65, 152–158.

Hahn UK, Bender RC, Bayne CJ (**2001**). Involvement of nitric oxide in killing of *Schistosoma mansoni* sporocysts by hemocytes from resistant *Biomphalaria glabrata*. *J. Parasitol.* 87, 778–785.

Halonen SK, Chiu FC, Weiss LM (**1998**). Effect of cytokines on growth of *Toxoplasma gondii* in murine astrocytes. *Infect. Immun.* 66, 4989–4993.

Halonen SK, Lyman WD, Chiu FC (**1996**). Growth and development of *Toxoplasma gondii* in human neurons and astrocytes. *J. Neuropathol. Exp. Neurol.* 55, 1150–6.

Halonen SK, Weiss LM (**2000**). Investigation into the mechanism of gamma interferon-mediated inhibition of *Toxoplasma gondii* in murine astrocytes. *Infect. Immun.* 68, 3426–3430.

Hamby ME, Uliasz TF, Hewett SJ, Hewett JA (**2006**). Characterization of an improved procedure for the removal of microglia from confluent monolayers of primary astrocytes. *J. Neurosci. Methods* 150, 128–37.

Hamilton CM, Brandes S, Holland C V, Pinelli E (**2008**). Cytokine expression in the brains of *Toxocara canis*-infected mice. *Parasite Immunol.* 30, 181–5.

Han H-E, Kim T-K, Son H-J, Park WJ, Han P-L (**2013**). Activation of autophagy pathway suppresses the expression of iNOS, IL6 and cell death of LPS-stimulated microglia cells. *Biomol. Ther.* 21, 21–8.

Hao C, Guilbert LJ, Fedoroff S (**1990**). Production of colony-stimulating factor-1 (CSF-1) by mouse astroglia *in vitro*. *J. Neurosci. Res.* 27, 314–23.

Harms AS, Lee J-K, Nguyen TA, Chang J, Ruhn KM, Treviño I, Tansey MG (**2012**). Regulation of microglia effector functions by tumor necrosis factor signaling. *Glia* 60, 189–202.

Hartmann S, Schönemeyer A, Sonnenburg B, Vray B, Lucius R (**2002**). Cystatins of filarial nematodes up-regulate the nitric oxide production of interferon-gamma-activated murine macrophages. *Parasite Immunol.* 24, 253–62.

Haseloff RF, Blasig IE, Bauer HC, Bauer H (**2005**). In search of the astrocytic factor(s) modulating blood-brain barrier functions in brain capillary endothelial cells in vitro. *Cell. Mol. Neurobiol.* 25, 25–39.

Heneka MT, Kummer MP, Latz E (**2014**). Innate immune activation in neurodegenerative disease. *Nat. Rev. Immunol.* 14, 463–77.

Henn A, Lund S, Hedtjärn M, Schrattenholz A, Pörzgen P, Leist M (**2009**). The suitability of BV2 cells as alternative model system for primary microglia cultures or for animal experiments examining brain inflammation. *ALTEX* 26, 83–94.

Henn FA, Haljamäe H, Hamberger A (**1972**). Glial cell function: active control of extracellular K+ concentration. *Brain Res.* 43, 437–43.

Hibbs JB, Taintor RR, Vavrin Z (**1987a**). Macrophage cytotoxicity: role for L-arginine deiminase and imino nitrogen oxidation to nitrite. *Science* 235, 473–6.

Hibbs JB, Vavrin Z, Taintor RR (**1987b**). L-arginine is required for expression of the activated macrophage effector mechanism causing selective metabolic inhibition in target cells. *J. Immunol.* 138, 550–65.

Hirata M, Hirata K, Kage M, Zhang M, Hara T, Fukuma T (**2001**). Effect of nitric oxide synthase inhibition on *Schistosoma japonicum* egg-induced granuloma formation in the mouse liver. *Parasite Immunol.* 23, 281–9.

Horák P, Dvořák J, Kolářová L, Trefil L (**1999**). *Trichobilharzia regenti*, a pathogen of the avian and mammalian central nervous systems. *Parasitology* 119, 577–81.

Horák P, Kolářová L (**2011**). Snails, waterfowl and cercarial dermatitis. *Freshw. Biol.* 56, 779–790.

Horák P, Kolářová L, Dvořák J (**1998**). *Trichobilharzia regenti* n. sp. (Schistosomatidae, Bilharziellinae), a new nasal schistosome from Europe. *Parasite* 5, 349–57.

Horák P, Mikeš L, Lichtenbergová L, Skála V, Soldánová M, Brant SV (**2015**). Avian schistosomes and outbreaks of cercarial dermatitis. *Clin. Microbiol. Rev.* 28, 165–190.

Horák P, Mikeš L, Rudolfová J, Kolářová L (**2008**). Penetration of *Trichobilharzia* cercariae into mammals: dangerous or negligible event? *Parasite* 15, 299–303.

Horvath RJ, Nutile-McMenemy N, Alkaitis MS, Deleo JA (**2008**). Differential migration, LPS-induced cytokine, chemokine, and NO expression in immortalized BV-2 and HAPI cell lines and primary microglial cultures. *J. Neurochem.* 107, 557–69.

Hozumi I, Chiu FC, Norton WT (**1990**). Biochemical and immunocytochemical changes in glial fibrillary acidic protein after stab wounds. *Brain Res.* 524, 64–71.

Hrádková K, Horák P (**2002**). Neurotropic behaviour of *Trichobilharzia regenti* in ducks and mice. *J. Helminthol.* 76, 137–41.

Hsieh CL, Koike M, Spusta SC, Niemi EC, Yenari M, Nakamura MC, Seaman WE (**2009**). A role for TREM2 ligands in the phagocytosis of apoptotic neuronal cells by microglia. *J. Neurochem.* 109, 1144–56.

Hu S, Martella A, Anderson WR, Chao CC (**1994**). Role of cytokines in lipopolysaccharide-induced functional and structural abnormalities of astrocytes. *Glia* 10, 227–34.

Huh S, Wang KC, Hong ST, Chai JY, Lee SH, Choi KS, Chi JG (**1993**). Histopathological changes of the cat brain in experimental sparganosis. *Pathol. Res. Pract.* 189, 1181–6.

Hunter CA, Abrams JS, Beaman MH, Remington JS (**1993**). Cytokine mRNA in the central nervous system of SCID mice infected with *Toxoplasma gondii*: Importance of T-cell-independent regulation of resistance to *T. gondii*. *Infect. Immun.* 61, 4038–4044.

Hunter CA, Gow JW, Kennedy PGE, Jennings FW, Murray M (**1991**). Immunopathology of experimental African sleeping sickness: Detection of cytokine mRNA in the brains of *Trypanosoma brucei brucei*-infected mice. *Infect. Immun.* 59, 4636–4640.

Hunter CA, Roberts CW, Alexander J (**1992a**). Kinetics of cytokine mRNA production in the brains of mice with progressive toxoplasmic encephalitis. *Eur. J. Immunol.* 22, 2317–2322.

Hunter CA, Roberts CW, Murray M, Alexander J (**1992b**). Detection of cytokine mRNA in the brains of mice with toxoplasmic encephalitis. *Parasite Immunol.* 14, 405–413.

Iglesias BM, Cerase J, Ceracchini C, Levi G, Aloisi F (**1997**). Analysis of B7-1 and B7-2 costimulatory ligands in cultured mouse microglia: upregulation by interferon-γ and lipopolysaccharide and downregulation by interleukin-10, prostaglandin E2 and cyclic AMP-elevating agents. *J. Neuroimmunol.* 72, 83–93.

Ito D, Imai Y, Ohsawa K, Nakajima K, Fukuuchi Y, Kohsaka S (**1998**). Microglia-specific localisation of a novel calcium binding protein, Iba1. *Brain Res. Mol. Brain Res.* 57, 1–9.

Ito D, Tanaka K, Suzuki S, Dembo T, Fukuuchi Y (**2001**). Enhanced expression of Iba1, ionized calcium-binding adapter molecule 1, after transient focal cerebral ischemia in rat brain. *Stroke.* 32, 1208–15.

Iyengar R, Stuehr DJ, Marletta MA (**1987**). Macrophage synthesis of nitrite, nitrate, and N-nitrosamines: precursors and role of the respiratory burst. *Proc. Natl. Acad. Sci.* 84, 6369–73.

Jährling N, Becker K, Dodt H-U (**2009**). 3D-reconstruction of blood vessels by ultramicroscopy. *Organogenesis* 5, 227–30.

Jährling N, Becker K, Kramer E, Dodt H (**2008**). 3D-visualization of nerve fiber bundles by ultramicroscopy. *Med. Laser Appl.* 23, 209–215.

James SL, Glaven J (**1989**). Macrophage cytotoxicity against schistosomula of *Schistosoma mansoni* involves arginine-dependent production of reactive nitrogen intermediates. *J. Immunol.* 143, 4208–12.

Janecek E, Beineke A, Schnieder T, Strube C (**2014**). Neurotoxocarosis: marked preference of *Toxocara canis* for the cerebrum and *T. cati* for the cerebellum in the paratenic model host mouse. *Parasit. Vectors* 7, 194.

Janota I, Doshi B (**1979**). Cerebral malaria in the United Kingdom. *J. Clin. Pathol.* 32, 769–72.

Janzer RC, Raff MC (**1987**). Astrocytes induce blood-brain barrier properties in endothelial cells. *Nature* 325, 253–7.

Jekabsone A, Mander PK, Tickler A, Sharpe M, Brown GC (**2006**). Fibrillar beta-amyloid peptide Abeta1-40 activates microglial proliferation via stimulating TNF-alpha release and H_2O_2 derived from NADPH oxidase: a cell culture study. *J. Neuroinflammation* 3, 24.

Jennings VM, Lal AA, Hunter RL (**1998**). Evidence for multiple pathologic and protective mechanisms of murine cerebral malaria. *Infect. Immun.* 66, 5972–9.

Jin Y, Choi IY, Kim C, Hong S, Kim W-K (**2009**). Excretory-secretory products from *Paragonimus westermani* increase nitric oxide production in microglia in PKC-dependent and -independent manners. *Neurosci. Res.* 65, 141–7.

Jin Y, Lee J-C, Choi IY, Kim EA, Shin MH, Kim W-K (**2006**). Excretory-secretory products produced by *Paragonimus westermani* differentially regulate the nitric oxide production and viability of microglial cells. *Int. Arch. Allergy Immunol.* 139, 16–24.

Jones LL, Margolis RU, Tuszynski MH (**2003**). The chondroitin sulfate proteoglycans neurocan, brevican, phosphacan, and versican are differentially regulated following spinal cord injury. *Exp. Neurol.* 182, 399–411.

Jones TC, Bienz KA, Erb P (**1986**). In vitro cultivation of *Toxoplasma gondii* cysts in astrocytes in the presence of gamma interferon. *Infect. Immun.* 51, 147–156.

Jouet D, Skírnisson K, Kolárová L, Ferté H (**2010**). Final hosts and variability of *Trichobilharzia regenti* under natural conditions. *Parasitol. Res.* 107, 923–30.

Jun CD, Kim SH, Soh CT, Kang SS, Chung HT (**1993**). Nitric oxide mediates the toxoplasmastatic activity of murine microglial cells *in vitro*. *Immunol. Invest.* 22, 487–501.

Kacem K, Lacombe P, Seylaz J, Bonvento G (**1998**). Structural organization of the perivascular astrocyte endfeet and their relationship with the endothelial glucose transporter: a confocal microscopy study. *Glia* 23, 1–10.

Kanazawa T, Asahi H, Hata H, Mochida K, Kagei N, Stadecker MJ (**1993**). Arginine-dependent generation of reactive nitrogen intermediates is instrumental in the *in vitro* killing of protoscoleces of *Echinococcus multilocularis* by activated macrophages. *Parasite Immunol.* 15, 619–23.

Kasný M, Mikes L, Dalton JP, Mountford AP, Horák P (**2007**). Comparison of cysteine peptidase activities in *Trichobilharzia regenti* and *Schistosoma mansoni* cercariae. *Parasitology* 134, 1599–609.

Keita M, Bouteille B, Enanga B, Vallat JM, Dumas M (**1997**). *Trypanosoma brucei brucei*: a long-term model of human African trypanosomiasis in mice, meningo-encephalitis, astrocytosis, and neurological disorders. *Exp. Parasitol.* 85, 183–192.

Kelvin E, Carpio A, Bagiella E, Leslie D, Leon P, Andrews H, Hauser WA (**2011**). Seizure in people with newly diagnosed active or transitional neurocysticercosis. *Seizure* 20, 119–25.

Kobayashi K, Imagama S, Ohgomori T, Hirano K, Uchimura K, Sakamoto K, Hirakawa A, Takeuchi H, Suzumura A, Ishiguro N, Kadomatsu K (**2013**). Minocycline selectively inhibits M1 polarization of microglia. *Cell Death Dis.* 4, e525.

Kofler J, Wiley CA (**2011**). Microglia: key innate immune cells of the brain. *Toxicol. Pathol.* 39, 103–14.

Kolářová L, Horák P, Čada F (**2001**). Histopathology of CNS and nasal infections caused by *Trichobilharzia regenti* in vertebrates. *Parasitol. Res.* 87, 644–650.

Kolářová L, Horák P, Skírnisson K, Marečková H, Doenhoff M (**2013**). Cercarial dermatitis, a neglected allergic disease. *Clin. Rev. Allergy Immunol.* 45, 63–74.

Kolbeková P, Kolářová L, Větvička D, Syrůček M (**2011**). Imaging of *Toxocara canis* larvae labelled by CFSE in BALB/c mice. *Parasitol. Res.* 108, 1007–14.

Kołodziej-Sobocińska M, Dziemian E, Machnicka-Rowińska B (**2006**). Inhibition of nitric oxide production by aminoguanidine influences the number of *Trichinella spiralis* parasites in infected "low responders" (C57BL/6) and "high responders" (BALB/c) mice. *Parasitol. Res.* 99, 194–196.

Kouřilová P, Hogg KG, Kolářová L, Mountford AP (**2004a**). Cercarial dermatitis caused by bird schistosomes comprises both immediate and late phase cutaneous hypersensitivity reactions. *J. Immunol.* 172, 3766–74.

Kouřilová P, Syrůček M, Kolářová L (**2004b**). The severity of mouse pathologies caused by the bird schistosome *Trichobilharzia regenti* in relation to host immune status. *Parasitol. Res.* 93, 8–16.

Kreutzberg GW (**1996**). Microglia: a sensor for pathological events in the CNS. *Trends Neurosci.* 19, 312–8.

Lawrence CE, Paterson JC, Wei XQ, Liew FY, Garside P, Kennedy MW (**2000**). Nitric oxide mediates intestinal pathology but not immune expulsion during Trichinella spiralis infection in mice. *J. Immunol.* 164, 4229–34.

Lee J-C, Cho G-S, Kwon JH, Shin MH, Lim JH, Kim W-K (**2006**). Macrophageal/microglial cell activation and cerebral injury induced by excretory-secretory products secreted by Paragonimus westermani. *Neurosci. Res.* 54, 133–9.

Lee SC, Liu W, Brosnan CF, Dickson DW (**1994**). GM-CSF promotes proliferation of human fetal and adult microglia in primary cultures. *Glia* 12, 309–18.

Lee SC, Liu W, Roth P, Dickson DW, Berman JW, Brosnan CF (**1993**). Macrophage colony-stimulating factor in human fetal astrocytes and microglia. Differential regulation by cytokines and lipopolysaccharide, and modulation of class II MHC on microglia. *J. Immunol.* 150, 594–604.

Lee SJ, Drabik K, Van Wagoner NJ, Lee S, Choi C, Dong Y, Benveniste EN (**2000**). ICAM-1-induced expression of proinflammatory cytokines in astrocytes: involvement of extracellular signal-regulated kinase and p38 mitogen-activated protein kinase pathways. *J. Immunol.* 165, 4658–66.

Lee Y-J, Park C-E, Kim J-H, Sohn H-J, Lee J, Jung S-Y, Shin H-J (**2011**). *Naegleria fowleri* lysate induces strong cytopathic effects and pro-inflammatory cytokine release in rat microglial cells. *Korean J. Parasitol.* 49, 285–90.

Lemos KR, Marques LC, Aquino LPCT, Alessi AC, Zacarias RZ (**2008**). Astrocytic and microglial response and histopathological changes in the brain of horses with experimental chronic *Trypanosoma evansi* infection. *Rev. Inst. Med. Trop. Sao Paulo* 50, 243–249.

Li CK, Seth R, Gray T, Bayston R, Mahida YR, Wakelin D (**1998**). Production of proinflammatory cytokines and inflammatory mediators in human intestinal epithelial cells after invasion by *Trichinella spiralis*. *Infect. Immun.* 66, 2200–6.

Li S, Yang F, Ji P, Zeng X, Wu X, Wei J, Ouyang L, Liang J, Zheng H, Wu Z, Lv Z (**2014**). Eosinophil chemotactic chemokine profilings of the brain from permissive and non-permissive hosts infected with *Angiostrongylus cantonenis*. *Parasitol. Res.* 113, 517–25.

Li Z, Chen X, Zen X, Liang J, Wei J, Lv Z, Sun X, Wu Z-D (**2014**). MicroRNA expression profile in the third- and fourth-stage larvae of *Angiostrongylus cantonensis*. *Parasitol. Res.* 113, 1883–96.

Li Z-Y, Lv Z-Y, Wei J, Liao Q, Zheng H-Q, Wu Z-D (**2012**). Cloning and characterization of a novel gene encoding 16 kDa protein (Ac16) from *Angiostrongylus cantonensis*. *Parasitol. Res.* 110, 2145–53.

Liao C-W, Fan C-K, Kao T-C, Ji D-D, Su K-E, Lin Y-H, Cho W-L (**2008**). Brain injury-associated biomarkers of TGF-beta1, S100B, GFAP, NF-L, tTG, AbetaPP, and tau were concomitantly enhanced and the UPS was impaired during acute brain injury caused by *Toxocara canis* in mice. *BMC Infect. Dis.* 8, 84.

Lichtenbergová L, Kolbeková P, Kouřilová P, KašnÝ M, Mikeš L, Haas H, Schramm G, Horák P, Kolářová L, Mountford AP (**2008**). Antibody responses induced by *Trichobilharzia regenti*

antigens in murine and human hosts exhibiting cercarial dermatitis. *Parasite Immunol.* 30, 585–595.

Lichtenbergová L, Lassmann H, Jones M, Kolářová L, Horák P (**2011**). *Trichobilharzia regenti*: Host immune response in the pathogenesis of neuroinfection in mice. *Exp. Parasitol.* 128, 328–35.

Ligasová A, Bulantová J, Sebesta O, Kašný M, Koberna K, Mikeš L (**2011**). Secretory glands in cercaria of the neuropathogenic schistosome *Trichobilharzia regenti* – ultrastructural characterization, 3-D modelling, volume and pH estimations. *Parasit. Vectors* 4, 162.

Liu S, Liu Y, Hao W, Wolf L, Kiliaan AJ, Penke B, Rübe CE, Walter J, Heneka MT, Hartmann T, Menger MD, Fassbender K (**2012**). TLR2 is a primary receptor for Alzheimer's amyloid β peptide to trigger neuroinflammatory activation. *J. Immunol.* 188, 1098–107.

Loddick SA, Turnbull A V, Rothwell NJ (**1998**). Cerebral interleukin-6 is neuroprotective during permanent focal cerebral ischemia in the rat. *J. Cereb. Blood Flow Metab.* 18, 176–9.

Londoño DP, Alvarez JI, Trujillo J, Jaramillo MM, Restrepo BI (**2002**). The inflammatory cell infiltrates in porcine cysticercosis: immunohistochemical analysis during various stages of infection. *Vet. Parasitol.* 109, 249–59.

Lu C-Y, Lai S-C (**2013a**). Induction of matrix metalloproteinase-2 and -9 via Erk1/2-NF-κB pathway in human astroglia infected with *Toxoplasma gondii*. *Acta Trop.* 127, 14–20.

Lu C-Y, Lai S-C (**2013b**). Matrix metalloproteinase-2 and -9 lead to fibronectin degradation in astroglia infected with *Toxoplasma gondii*. *Acta Trop.* 125, 320–9.

Lüder CG, Giraldo-Velásquez M, Sendtner M, Gross U (**1999**). *Toxoplasma gondii* in primary rat CNS cells: differential contribution of neurons, astrocytes, and microglial cells for the intracerebral development and stage differentiation. *Exp. Parasitol.* 93, 23–32.

Ma N, Madigan MC, Chan-Ling T, Hunt NH (**1997**). Compromised blood-nerve barrier, astrogliosis, and myelin disruption in optic nerves during fatal murine cerebral malaria. *Glia* 19, 135–151.

Mack CL, Vanderlugt-Castaneda CL, Neville KL, Miller SD (**2003**). Microglia are activated to become competent antigen presenting and effector cells in the inflammatory environment of the Theiler's virus model of multiple sclerosis. *J. Neuroimmunol.* 144, 68–79.

Magnusson JP, Goritz C, Tatarishvili J, Dias DO, Smith EMK, Lindvall O, Kokaia Z, Frisen J (**2014**). A latent neurogenic program in astrocytes regulated by Notch signaling in the mouse. *Science* 346, 237–241.

Mander PK, Jekabsone A, Brown GC (**2006**). Microglia proliferation is regulated by hydrogen peroxide from NADPH oxidase. *J. Immunol.* 176, 1046–52.

Marek R, Caruso M, Rostami A, Grinspan JB, Das Sarma J (**2008**). Magnetic cell sorting: a fast and effective method of concurrent isolation of high purity viable astrocytes and microglia from neonatal mouse brain tissue. *J. Neurosci. Methods* 175, 108–18.

Martinez FO, Gordon S (**2014**). The M1 and M2 paradigm of macrophage activation: time for reassessment. *F1000Prime Rep.* 6, 13.

Masocha W, Rottenberg ME, Kristensson K (**2006**). Minocycline impedes African trypanosome invasion of the brain in a murine model. *Antimicrob. Agents Chemother.* 50, 1798–1804.

Matsumoto Y, Ohmori K, Fujiwara M (**1992**). Immune regulation by brain cells in the central nervous system: microglia but not astrocytes present myelin basic protein to encephalitogenic T cells under *in vivo*-mimicking conditions. *Immunology* 76, 209–16.

McCarthy KD, de Vellis J (**1980**). Preparation of separate astroglial and oligodendroglial cell cultures from rat cerebral tissue. *J. Cell Biol.* 85, 890–902.

McGarry HF, Plant LD, Taylor MJ (**2005**). Diethylcarbamazine activity against *Brugia malayi* microfilariae is dependent on inducible nitric-oxide synthase and the cyclooxygenase pathway. *Filaria J.* 4, 4.

McKeon R, Jurynec M, Buck C (**1999**). The chondroitin sulfate proteoglycans neurocan and phosphacan are expressed by reactive astrocytes in the chronic CNS glial scar. *J. Neurosci.* 19, 10778–88.

McKeon R, Schreiber R, Rudge J, Silver J (**1991**). Reduction of neurite outgrowth in a model of glial scarring following CNS injury is correlated with the expression of inhibitory molecules on reactive astrocytes. *J. Neurosci.* 11, 3398–411.

McLaren DJ, James SL (**1985**). Ultrastructural studies of the killing of schistosomula of *Schistosoma mansoni* by activated macrophages in vitro. *Parasite Immunol.* 7, 315–31.

Medana IM, Hunt NH, Chan-Ling T (**1997a**). Early activation of microglia in the pathogenesis of fatal murine cerebral malaria. *Glia* 19, 91–103.

Medana IM, Hunt NH, Chaudhri G (**1997b**). Tumor necrosis factor-alpha expression in the brain during fatal murine cerebral malaria: evidence for production by microglia and astrocytes. *Am. J. Pathol.* 150, 1473–1486.

Mikes L, Zìdková L, Kasný M, Dvorák J, Horák P (**2005**). *In vitro* stimulation of penetration gland emptying by *Trichobilharzia szidati* and *T. regenti* (Schistosomatidae) cercariae. Quantitative collection and partial characterization of the products. *Parasitol. Res.* 96, 230–41.

Miller KR, Prokop S, Heppner FL (**2013**). Roles of activated microglia. *In: Kettenmann H, Ransom BR (Eds), Neuroglia*. Oxford University Press, New York, pp. 626–637.

Mills CD, Kincaid K, Alt JM, Heilman MJ, Hill AM (**2000**). M-1/M-2 macrophages and the Th1/Th2 paradigm. *J. Immunol.* 164, 6166–6173.

Mishra BB, Gundra UM, Teale JM (**2008**). Expression and distribution of Toll-like receptors 11-13 in the brain during murine neurocysticercosis. *J. Neuroinflammation* 5, 53.

Mishra BB, Mishra PK, Teale JM (**2006**). Expression and distribution of Toll-like receptors in the brain during murine neurocysticercosis. *J. Neuroimmunol.* 181, 46–56.

Monnier PP, Sierra A, Schwab JM, Henke-Fahle S, Mueller BK (**2003**). The Rho/ROCK pathway mediates neurite growth-inhibitory activity associated with the chondroitin sulfate proteoglycans of the CNS glial scar. *Mol. Cell. Neurosci.* 22, 319–30.

Morocoima A, Socorro G, Avila R, Hernández A, Merchán S, Ortiz D, Primavera G, Chique J, Herrera L, Urdaneta-Morales S (**2012**). *Trypanosoma cruzi*: experimental parasitism in the central nervous system of albino mice. *Parasitol. Res.* 111, 2099–107.

Moyano LM, Saito M, Montano SM, Gonzalvez G, Olaya S, Ayvar V, González I, Larrauri L, Tsang VCW, Llanos F, Rodríguez S, Gonzalez AE, Gilman RH, Garcia HH (**2014**). Neurocysticercosis as a cause of epilepsy and seizures in two community-based studies in a cysticercosis-endemic region in Peru. *PLoS Negl. Trop. Dis.* 8, e2692.

Ndimubanzi PC, Carabin H, Budke CM, Nguyen H, Qian Y-J, Rainwater E, Dickey M, Reynolds S, Stoner JA (**2010**). A systematic review of the frequency of neurocyticercosis with a focus on people with epilepsy. *PLoS Negl. Trop. Dis.* 4, e870.

Niederkorn JY (**2006**). See no evil, hear no evil, do no evil: the lessons of immune privilege. *Nat. Immunol.* 7, 354–9.

Nikodemova M, Watters JJ (**2012**). Efficient isolation of live microglia with preserved phenotypes from adult mouse brain. *J. Neuroinflammation* 9, 147.

Nimmerjahn A, Kirchhoff F, Helmchen F (**2005**). Resting microglial cells are highly dynamic surveillants of brain parenchyma *in vivo*. *Science* 308, 1314–8.

Norden DM, Godbout JP (**2013**). Microglia of the aged brain: primed to be activated and resistant to regulation. *Neuropathol. Appl. Neurobiol.* 39, 19–34.

O'Connor RA, Devaney E (**2002**). Nitric oxide limits the expansion of antigen-specific T cells in mice infected with the microfilariae of *Brugia pahangi*. *Infect. Immun.* 70, 5997–6004.

O'Connor RA, Jenson JS, Devaney E (**2000**). NO contributes to proliferative suppression in a murine model of filariasis. *Infect. Immun.* 68, 6101–7.

O'Donnell VB, Eiserich JP, Chumley PH, Jablonsky MJ, Krishna NR, Kirk M, Barnes S, Darley-Usmar VM, Freeman BA (**1999**). Nitration of unsaturated fatty acids by nitric oxide-derived reactive nitrogen species peroxynitrite, nitrous acid, nitrogen dioxide, and nitronium ion. *Chem. Res. Toxicol.* 12, 83–92.

Oberdörfer C, Adams O, MacKenzie CR, De Groot CJA, Däubener W (**2003**). Role of IDO activation in anti-microbial defense in human native astrocytes. *Adv. Exp. Med. Biol.* 527, 15–26.

Ohsawa K, Imai Y, Kanazawa H, Sasaki Y, Kohsaka S (**2000**). Involvement of Iba1 in membrane ruffling and phagocytosis of macrophages/microglia. *J. Cell Sci.* 113, 3073–3084.

Olson JK, Miller SD (**2004**). Microglia initiate central nervous system innate and adaptive immune responses through multiple TLRs. *J. Immunol.* 173, 3916–24.

Oswald IP, Eltoum I, Wynn TA, Schwartz B, Caspar P, Paulin D, Sher A, James SL (**1994**). Endothelial cells are activated by cytokine treatment to kill an intravascular parasite, *Schistosoma mansoni*, through the production of nitric oxide. *Proc. Natl. Acad. Sci.* 91, 999–1003.

Pacher P, Beckman JS, Liaudet L (**2007**). Nitric oxide and peroxynitrite in health and disease. *Physiol. Rev.* 87, 315–424.

Paolicelli RC, Bolasco G, Pagani F, Maggi L, Scianni M, Panzanelli P, Giustetto M, Ferreira TA, Guiducci E, Dumas L, Ragozzino D, Gross CT (**2011**). Synaptic pruning by microglia is necessary for normal brain development. *Science* 333, 1456–8.

Paveley RA, Aynsley SA, Cook PC, Turner JD, Mountford AP (**2009**). Fluorescent imaging of antigen released by a skin-invading helminth reveals differential uptake and activation profiles by antigen presenting cells. *PLoS Negl. Trop. Dis.* 3, e528.

Pech V (**2013**). Perorální infekce ptáků a savců neuropatogenní motolicí *Trichobilharzia regenti*. Master's thesis. Charles University in Prague, Faculty of Science. [In Czech].

Pekny M, Wilhelmsson U, Pekna M (**2014**). The dual role of astrocyte activation and reactive gliosis. *Neurosci. Lett.* 565, 30–8.

Perea G, Navarrete M, Araque A (**2009**). Tripartite synapses: astrocytes process and control synaptic information. *Trends Neurosci.* 32, 421–31.

Peress NS, Fleit HB, Perillo E, Kuljis R, Pezzullo C (**1993**). Identification of Fc gamma RI, II and III on normal human brain ramified microglia and on microglia in senile plaques in Alzheimer's disease. *J. Neuroimmunol.* 48, 71–9.

Peterson PK, Gekker G, Hu S, Chao CC (**1995**). Human astrocytes inhibit intracellular multiplication of *Toxoplasma gondii* by a nitric oxide-mediated mechanism. *J. Infect. Dis.* 171, 516–518.

Peterson PK, Gekker G, Hu S, Chao CC (**1993**). Intracellular survival and multiplication of *Toxoplasma gondii* in astrocytes. *J. Infect. Dis.* 168, 1472–1478.

Pfefferkorn ER (**1984**). Interferon gamma blocks the growth of *Toxoplasma gondii* in human fibroblasts by inducing the host cells to degrade tryptophan. *Proc. Natl. Acad. Sci.* 81, 908–12.

Pfefferkorn ER, Eckel M, Rebhun S (**1986**). Interferon-gamma suppresses the growth of *Toxoplasma gondii* in human fibroblasts through starvation for tryptophan. *Mol. Biochem. Parasitol.* 20, 215–24.

Pittella J (**1985**). Vascular changes in cerebral schistosomiasis mansoni: a histopathological study of fifteen cases. *Am. J. Trop. Med. Hyg.* 34, 898–902.

Powell EM, Geller HM (**1999**). Dissection of astrocyte-mediated cues in neuronal guidance and process extension. *Glia* 26, 73–83.

Quan N, Mhlanga JDM, Whiteside MB, McCoy AN, Kristensson K, Herkenham M (**1999**). Chronic overexpression of proinflammatory cytokines and histopathology in the brains of rats infected with *Trypanosoma brucei*. *J. Comp. Neurol.* 414, 114–130.

Quijano C, Alvarez B, Gatti RM, Augusto O, Radi R (**1997**). Pathways of peroxynitrite oxidation of thiol groups. *Biochem. J.* 322, 167–73.

Ragnarson B, Bengtsson L, Haegerstrand A (**1992**). Labeling with fluorescent carbocyanine dyes of cultured endothelial and smooth muscle cells by growth in dye-containing medium. *Histochemistry* 97, 329–33.

Rajan T V, Porte P, Yates JA, Keefer L, Shultz LD (**1996**). Role of nitric oxide in host defense against an extracellular, metazoan parasite, *Brugia malayi*. *Infect. Immun.* 64, 3351–3.

Rajbhandari L, Tegenge MA, Shrestha S, Ganesh Kumar N, Malik A, Mithal A, Hosmane S, Venkatesan A (**2014**). Toll-like receptor 4 deficiency impairs microglial phagocytosis of degenerating axons. *Glia* 62, 1982–91.

Rakic P (**1971**). Guidance of neurons migrating to the fetal monkey neocortex. *Brain Res.* 33, 471–6.

Ransohoff RM, Engelhardt B (**2012**). The anatomical and cellular basis of immune surveillance in the central nervous system. *Nat. Rev. Immunol.* 12, 623–35.

Redlich S, Ribes S, Schütze S, Eiffert H, Nau R (**2013**). Toll-like receptor stimulation increases phagocytosis of *Cryptococcus neoformans* by microglial cells. *J. Neuroinflammation* 10, 71.

Reichert F, Rotshenker S (**2003**). Complement-receptor-3 and scavenger-receptor-AI/II mediated myelin phagocytosis in microglia and macrophages. *Neurobiol. Dis.* 12, 65–72.

Restrepo B, Alvarez J, Castano J, Arias L, Restrepo M, Trujillo J, Colegial C, Teale J (**2001**). Brain granulomas in neurocysticercosis patients are associated with a Th1 and Th2 profile. *Infect. Immun.* 69, 4554.

Ribes S, Ebert S, Czesnik D, Regen T, Zeug A, Bukowski S, Mildner A, Eiffert H, Hanisch U-K, Hammerschmidt S, Nau R (**2009**). Toll-like receptor prestimulation increases phagocytosis of *Escherichia coli* DH5alpha and *Escherichia coli* K1 strains by murine microglial cells. *Infect. Immun.* 77, 557–64.

Rock RB, Gekker G, Hu S, Sheng WS, Cheeran M, Lokensgard JR, Peterson PK (**2004**). Role of microglia in central nervous system infections. *Clin. Microbiol. Rev.* 17, 942–64, table of contents.

Roitbak T, Syková E (**1999**). Diffusion barriers evoked in the rat cortex by reactive astrogliosis. *Glia* 28, 40–8.

Rozenfeld C, Martinez R, Figueiredo RT, Bozza MT, Lima FRS, Pires AL, Silva PM, Bonomo A, Lannes-Vieira J, De Souza W, Moura-Neto V (**2003**). Soluble factors released by *Toxoplasma gondii*-infected astrocytes down-modulate nitric oxide production by gamma interferon-activated microglia and prevent neuronal degeneration. *Infect. Immun.* 71, 2047–57.

Rozenfeld C, Martinez R, Seabra S, Sant'anna C, Gonçalves JGR, Bozza M, Moura-Neto V, De Souza W (**2005**). *Toxoplasma gondii* prevents neuron degeneration by interferon-gamma-activated microglia in a mechanism involving inhibition of inducible nitric oxide synthase and transforming growth factor-beta1 production by infected microglia. *Am. J. Pathol.* 167, 1021–31.

Rudge JS, Silver J (**1990**). Inhibition of neurite outgrowth on astroglial scars *in vitro*. *J. Neurosci.* 10, 3594–603.

Sajid M, McKerrow JH, Hansell E, Mathieu MA, Lucas KD, Hsieh I, Greenbaum D, Bogyo M, Salter JP, Lim KC, Franklin C, Kim J-H, Caffrey CR (**2003**). Functional expression and characterization of *Schistosoma mansoni* cathepsin B and its trans-activation by an endogenous asparaginyl endopeptidase. *Mol. Biochem. Parasitol.* 131, 65–75.

Saura J (**2007**). Microglial cells in astroglial cultures: a cautionary note. *J. Neuroinflammation* 4, 26.

Saura J, Tusell JM, Serratosa J (**2003**). High-yield isolation of murine microglia by mild trypsinization. *Glia* 44, 183–9.

Schluesener HJ, Kremsner PG, Meyermann R (**1998**). Widespread expression of MRP8 and MRP14 in human cerebral malaria by microglial cells. *Acta Neuropathol.* 96, 575–80.

Schlüter D, Kaefer N, Hof H, Wiestler OD, Deckert-Schlüter M (**1997**). Expression pattern and cellular origin of cytokines in the normal and *Toxoplasma gondii*-infected murine brain. *Am. J. Pathol.* 150, 1021–35.

Sharafeldin A, Eltayeb R, Pashenkov M, Bakhiet M (**2000**). Chemokines are produced in the brain early during the course of experimental African trypanosomiasis. *J. Neuroimmunol.* 103, 165–70.

Sheng W, Zong Y, Mohammad A, Ajit D, Cui J, Han D, Hamilton JL, Simonyi A, Sun AY, Gu Z, Hong J-S, Weisman GA, Sun GY (**2011**). Pro-inflammatory cytokines and lipopolysaccharide induce changes in cell morphology, and upregulation of ERK1/2, iNOS and $sPLA_2$-IIA expression in astrocytes and microglia. *J. Neuroinflammation* 8, 121.

Sikasunge C, Johansen M, Phiri I, Willingham A, Leifsson P (**2009**). The immune response in *Taenia solium* neurocysticercosis in pigs is associated with astrogliosis, axonal degeneration and altered blood-brain barrier permeability. *Vet. Parasitol.* 160, 242–50.

Silva RR, Mariante RM, Silva AA, dos Santos ALB, Roffê E, Santiago H, Gazzinelli RT, Lannes-Vieira J (**2015**). Interferon-gamma promotes infection of astrocytes by *Trypanosoma cruzi*. *PLoS One* 10, e0118600.

Smith AM, Gibbons HM, Oldfield RL, Bergin PM, Mee EW, Curtis MA, Faull RLM, Dragunow M (**2013**). M-CSF increases proliferation and phagocytosis while modulating receptor and transcription factor expression in adult human microglia. *J. Neuroinflammation* 10, 85.

Smith JA, Das A, Ray SK, Banik NL (**2012**). Role of pro-inflammatory cytokines released from microglia in neurodegenerative diseases. *Brain Res. Bull.* 87, 10–20.

Smith-Thomas L, Fok-Seang J, Stevens J, Du J, Muir E, Faissner A, Geller H, Rogers J, Fawcett J (**1994**). An inhibitor of neurite outgrowth produced by astrocytes. *J. Cell Sci.* 107, 1687–95.

Sofroniew M V (**2009**). Molecular dissection of reactive astrogliosis and glial scar formation. *Trends Neurosci.* 32, 638–47.

Sofroniew M V, Vinters H V (**2010**). Astrocytes: biology and pathology. *Acta Neuropathol.* 119, 7–35.

Stansley B, Post J, Hensley K (**2012**). A comparative review of cell culture systems for the study of microglial biology in Alzheimer's disease. *J. Neuroinflammation* 9, 115.

Steers NJ, Rogan MT, Heath S (**2001**). *In vitro* susceptibility of hydatid cysts of *Echinococcus granulosus* to nitric oxide and the effect of the laminated layer on nitric oxide production. *Parasite Immunol.* 23, 411–7.

Stence N, Waite M, Dailey ME (**2001**). Dynamics of microglial activation: a confocal time-lapse analysis in hippocampal slices. *Glia* 33, 256–66.

Stewart VC, Sharpe MA, Clark JB, Heales SJ (**2000**). Astrocyte-derived nitric oxide causes both reversible and irreversible damage to the neuronal mitochondrial respiratory chain. *J. Neurochem.* 75, 694–700.

Strack A, Asensio VC, Campbell IL, Schlüter D, Deckert M (**2002**). Chemokines are differentially expressed by astrocytes, microglia and inflammatory leukocytes in *Toxoplasma* encephalitis and critically regulated by interferon-gamma. *Acta Neuropathol.* 103, 458–68.

Streit WJ (**2013**). Microglia in cell culture. *In: Kettenmann H, Ransom BR (Eds), Neuroglia*. Oxford University Press, New York, pp. 92–93.

Streit WJ, Hurley SD, McGraw TS, Semple-Rowland SL (**2000**). Comparative evaluation of cytokine profiles and reactive gliosis supports a critical role for interleukin-6 in neuron-glia signaling during regeneration. *J. Neurosci. Res.* 61, 10–20.

Streit WJ, Kreutzberg GW (**1987**). Lectin binding by resting and reactive microglia. *J. Neurocytol.* 16, 249–60.

Stuehr DJ (**1999**). Mammalian nitric oxide synthases. *Biochim. Biophys. Acta* 1411, 217–30.

Stuehr DJ, Marletta MA (**1987**). Induction of nitrite/nitrate synthesis in murine macrophages by BCG infection, lymphokines, or interferon-gamma. *J. Immunol.* 139, 518–25.

Stuehr DJ, Marletta MA (**1985**). Mammalian nitrate biosynthesis: mouse macrophages produce nitrite and nitrate in response to *Escherichia coli* lipopolysaccharide. *Proc. Natl. Acad. Sci.* 82, 7738–42.

Sun Y, Chauhan A, Sukumaran P, Sharma J, Singh BB, Mishra BB (**2014**). Inhibition of store-operated calcium entry in microglia by helminth factors: implications for immune suppression in neurocysticercosis. *J. Neuroinflammation* 11, 210.

Suzuki Y, Claflin J, Wang X, Lengi A, Kikuchi T (**2005**). Microglia and macrophages as innate producers of interferon-gamma in the brain following infection with *Toxoplasma gondii*. *Int. J. Parasitol.* 35, 83–90.

Suzumura A, Marunouchi T, Yamamoto H (**1991**). Morphological transformation of microglia *in vitro*. *Brain Res.* 545, 301–306.

Tam WY, Ma CHE (**2014**). Bipolar/rod-shaped microglia are proliferating microglia with distinct M1/M2 phenotypes. *Sci. Rep.* 4, 7279.

Tang X, Davies JE, Davies SJA (**2003**). Changes in distribution, cell associations, and protein expression levels of NG2, neurocan, phosphacan, brevican, versican V2, and tenascin-C during acute to chronic maturation of spinal cord scar tissue. *J. Neurosci. Res.* 71, 427–44.

Tang Y, Le W (**2015**). Differential roles of M1 and M2 microglia in neurodegenerative diseases. *Mol. Neurobiol.* [Epub ahead of print].

Taramelli D, Basilico N, Pagani E, Grande R, Monti D, Ghione M, Olliaro P (**1995**). The heme moiety of malaria pigment (beta-hematin) mediates the inhibition of nitric oxide and tumor necrosis factor-alpha production by lipopolysaccharide-stimulated macrophages. *Exp. Parasitol.* 81, 501–511.

Taylor MJ, Cross HF, Bilo K (**2000**). Inflammatory responses induced by the filarial nematode *Brugia malayi* are mediated by lipopolysaccharide-like activity from endosymbiotic Wolbachia bacteria. *J. Exp. Med.* 191, 1429–36.

Taylor MJ, Cross HF, Mohammed AA, Trees AJ, Bianco AE (**1996**). Susceptibility of *Brugia malayi* and *Onchocerca lienalis* microfilariae to nitric oxide and hydrogen peroxide in cell-free culture and from IFN gamma-activated macrophages. *Parasitology* 112, 315–322.

Thomas GR, McCrossan M, Selkirk ME (**1997**). Cytostatic and cytotoxic effects of activated macrophages and nitric oxide donors on Brugia malayi. *Infect. Immun.* 65, 2732–9.

Uddin J, Garcia HH, Gilman RH, Gonzalez AE, Friedland JS (**2005**). Monocyte-astrocyte networks and the regulation of chemokine secretion in neurocysticercosis. *J. Immunol.* 175, 3273–81.

Vargas-Zambrano JC, Lasso P, Cuellar A, Puerta CJ, González JM (**2013**). A human astrocytoma cell line is highly susceptible to infection with *Trypanosoma cruzi*. *Mem. Inst. Oswaldo Cruz* 108, 212–219.

Verma SK, Joseph SK, Verma R, Kushwaha V, Parmar N, Yadav PK, Thota JR, Kar S, Murthy PK (**2015**). Protection against filarial infection by 45-49 kDa molecules of *Brugia malayi* via IFN-γ-mediated iNOS induction. *Vaccine* 33, 527–34.

Vermeiren C, Najimi M, Vanhoutte N, Tilleux S, de Hemptinne I, Maloteaux J-M, Hermans E (**2005**). Acute up-regulation of glutamate uptake mediated by mGluR5a in reactive astrocytes. *J. Neurochem.* 94, 405–16.

Vijayan VK, Lee YL, Eng LF (**1990**). Increase in glial fibrillary acidic protein following neural trauma. *Mol. Chem. Neuropathol.* 13, 107–18.

Voutsinos-Porche B, Bonvento G, Tanaka K, Steiner P, Welker E, Chatton J-Y, Magistretti PJ, Pellerin L (**2003**). Glial glutamate transporters mediate a functional metabolic crosstalk between neurons and astrocytes in the mouse developing cortex. *Neuron* 37, 275–86.

Wake H, Moorhouse AJ, Miyamoto A, Nabekura J (**2013**). Microglia: actively surveying and shaping neuronal circuit structure and function. *Trends Neurosci.* 36, 209–17.

Wandurska-Nowak E, Hadaś E, Derda M, Wojt W (**2003**). Effect of nitric oxide releasing drugs on the intensity of infection during experimental trichinellosis in mice. *Parasitol. Res.* 90, 164–5.

Wandurska-Nowak E, Wiśniewska J (**2002**). Release of nitric oxide during experimental trichinellosis in mice. *Parasitol. Res.* 88, 708–11.

Wang X, Suzuki Y (**2007**). Microglia produce IFN-γ independently from T-cells during acute toxoplasmosis in the brain. *J. Interf. Cytokine Res.* 27, 599–605.

Wei J, Wu F, Sun X, Zeng X, Liang J-Y, Zheng H-Q, Yu X-B, Zhang K-X, Wu Z-D (**2013**). Differences in microglia activation between rats-derived cell and mice-derived cell after stimulating by soluble antigen of IV larva from *Angiostrongylus cantonensis in vitro*. *Parasitol. Res.* 112, 207–14.

Wiese L, Kurtzhals JAL, Penkowa M (**2006**). Neuronal apoptosis, metallothionein expression and proinflammatory responses during cerebral malaria in mice. *Exp. Neurol.* 200, 216–226.

Wilhelmsson U, Bushong EA, Price DL, Smarr BL, Phung V, Terada M, Ellisman MH, Pekny M (**2006**). Redefining the concept of reactive astrocytes as cells that remain within their unique domains upon reaction to injury. *Proc. Natl. Acad. Sci.* 103, 17513–17518.

Winkler S, El Menyawi I, Linnau KF, Graninger W (**1998**). Short report: total serum levels of the nitric oxide derivatives nitrite/nitrate during microfilarial clearance in human filarial disease. *Am. J. Trop. Med. Hyg.* 59, 523–5.

Wlodarczyk A, Løbner M, Cédile O, Owens T (**2014**). Comparison of microglia and infiltrating $CD11c^+$ cells as antigen presenting cells for T cell proliferation and cytokine response. *J. Neuroinflammation* 11, 57.

Wong PS-Y, Eiserich JP, Reddy S, Lopez CL, Cross CE, van der Vliet A (**2001**). Inactivation of glutathione S-transferases by nitric oxide-derived oxidants: Exploring a role for tyrosine nitration. *Arch. Biochem. Biophys.* 394, 216–228.

Wynn TA, Oswald IP, Eltoum IA, Caspar P, Lowenstein CJ, Lewis FA, James SL, Sher A (**1994**). Elevated expression of Th1 cytokines and nitric oxide synthase in the lungs of vaccinated mice after challenge infection with *Schistosoma mansoni*. *J. Immunol.* 153, 5200–9.

Yu WH, Kumar A, Peterhoff C, Shapiro Kulnane L, Uchiyama Y, Lamb BT, Cuervo AM, Nixon RA (**2004**). Autophagic vacuoles are enriched in amyloid precursor protein-secretase activities: implications for beta-amyloid peptide over-production and localization in Alzheimer's disease. *Int. J. Biochem. Cell Biol.* 36, 2531–40.

Zahoor Z, Davies AJ, Kirk RS, Rollinson D, Walker AJ (**2009**). Nitric oxide production by *Biomphalaria glabrata* haemocytes: effects of *Schistosoma mansoni* ESPs and regulation through the extracellular signal-regulated kinase pathway. *Parasit. Vectors* 2, 18.

Zeghir-Bouteldja R, Amri M, Aitaissa S, Bouaziz S, Mezioug D, Touil-Boukoffa C (**2009**). *In vitro* study of nitric oxide metabolites effects on human hydatid of *Echinococcus granulosus*. *J. Parasitol. Res.* 2009, 1–7.

Zeinstra E, Wilczak N, Streefland C, De Keyser J (**2000**). Astrocytes in chronic active multiple sclerosis plaques express MHC class II molecules. *Neuroreport* 11, 89–91.

Zhang Y, Chen H, Chen Y, Wang L, Cai Y, Li M, Wen H, Du J, An R, Luo Q, Wang X, Lun Z-R, Xu Y, Shen J (**2014**). Activated microglia contribute to neuronal apoptosis in toxoplasmic encephalitis. *Parasit. Vectors* 7, 372.

Zhao J, Lv Z, Wang F, Wei J, Zhang Q, Li S, Yang F, Zeng X, Wu X, Wu Z (**2013**). Ym1, an eosinophilic chemotactic factor, participates in the brain inflammation induced by *Angiostrongylus cantonensis* in mice. *Parasitol. Res.* 112, 2689–95.

9. SUPPLEMENTS

9.1. *T. regenti* larval stages staining for ultramicroscopic examination

Two approaches were applied: staining of either cercariae before penetration into the host (see 9.1.1.) or staining of schistosomula *in situ*, i.e. in the spinal cord. This supplement presents brief protocols which were tested but gave negative results.

9.1.1. Staining of cercariae

9.1.1.1. Qtracker® 605 Cell Labelling Kit (Invitrogen)

This kit contains fluorescently tagged nanocrystals designed for long-term labelling of *in vitro* grown cells. One micromolar pre-mix of nanocrystals in PBS was prepared and subsequently mixed with water containing cercariae (1000/ml) to reach 20, 10, 5, and 2.5 nM final concentrations according to manufacturer's recommendation. The mixture was incubated in the dark at room temperature or at 37 °C for ¾ to 5 hours. Afterwards, viability of cercariae and the quality of staining were evaluated under the fluorescence microscope. The results are summarised in Table 9.1., representative photo from staining experiments is shown in Fig. 9.1A. Qtracker® Cell Labelling Kit was found not to be capable of labelling of cercariae.

Table 9.1. Staining of cercariae by Qtracker® 605 Cell Labelling Kit. Viability of cercariae: + living and motile cercariae, (+) non-motile cercariae with vacuolised tegument. Quality of staining: (+) red signal appears only around penetration glands opening or at the site of tail detachment, – no red signal detected. N.D. = not done.

Concentration of nanocrystals	Incubation time	Viability of cercariae		Quality of staining	
		RT	37 °C	RT	37 °C
20 nM	3 h	+	N.D.	(+)	N.D.
10 nM	45 min	+	N.D.	–	N.D.
	90 min	+	N.D.	(+)	N.D.
	3 h	+	N.D.	–	N.D.
	5 h	+	(+)	–	(+)
5 nM	45 min	+	N.D.	–	N.D.
	90 min	+	(+)	(+)	(+)
2.5 nM	45 min	+	N.D.	–	N.D.
	90 min	+	N.D.	–	N.D.

9.1.1.2. DiIC$_{16}$ (Invitrogen)

DiIC$_{16}$ is a fluorescent lipophilic molecule which is easily incorporated into cell membranes. Crystals of DiIC$_{16}$ were dissolved in 99.5% ethanol to prepare 0.25% (w/v) stock solution. It was diluted by

adding of water with cercariae (1000/ml) to get these final $DiIC_{16}$ concentrations: 50, 25, and 5 μg/ml. Working concentration range was set according to Ragnarson *et al*. (1992). Incubation was performed in the dark for 24 hours (RT). Viability of cercariae and the quality of staining were evaluated under the fluorescence microscope after 1, 6, and 24 hours. Table 9.2. presents the results of experiments and Figure 9.1B. illustrates the representative appearance of cercariae after staining. $DiIC_{16}$ was assessed not to be useful for labelling of cercariae.

Table 9.2. Staining of cercariae by $DiIC_{16}$. Viability of cercariae: + living and motile cercariae, (+) living cercariae, most of them with detached tails. Quality of staining: (+) red signal appears only around cercariae staining probably excretory/secretory products, – no red signal detected.

$DiIC_{16}$ concentration	Incubation time	Viability of cercariae	Quality of staining
50 μg/ml	1 h	(+)	(+)
	6 h	(+)	–
	24 h	(+)	–
25 μg/ml	1 h	(+)	–
	6 h	(+)	–
	24 h	(+)	–
5 μg/ml	1 h	+	(+)
	6 h	(+)	–
	24 h	(+)	–

9.1.1.3. CellTrace™ Far Red DDAO-SE (Invitrogen)

This fluorescent compound is commonly used for long-term cell labelling. One microliter from 2 mM stock solution was mixed with 3 ml of dechlorinated water and 750 μl of this mixture was next mixed with 250 μl of water containing cercariae (1000/ml), i.e. final concentration was 0.5 μM. The incubation was done in the dark for 30 minutes (RT). Examination under the fluorescence microscope revealed that cercariae were alive. However, most of them had detached tails; this was the site where the dye was bound (Fig. 9.1C). Therefore, CellTrace™ Far Red DDAO-SE was regarded as not suitable for staining of cercariae.

9.1.2. *In situ* staining of schistosomula

A possibility of labelling schistosomula directly in the spinal cord using the principle of indirect immunofluorescence was tested. C57BL/6 mouse was infected with 2000 cercariae (see 4.3.2.), sacrificed 6 DPI and perfused transcardially by heparinised PBS and 4% paraformaldehyde (see 4.4.2.). The extracted spinal cord was post-fixed in 4% paraformaldehyde overnight at 4 °C and subsequently processed according to protocol based on Jährling *et al*. (2008).

The next day, the spinal cord was cut into 1 cm long pieces which were washed 3× 50 minutes in 0.5% Triton X-100 in TBS. Incubation with a serum from a mouse reinfected with *T. regenti* (four infections repeated at 10-day interval, serum obtained 10 days after the 4th infection) followed. The mouse serum was diluted 1:100 or 1:150 in blocking solution (20% [v/v] dimethyl sulfoxide/foetal calf serum); the incubation lasted 36 hours. Samples were then washed 3× 60 minutes with 0.5% Triton X-100/TBS and incubated with goat anti-mouse Alexa Fluor® 568 (1:1000 in blocking solution, Invitrogen) for 18 hours in the dark. Afterwards, samples were being rinsed 3× 60 minutes with 0.5% Triton X-100/PBS. Squashed-tissue samples were prepared and examined under the fluorescence microscope for the presence of schistosomula; quality of their staining was evaluated.

In total, three experiments were made and only two schistosomula were found migrating through the spinal cord. When being examined under the fluorescence microscope, they did not show any antibody-specific signal and it was not possible to distinguish them from the nervous tissue due to the high background (Fig. 9.1D) caused probably by myelin auto-fluorescence and/or unspecific secondary antibody binding. To conclude, indirect immunofluorescence is not applicable to detect schistosomula *in situ*.

Figure 9.1. Staining of *T. regenti* cercariae and schistosomula. (A) Staining of cercariae by Qtracker® 605 Cell Labelling Kit. Cercariae are labelled only at the site of tail detachment. Concentration of nanocrystals: 10 nM, incubation for 5 hours at 37 °C. Scale bar 50 μm. (B) Staining of cercariae by $DiIC_{16}$. The body of cercariae is labelled but the tail has detached. Concentration of $DiIC_{16}$: 25 μg/ml, incubation for 1 hours (RT). Scale bar 50 μm. (C) Staining of cercariae by CellTrace™ Far Red DDAO-SE. The only site labelled was the site of tail detachment. Concentration of DDAO-SE: 0.5 μM, incubation for 30 minutes (RT). Scale bar 50 μm. (D) Staining of schistosomula *in situ* utilizing indirect immunofluorescence. The pictures from light (D1) and fluorescence (D2) microscope demonstrate that schistosomula migrating through the spinal cord are not distinguishable from the nervous tissue by using indirect immunofluorescence. Primary antibody dilution 1:100. Scale bars 50 μm.